

0041

AISC E&R Library



8262

→ RESEARCH
LIBRARY

2095

**TESTS OF FULL-SCALE BEAM-TO-COLUMN
CONNECTIONS**

by

Reidar Bjorhovde
The Bjorhovde Group, Tucson, Arizona

Lawrence J. Goland
Southwest Research Institute, San Antonio, Texas

Daniel J. Benac
Bryant-Lee Associates, San Antonio, Texas

August 1999

ABSTRACT

The 1994 Northridge earthquake appeared to demonstrate that steel-framed structures and particularly certain of the beam-to-column connections were unable to perform adequately under seismic conditions. Several major research efforts were undertaken to determine the causes of the failures, and to pinpoint issues related to material performance, design, detailing and fabrication. Old and new connection types have been investigated, with the aim of ensuring satisfactory service of steel structures under future earthquakes.

The research program that is detailed in this report was undertaken as the result of certain connection fractures that were discovered during the fabrication of the connections for a major California structure. Standard details and fabrication practices had been utilized for the structure, yet cracking took place in certain areas of the connections. An intensive evaluation of the particular structure was conducted, and it was subsequently determined that the major reason for the cracking was the presence of hydrogen during the welding of the elements. The repair procedures that were put in place yielded fully satisfactory assemblies. Nevertheless, it was decided that a cohesive and detailed study was needed to remove any and all uncertainties regarding the steel material and the connections that had been used.

A total of 17 full-scale beam-to-column connections were tested. All used W14x176 columns and W21x122 beams in ASTM A572 Grade 50 steel. Eight tests had connections identical to those of the California structure; these used cover-plated beams and complete joint penetration continuity plates to column welds. The other nine specimens incorporated revisions that were intended to provide improved connection performance as well as fabrication ease and economy. In particular, the continuity plates were fillet welded to the column, and thinner cover plates were used for eight of the tests. The ninth specimen was identical to the original design, but with a transition fillet weld added between the beam and the column. Among the second group of eight specimens were two that had repositioned continuity plates as well as the transition fillet weld between the beam and the column.

The tests also aimed at determining the effects of the straightening protocol that had been used for the columns. Among the 17 tests, 13 had rotary straightened columns, 2 columns were gag straightened, and 2 were unstraightened. Finally, test loading and control were done in conformance with the criteria of the Applied Technology Council (ATC), with eight tests using slow cyclic (quasi-static) loading and nine being loaded according to a 1 Hz dynamic protocol.

The full-scale connection tests showed that the original (as-built) connections were able to perform adequately and in agreement with the Federal Emergency Management Agency's (FEMA) requirements. Most of the revised connections were also able to meet the FEMA criteria for new construction; these are more demanding in plastic rotation capacity than those used for as-built construction. However, the performance of one of the revised connection types was far superior in all respects; this was the specimen that utilized fillet welded, repositioned continuity plates and a transition fillet weld from the beam to the column. It is referred to as Type 3 below.

The Type 3 connections performed extremely well, exhibiting very large plastic rotation capacities and late onset of cracking and eventual failure. It was also found that although cracks developed and propagated through portions of the column material, the propagation was slow and stable, with numerous crack arrest events during the tests. This also occurred for the cracks that propagated into the k-area of the columns, demonstrating that a crack in this region will not propagate in brittle fashion, given appropriate connection details and fracture paths.

Overall, the test results demonstrated conclusively that there are no significant performance differences between assemblies using rotary straightened, gag straightened and unstraightened columns. The type of loading protocol was also found to be unimportant, although it appeared that the demands imposed by the dynamic loading were more severe than those of the quasi-static protocol.

TABLE OF CONTENTS

	Abstract	ii
	Executive Summary	x
1.	Introduction	1
2.	Scope and Aims of Testing Program	4
	2.1 General Program Criteria	4
	2.2 Specimen Design and Fabrication	4
	2.3 Loading Protocols	5
	2.4 Straightening Protocols for Connection Assembly Members	6
	2.5 Connection Details	7
	2.6 Replication of Test Performance	9
	2.7 Data Collection	9
3.	Selection and Design of Connection Specimens	10
	3.1 General Description	10
	3.2 Overall Testing Rationale	13
	3.3 Specimen Materials	16
	3.4 Fabrication of Test Specimens	17
4.	Testing Protocols, Computations and Equipment	19
	4.1 General Description	19
	4.2 Test Frame and Specimen Installation	20
	4.3 Measurement Needs and Instrumentation	21
	4.4 Loads and Load Application System	22
	4.5 Testing and Loading Protocols	22
	4.6 Computation of Displacements and Rotations	26

5.	Material Properties	32
5.1	General Observations	32
5.2	Tensile Properties	32
5.3	Charpy Impact Testing	37
5.4	Hardness	42
5.5	Grain Size and Chemistry	46
6.	Performance of As-Built Connections with Rotary Straightened Columns	47
6.1	Connection Design and Materials	47
6.2	Quasi-Static Tests	47
6.3	Dynamic Tests	49
6.4	Assessment of Performance	52
7.	Performance of As-Built Connections with Gag Straightened Columns	53
7.1	Connection Design and Materials	53
7.2	Test Results	54
7.3	Assessment of Performance	55
8.	Performance of As-Built Connection with Unstraightened Column	56
8.1	Connection Design and Materials	56
8.2	Straightening Protocol	57
8.3	Test Results	57
8.4	Assessment of Performance	58
9.	Performance of Revised As-Built Connection Type 1	58
9.1	Connection Design and Materials	58
9.2	Straightening Protocol	59
9.3	Quasi-Static Tests	59
9.4	Dynamic Tests	61
9.5	Assessment of Performance	62

10.	Performance of Revised As-Built Connection Type 2	62
	10.1 Connection Design and Materials	62
	10.2 Test Results	64
	10.3 Comparison of Performance with Other Connections	65
11.	Performance of Revised As-Built Connection Type 3	66
	11.1 Connection Design and Materials	66
	11.2 Test Results	67
	11.3 Assessment of Performance	71
12.	Review of Overall Test Program and Connection Performance: Conclusions and Recommendations	73
	12.1 Connection Testing Program	73
	12.2 Measurements of Plastic Rotation	74
	12.3 Performance of As-Built Connections	74
	12.4 Performance of Revised Connections	75
	12.5 Influence of Straightening Protocol	75
13.	References	76
14.	Figures	78
	Fig. 1 As-Built Connection	79
	Fig. 2 Location of k-region in W-shape	80
	Fig. 3 Revised As-Built Connection Type 1	81
	Fig. 4 Revised As-Built Connection Type 2	82
	Fig. 5 Revised As-Built Connection Type 3	83
	Fig. 6 Configuration of Test Frame and Installed Specimen	84
	Fig. 7 Photograph of Installed Specimen	85
	Fig. 8 Photograph of Column Pinned Base	86
	Fig. 9 Photograph of Actuator and Beam End	87
	Fig. 10 Beam Tip Cyclic Displacement Profile	88
	Fig. 11 Finite Element Model of Test Specimen	89
	Fig. 12 Nomenclature for Beam Tip Displacement Calculations	90
	Fig. 13 Material Property Specimen Locations in Column	91
	Fig. 14 Photographs of Samples for Hardness Testing	92

Fig. 15	Toughness vs. Temperature for k-Region of Straightened and Unstraightened Column Shapes	93
Fig. 16	Toughness vs. Temperature for Core and k-Region	94
Fig. 17	Toughness vs. Temperature for Core and k-Region of Rotary Straightened Column	95
Fig. 18	Toughness vs. Temperature for Core and k-Region of Gag Straightened Column	96
Fig. 19	Load-Displacement and Moment-Plastic Rotation Hysteresis Curves for Test A1	97
Fig. 20	Load-Displacement and Moment-Plastic Rotation Hysteresis Curves for Test A2	98
Fig. 21	Load-Displacement and Moment-Plastic Rotation Hysteresis Curves for Test A3	99
Fig. 22	Photographs of Cracks in Specimen A1	100
Fig. 23	Photographs of Fractured Specimen A2	101
Fig. 24	Photographs of Crack Adjacent to Weld in Specimen A3	102
Fig. 25	Photograph of Fracture Surface for Specimen A3	103
Fig. 26	Beam Tip Displacement vs. Time for Specimen A4	104
Fig. 27	Beam Tip Load vs. Time for Specimen A4	105
Fig. 28	Beam Tip Load vs. Displacement Hysteresis Curves for Specimen A4	106
Fig. 29	Moment vs. Plastic Rotation Hysteresis Curves for Specimen A4	107
Fig. 30	Moment vs. Plastic Rotation Hysteresis Curves for Specimen A5	108
Fig. 31	Photographs of Top and Bottom Fracture Locations for Specimen A4	109
Fig. 32	Photographs of Bottom Location for Specimen A5, Showing Crack at Toe of Cover Plate to Column Weld	110
Fig. 33	Photographs of Fracture Origin with Shear Lip at Cover Plate to Column Weld for Specimen A4	111
Fig. 34	Schematic Illustration of Crack Locations, Depths and Lengths for Specimens A4 and A5	112
Fig. 35	Photographs of Bottom Location Fracture at Fusion Line and Ductile Shear Failure of Web of Specimen A4	113
Fig. 36	Moment vs. Plastic Rotation Hysteresis Curves for Specimen A6	114
Fig. 37	Moment vs. Plastic Rotation Hysteresis Curves for Specimen A7	115

Fig. 38	Top Location of Specimen A6, Showing (a) Crack in k-Region and (b) Separation of Continuity Plate	116
Fig. 39	Fracture Origin at Top Cover Plate to Column Weld for Specimen A6. Short Arrows Indicate Origin, Long Arrows Show Crack Propagation Direction	117
Fig. 40	Load-Displacement and Moment-Plastic Rotation Hysteresis Curves for Test A8	118
Fig. 41	Load-Displacement and Moment-Plastic Rotation Hysteresis Curves for Test R1-1	119
Fig. 42	Load-Displacement and Moment-Plastic Rotation Hysteresis Curves for Test R1-2	120
Fig. 43	Load-Displacement and Moment-Plastic Rotation Hysteresis Curves for Test R1-3	121
Fig. 44	Photographs of Crack Adjacent to Weld in Specimen R1-3	122
Fig. 45	Load-Displacement and Moment-Plastic Rotation Hysteresis Curves for Test R1-6	123
Fig. 46	Moment vs. Plastic Rotation Hysteresis Curves for Specimen R1-4	124
Fig. 47	Moment vs. Plastic Rotation Hysteresis Curves for Specimen R1-5	125
Fig. 48	Bottom Location for Specimen R1-4 Showing (a) Crack Extension in k-Region and (b) Failure of Continuity Plate Weld	126
Fig. 49	Bottom (a) and Top (b) Locations of Cover Plate to Column Weld for Specimen R1-5. Arrows Indicate Crack between Cover Plate and Flange	127
Fig. 50	Schematic Illustration of Crack Locations, Depths and Lengths for Specimens R1-4 and R1-5	128
Fig. 51	Moment vs. Plastic Rotation Hysteresis Curves for Specimen R2	129
Fig. 52	Schematic Illustration of Crack Locations, Depths and Lengths for Specimens R2, A6 and A7	130
Fig. 53	Moment vs. Plastic Rotation Hysteresis Curves for Specimen R3-1	131
Fig. 54	Moment vs. Plastic Rotation Hysteresis Curves for Specimen R3-2	132
Fig. 55	Photographs of Cover Plate to Column Weld at Bottom (a) and Top (b), for Specimen R3-1, with no Fracture at the Weld Toe	133

Fig. 56	Column Flange near Bottom Cover Plate for Specimen R3-1, with Small Crack Extending into Column	134
Fig. 57	Photographs of Sectioned Top Cover Plate Location for Specimen R3-1, with Arrow A Showing Crack between Cover Plate and Beam Flange, and Arrow B Showing Crack in Continuity Plate Fillet Weld	135
Fig. 58	Photographs of Exposed Crack for Specimen R3-1. Arrows Show Crack Origin Along Weld Root. Dashed Line Separates Flange (A) from Weld (B).	136
Fig. 59	Top Cover Plate to Column Weld for Specimen R3-2. Arrows Show Fractured Cover Plate and Flange	137
Fig. 60	Fracture Path Along k-Region for Specimen R3-2. Arrow A Shows Location of k-Region Crack.	138
Fig. 61	Photographs of Specimen R3-2, with Arrows Showing Cracks at (a) Column Flange at Bottom Cover Plate and (b) Bottom Continuity Plate	139
Fig. 62	Fractured k-Region for Specimen R3-2. Arrow A Shows Origin at Edge of Continuity Plate Weld. Small Arrows Show Crack Arrest Marks.	140
Fig. 63	Fractured k-Region for Specimen R3-2. Small Arrows Show Six of the Seven Crack Arrest Marks. Arrow A Shows Origin Location Near the Continuity Plate Fillet Weld	141
Fig. 64	Fracture Surfaces at the Top Cover Plate for Specimen R3-2. Arrows Indicate Fracture Origin at Weld Root between Cover Plate and Beam Flange. Arrow A Indicates Crack Arrest Mark in Flange.	142
Fig. 65	Fractures of Specimen R3-2: (a) Shows Origin at Weld Root between Cover Plate and Flange; (b) Shows Fracture Transition near k-Region. Arrows Indicate Crack Propagation Direction. Arrow A Indicates Shear Lip on Flange.	143
Fig. 66	Schematic Illustration of Crack Locations, Depths and Lengths for Specimens R3-1 and R3-2	144

00481

EXECUTIVE SUMMARY

The 1994 Northridge earthquake appeared to demonstrate that steel-framed structures and particularly certain of the beam-to-column connections were unable to perform adequately under seismic conditions. It is now clear that some of the damage that was discovered had occurred prior to the earthquake, and that similar incidences of failures had taken place in structures where no seismic activity had been present. However, several major research efforts were undertaken to determine the causes of the failures, and to pinpoint issues related to material performance, design, detailing and fabrication. Old and new connection types have been investigated, with the aim of ensuring satisfactory service of steel structures under future earthquakes.

The research program that is detailed in this report was undertaken as the result of certain connection fractures that were discovered during the fabrication of the connections for a major California structure. Standard details and fabrication practices had been utilized for the structure, yet cracking took place in certain areas of the connections. An intensive evaluation of the particular structure was conducted, and it was subsequently determined that the major reason for the cracking was the presence of hydrogen during the welding of the elements. The repair procedures that were put in place yielded fully satisfactory assemblies. Nevertheless, it was decided that a cohesive and detailed study was needed to remove any and all uncertainties regarding the steel material and the connections that had been used.

The Executive Summary Table gives an oversight of the research program and the key parameters that were investigated. A total of 17 full-scale beam-to-column connections were fabricated and tested. All used W14x176 columns and W21x122 beams in ASTM A572 Grade 50 steel.

Executive Summary Table

Key Features of Connection Testing Program

No. Tests	Conn. Type	Connection Description ¹	Straight. Protocol ²	Loading Protocol ³	FEMA Criterion ⁴ Met?
8	As-Built (AB)	CJP welds beam to col. and contin. plates to col; 1-5/8" cover pl.; A325 HS bolts for beam web	5 R 2 G 1 U	4 Q 4 D	4 R: yes 1 R: no 2 G: yes 1 U: yes
6	Revised Type 1 (RAB 1)	As AB, but 1" cover pl. and fillet welds for continuity plates	5 R 1 U	4 Q 2 D	3 R: yes 2 R: no 1 U: no
1	Revised Type 2 (RAB 2)	As AB, plus 1/2" fillet weld transition from beam to column	1 R	1 D	1 R: yes
2	Revised Type 3 (RAB 3)	As RAB 1, plus 1/2" fillet weld transition and repositioned continuity plates	2 R	2 D	2 R: yes

Notes for Executive Summary Table:

- Note 1 CJP = complete joint penetration
- Note 2 Straightening protocols are designated as R = rotary straightened; G = gag straightened; U = unstraightened
- Note 3 Loading protocols are designated as Q = slow cyclic (quasi-static) testing; D = dynamic (1 Hz frequency) testing
- Note 4 FEMA acceptance criteria are:
 For as-built or rehabilitated construction: minimum 1 complete cycle at 0.025 radians plastic rotation
 For new construction: minimum 1 complete cycle at 0.030 radians plastic rotation

The first four connections were identical to the connections that had been used in the California structure where the original cracking had been detected. These used cover-plated, complete joint penetration (CJP) welds to attach the beam to the column, and CJP welds were used for the continuity plates that were placed in the web area of the column. The beam web connection used A325 high strength bolts. The testing was performed in accordance with the recommendations of the Applied Technology Council (ATC), using a slow cyclic (quasi-static) loading protocol to simulate the earthquake loading on the structure. The connections were heavily instrumented with LVDT-s and strain gages, to monitor the response of the material and the various connection elements during the tests. Further, it was decided to examine the potential influence of the column straightening protocol that had been used by the steel producer to achieve members that would meet the straightness criteria of the ASTM materials delivery standard. Thus, three of the four connections had rotary straightened columns; the fourth used an unstraightened member.

The next four specimens utilized a revised (Type 1) connection, with thinner cover plates and fillet welds for the continuity plates. The use of fillet welds, in particular, was a major departure from at-the-time practice. Three of the specimens used rotary straightened columns; the fourth had an unstraightened member.

Following the tests of the first eight beam-to-column connections, it was decided to expand the research program to examine the response characteristics of assemblies using gag straightened columns. It was also decided to make use of a dynamic loading protocol, with the aim of achieving even better correlation with the effect of the seismic loads on the connections. The levels of loading and displacement were the same as for the quasi-statically loaded connections, but the loads were cycled

with a 1 Hz (one cycle per second) frequency. It was felt that this would be a more severe test for the assemblies.

The second group of beam-to-column connections included a total of nine specimens. Four of these were identical to the initial connection types, assuring direct correlation between specimens tested under the two types of loading protocol. Two of the four had rotary straightened columns, and two had gag straightened columns, permitting an evaluation of the effects of rotary versus gag straightening.

Included in the second group of test specimens were also two that were identical to the revised Type 1 connection. The columns for these assemblies were rotary straightened, and the loading protocol was dynamic. This would provide for a direct correlation with the identical connections tested quasi-statically.

A separate, revised (Type 2) connection was identical to the original specimens, with the only change being a 1/2 inch transition fillet weld between the cover plate and the column flange. It was felt that this might provide a better force and deformation transfer path for the connection in an area where cracks had been proven to initiate the eventual overall failures. The column was rotary straightened, and the testing was dynamic.

The final two specimens were revised (Type 3) from the other designs. It was identical to the Type 1 revised connections, but also used the 1/2 inch transition fillet weld that was utilized for Type 2. In addition, the continuity plates were repositioned, to allow for an improved load and fracture path for the connection. The columns were rotary straightened, and the loading protocol was dynamic.

00485

Extensive testing was performed for the column materials in the connection specimens, since the cracking and eventual connection failure would occur within these members. The steel grade was ASTM A572 (50), and the tensile property and chemical analysis tests showed that the steel in all of the specimens was in accord with the ASTM standard. The tension test specimens were taken from the ASTM-required locations within the flanges; in addition, tests were also performed for the web and k-region material. As expected, the tensile properties of the web and flange steel met and reasonably exceeded the ASTM minimum requirements. The k-region of the rotary straightened columns had higher yield and tensile strengths and lower ductility. The gag straightened and unstraightened members showed nearly uniform strength and ductility properties at all locations. These results were all as expected.

Charpy V-Notch (CVN) specimens for fracture toughness testing were taken from the ASTM-required flange locations, in addition to areas in the web, core and k-region of the columns. As expected, the flange and web materials in the rotary straightened columns exhibited excellent toughness; the core and especially the k-region steel was much less tough. Gag straightened and unstraightened columns did not display the k-region decreases in toughness.

Rockwell B hardness tests were conducted for the steel in flange-to-web T-intersection, mapping the hardness variability within this area of the column shapes. As expected, the k-region of rotary straightened shapes exhibited higher hardness in the areas where the CVN toughness was low. The data also delineated the location of the high hardness area, commonly referred to as the k-region or k-area; these results were very much the same for all of the rotary straightened columns.

The full-scale connection tests showed that the original (as-built) connections were

00485

able to perform adequately and in agreement with the Federal Emergency Management Agency's (FEMA) requirements. Most of the revised connections were also able to meet the FEMA performance requirements for new construction; these criteria are more demanding in plastic rotation capacity than those used for as-built construction. However, the performance of the revised Type 2 and Type 3 connections was far superior in all respects.

The Type 3 connections in particular performed extremely well and significantly exceeded the FEMA requirements. They exhibited very large plastic rotation capacities and late onset of cracking and eventual failure. For these connections it was also found that although cracks developed and propagated through portions of the column material, the propagation was slow and stable, with numerous crack arrest events during the tests. This also occurred for the cracks that propagated into the k-area of the columns, demonstrating that a crack in this region will propagate in stable fashion, given appropriate connection details and fracture paths.

The connection test results demonstrated that there are no significant performance differences between assemblies using rotary straightened, gag straightened and unstraightened columns. The type of loading protocol was also found to be unimportant, although it appeared that the demands imposed by the dynamic loading were more severe than those of the quasi-static loading.

1. INTRODUCTION

Steel has been the primary construction material for a very large number of buildings, bridges and other structures for more than 100 years. Its elastic and inelastic responses to loads and load effects make it a material with predictable and reliable behavior under a wide range of service conditions. The ease and speed of fabrication and erection yield significant economies of construction.

As with other types of construction, the most complex elements of steel structures are the connections that are used to attach the individual framing members to each other. For buildings this is particularly true for the connections between beams and columns, where structural details and fabrication processes combine to produce true three-dimensional conditions.

To facilitate construction and allow for economies in usage, certain connection types over the years became very common, almost to the point of being standardized assemblies. They proved their adequacy through service in many buildings, designers were confident about design methods and details, and fabricators produced high-quality structures. Some of the connections were even specifically recognized by building codes as preferred solutions. In particular, beam-to-column connections utilizing welded joints between the beam and column flanges and bolted beam web connections were used extensively. Tests and analyses had shown that these connections were capable of producing appropriate moment and shear capacities, and their deformation characteristics were excellent.

Use of steel structures in areas of high seismicity were considered especially advantageous, due to the inherent inelastic deformation capacity or ductility of the

material. Time-honored design and fabrication practices proved their worth through a number of minor and major earthquakes. However, at the same time the understanding of seismic effects and structural behavior advanced significantly, and tools such as computers facilitated increasingly fine-tuned designs. Prompted by owners and architects, structural systems also changed, to allow for differing working and living space arrangements. As a result, structures in some ways became simpler, with fewer primary load-carrying elements, but at the cost of reduced redundancy. The effects of events such as earthquakes would therefore have to be accommodated by fewer structural members and especially connections.

The 1994 Northridge earthquake had a significant effect on state-of-the-art thinking about ductile structural response. A number of steel-framed structures were found to have cracks in their beam-to-column connections, and it was surmised that the earthquake had caused these failures. Although it is now clear that some or maybe many of the cracks had occurred before the earthquake, and that such cracking had taken place in structures elsewhere, where no seismicity had been present¹, it was also evident that material and structural behavior and design and fabrication approaches needed careful re-examination. Major research and development efforts ensued, some of which are coming to a conclusion as this time.

As a specific example of the non-earthquake-related cracking incidences, the fabricator for a California project experienced cracking in the column of beam-to-column assemblies during the shop fabrication. It is now clear that the cracking occurred as primarily as a result of improper welding procedures, especially by allowing for the

¹ The fractures that occurred in the structure for the hospital at Elmendorf Air Force Base in Alaska is a typical example (Engineering News-Record, May 27, 1996).

presence of hydrogen as a result of insufficient drying of welding electrodes. The connections were of the welded flange, bolted web variety, but also utilized welded cover plates as well as continuity plates (stiffeners) for the column. Details are shown in Fig. 1; this will be referred to throughout this report as the **As-Built Connection**. Although the beam and column sizes shown in the figure are not identical to those used in the project in question, they are representative examples of what was used.

The cracks in the connection shown in Fig. 1 were found in the web of the column, in the region of the cross section now commonly known as the "k-area" or "k-region". This is a small area of the wide-flange shape surrounding the location where the transition fillet from the flange enters the web. The k-dimension measures the distance from the outside of the flange to the end of the transition fillet. Figure 2 illustrates these terms.

Originally the earthquake-related and fabrication-related cracks were thought to have taken place in part as a result of inadequate material properties. Much discussion took place about yield stresses significantly higher than the specified minimum values, and some investigators tended to state that current steel mill practices therefore were faulty. Additional problems evolved as subsequent examinations found that the k-region of W-shapes was prone to exhibit high strength and hardness, but lower ductility and fracture toughness. These properties were related to the fact that many sizes of wide-flange shapes are rotary straightened in the mill in order to meet product straightness requirements. This is typical and world-wide practice, but nevertheless a phenomenon that merited study. These events form the background for the research program that is presented in this report.

2. SCOPE AND AIMS OF TESTING PROGRAM

2.1 General Program Criteria

In view of the importance of the subject matter, to society as well as the steel industry, Nucor-Yamato Steel Company of Blytheville, Arkansas, agreed to sponsor the connections research project that is detailed in this report. It was decided to focus the research program on full-scale testing of actual beam-to-column connections and variations thereof, utilizing realistic member sizes and details, accepted design approaches, and normal fabrication practices. This would ensure that the test results could be assessed in comparison with other connection experiments, but also that materials and members would be exposed to the type of in-service load and deformation demands that are associated with realistic structures.

2.2 Specimen Design and Fabrication

Specimen design and fabrication were performed in accordance with the requirements of the Uniform Building Code (UBC), which in turn is based on the criteria of the structural steel design Specification and the Code of Standard Practice of the American Institute of Steel Construction (AISC) (1). The UBC is also based on the Recommended Lateral Force Requirements of the Structural Engineers Association of California (SEAOC) (2). The materials and delivery standards of the American Society for Testing and Materials (ASTM) (3) were applied, as were the Structural Welding Code of the American Welding Society (AWS) (4).

To achieve optimal performance of structures and their elements, current seismic design principles utilize the "strong column, weak beam" concept, where plastic hinges will form in the beams at the ultimate limit state. This provides for improved structural redundancy and ductile failure modes for a structure as a whole. In the

planning of the research program it was decided to impose the most demanding conditions possible on the column and its material, primarily since the cracking that had taken place in the California structure had occurred in the columns. It was felt that this would represent a worst case scenario. The test specimens that were chosen for this research program therefore reflect assemblies with strong beams and weak columns, where plastic hinges will form in the panel zone of the column.

The expected flexural strength of the beam and the shear strength of the column panel zone were determined in accordance with the criteria of the AISC Seismic Provisions for Structural Steel Buildings (5). The requirements were satisfied.

2.3 Loading Protocols

A number of beam-to-column connection tests have been conducted in past research projects. Many of these tests were conducted with slowly increasing or effectively static loads. Recognizing the importance of dynamic and especially seismic response characteristics, in particular after the 1989 Loma Prieta and the 1994 Northridge earthquakes, the Applied Technology Council (ATC) developed testing criteria that were based on cyclic loads (6). These are often referred to as quasi-static testing conditions, since it was not attempted to model earthquake loading input. Rather, using a displacement control approach, the cyclic load was applied in alternate directions, using increasing amplitudes of the load application point. This is the load application method that was utilized for the first eight of the tests of the connection research program described in this report.

However, more recent studies by seismologists and structural engineers emphasized the need to have the test loading simulate seismic conditions as closely as possible. This led to the development of criteria that focused on loads applied at certain loading

or strain rates, to mimic the earthquake response of the structure. Although opinions still differ as to whether true dynamic loads impose more demanding and realistic conditions than quasi-static loads, the former in all likelihood reflect a worst case scenario. On this background it was decided to run the additional nine tests of the connection program at true dynamic loads, using a frequency of 1 Hz. Details of the equipment and the loading procedure are given in Chapter 4.

2.4 Straightening Protocols for Connection Assembly Members

It was noted in Chapter 1 that one of the issues that led to the decision to perform this program of connection tests was the performance of the steel itself in the web of the column. Specifically, cracks had developed in the k-region of some columns during welding. It was also noted that the k-region is deformed significantly because of the rotary (continuous) straightening that is used in steel mills to meet the straightness requirements of material delivery standards (3). As a result, the k-region steel of rotary straightened shapes tend to have higher strength and hardness than other areas of the cross section, but also lower ductility and toughness. Since this form of straightening is applied continuously, the localized areas of changed material characteristics appear along the complete element.

Another factor in the rotary straightening process is the initial out-of-straightness of the shape as it comes from the cooling bed in the steel mill. It is possible to have shapes that are very straight after the rolling; these require less straightening effort to meet the delivery criteria. On the other hand, some shape lengths may turn out to be fairly out-of-straight; these require higher straightening loads. Current mill practice dictates that all shapes are straightened to meet the ASTM requirements.

Heavy shapes are straightened by the application of concentrated loads at discrete

00493

points; this process is termed gag straightening. The gag load application differs from the rotary process to the effect that the load is not applied in the same way. Gag straightening therefore does not introduce areas of high strength and hardness in the manner of rotary straightening.

As will be described later in this report, the columns in some of the test specimens were rotary straightened; others were gag straightened. To investigate the effect of straightening *per se*, two of the specimens were also fabricated with unstraightened columns. This was done for demonstration purposes only, and to establish the other extreme condition for straightening. Unstraightened shapes are not commercially available products.

2.5 Connection Details

The as-built connection (see Fig. 1) utilized complete joint penetration (CJP) welds between the beam and column flanges, as well as a shear plate welded to the column flange with fillet welds. The beam web was bolted to the shear plate with 10 - 1-1/8 inch diameter A325 high strength bolts. In addition, this connection had 1-5/8 inch thick cover plates at the top and bottom of the beam; these were CJP-welded to the column flange and welded to the beam flange with 1 inch fillet welds. Finally, the as-built connection used 1-1/8 inch thick fitted column web continuity plates, CJP welded to the column flanges and web as shown in Fig. 1. The corners of the continuity plates were cropped (see Fig. 1) by one inch, to allow suitable placement with respect to the column flanges and the web, and to avoid welding in the flange to web transition fillet. They were placed with their centerline aligned with the interface between the beam flange and the cover plate. A total of eight such tests were planned.

Additional criteria were to be utilized for these tests, specifically such that some would have rotary straightened columns, some columns would have gag straightened and one used an unstraightened column. Further, some of the rotary straightened specimens were tested quasi-statically, others dynamically. All of these considerations were intended to allow for performance evaluations of the individual tests, as well as to assess the influence of the additional criteria. Overall testing program details are given in the next chapter.

Since the as-built connection had experienced difficulties during the shop fabrication, it was decided to examine modifications of the original design, with the aim of developing connections with improved fabrication conditions and performance under load. Referred to as **Revised As-Built Connection 1 (RAB 1)**, the first modified connection used thinner cover plates, and fillet welds were specified in lieu of the complete joint penetration welds for the continuity plates. This would result in lower welding residual stresses as well as fabrication economies, through the use of fillet welded continuity plates. Incorporating straightening and load application effects, six RAB 1 tests were planned.

Revised As-Built Connection 2 (RAB 2) was devised as an examination of the potential benefits of a better, more gradual transition of the area between the beam flange plate and the column. A fillet weld was deposited at the top and bottom cover plate to column joints. One such specimen was included in the testing program.

The **Revised As-Built Connection 3 (RAB 3)** aimed at assessing the performance of a connection with repositioned continuity plates. RAB 3 was purposely made identical to RAB 1, with the addition of the transition fillet weld between the cover plate and the column. The continuity plates were moved inward, in order to have their outside

00495

edges aligned with the beam flange to cover plate interface. Two such tests were included in the testing program, including straightening and dynamic loading effects.

2.6 Replication of Test Performance

Beam-to-column connection tests are particularly difficult to perform because of the many variables that influence the performance. It was decided to run several identical specimens of some of the connection assemblies, in an effort to satisfy replication needs as well as to confirm or deny the results obtained for any individual specimen.

2.7 Data Collection

In addition to the development of stress and strain data for each connection as a whole and displacement characteristics for the assemblies, it was determined that special attention had to be paid to connection rotation capacities. This was in part prompted by the criteria developed by ATC (6), but also due to the need for comparison and correlation with the results from connection tests conducted elsewhere. Of particular interest were the plastic rotation capacity as well as the cumulative plastic rotation capacity.

The plastic rotation capacity has been identified by the Federal Emergency Management Agency (FEMA) and its SAC project as a major measure of connection suitability for new and rehabilitated construction (7). Specific guidelines for testing and connection response needs have been developed. It was agreed that satisfactory performance of any connection would have been achieved upon reaching or exceeding the minimum requirements of the FEMA guidelines.

Since earthquake performance of a structure is often measured by its energy absorption capacity, it was also decided to determine the cumulative plastic rotation

00496

capacity for each of the connections. This is especially useful for elements tested under dynamic cyclic conditions. Japanese researchers have been computing CPRC values for connections tested after the 1995 Kobe earthquake; the approach is described in works by Nakashima et al. (8).

Additional details for the materials test results and connection performance data for the complete series of 17 tests presented in this report are provided in the reports by Strybos et al. (9) and Goland et al. (10, 11).

3. SELECTION AND DESIGN OF CONNECTION SPECIMENS

3.1 General Description of Specimens

Figure 1 shows the details of the As-Built Connection (AB) that formed the starting point for the study. Some of the elements of AB were used for all of the connection specimens in the program, as follows:

Beam size:	W21x122
Column size:	W14x176
Continuity plates:	1-1/8 inch thickness
Beam web shear plate:	5/8 inch thickness
Shear plate welds:	5/16 inch fillet welds
Beam web connection:	10 - 1-1/8 inch diameter A325 bolts

The shape (geometry in plan) of the top and bottom beam flange cover plates were the same; they were also the same for all connections in the research program. In practice the bottom cover plate is normally rectangular, to facilitate erection and field welding; it was decided to use the pointed plate geometry for both plates to promote connection simplicity. Further, the shop fabrication of

the test specimens allowed the assembly to be turned upside down to allow downhand welding of the cover plate to column flange CJP-s. The differences in the geometry of one cover plate would not influence the response of the connections. Finally, all connections used complete joint penetration welds for the beam to column flange weld and the cover plate to column flange weld.

The unique characteristics of the AB connection are:

Cover plate thickness:	1-5/8 inch
Cover plate to beam weld:	1 inch fillet
Continuity plate placement:	Mid-thickness of plate in line with beam flange and flange plate interface
Continuity plate welds:	Complete joint penetration
Column straightening protocol:	Rotary straightening for five specimens, gag straightening for two specimens, no straightening for one specimen
Loading protocol:	Four specimens were tested under quasi-static conditions, four under dynamic conditions
Total number of AB tests:	8

The Revised As-Built Connection 1 (RAB 1) is shown in Fig. 3. The unique characteristics of RAB 1 are:

Cover plate thickness:	1 inch
Cover plate to beam weld:	3/4 inch fillet
Continuity plate placement:	Mid-thickness of plate in line with beam flange and cover plate interface

Continuity plate welds: 9/16 inch fillet
 Column straightening protocol: Rotary straightening for five specimens, no straightening for one specimen
 Loading protocol: Four specimens were tested under quasi-static conditions, two under dynamic conditions
 Total number of RAB 1 tests: 6

The Revised As-Built Connection 2 (RAB 2) is shown in Fig. 4. It is identical to AB in all respects but one: a 1/2 inch fillet weld was added as a transition weld between the cover plates and the column flange. The characteristics of RAB 2 are:

Cover plate thickness: 1-5/8 inch
 Cover plate to beam weld: 1 inch fillet
 Cover plate to column flange transition weld: 1/2 inch fillet weld
 Continuity plate placement: Mid-thickness of plate in line with beam flange and flange plate interface
 Continuity plate welds: Complete joint penetration
 Column straightening protocol: Rotary straightening
 Loading protocol: Dynamic loading
 Total number of RAB 2 tests: 1

The Revised As-Built Connection 3 (RAB 3) is shown in Fig. 5. It is identical to RAB 1 with the exception of the location of the continuity plates and the cover plate transition weld. The characteristics of RAB 3 are as follows:

Cover plate thickness: 1 inch

Cover plate to beam weld:	3/4 inch fillet
Cover plate to column flange transition weld:	1/2 inch fillet weld
Continuity plate placement:	Outside edge of plate in line with beam flange and cover plate interface
Continuity plate welds:	9/16 inch fillet
Column straightening protocol:	Rotary straightening
Loading protocol:	Dynamic loading
Total number of RAB 3 tests:	2

As outlined, the testing program incorporated a total of 17 full-scale beam-to-column connection tests. The data are summarized in Table 1. Additional details are given in the three Southwest Research Institute reports (9, 10, 11), but it is noted that the test numbering system for these reports differs from the one used here.

3.2 Overall Testing Rationale

As shown in Table 1, the number of specimens and details, straightening conditions and loading protocols make it possible to evaluate a variety of influences, as follows.

- (i) Influence of loading protocol: Five identical AB (test nos. A1-A5) and another five identical RAB 1 specimens (test nos. R1-1 through R1-5) were tested with two different loading protocols. For each of these sets of five tests, quasi-static loading was used for three tests, and the other two used dynamic loading. This should determine the influence of the loading protocol, if any.
- (ii) Influence of straightening protocol: Four identical AB (test nos. A4-A7) specimens were tested, where two (A4-A5) had rotary straightened columns

Table 1

Data for Beam-to-Column Connection Testing Program

Test No.	New Test No.	Joint ¹	Modifications from original connection	Straight. Protocol ²	Loading Protocol ³
1	A1	AB	----	R	Q
2	A2	AB	----	R	Q
3	A3	AB	----	R	Q
9	A4	AB	----	R	D
10	A5	AB	----	R	D
15	A6	AB	----	G	D
16	A7	AB	----	G	D
7	A8	AB	----	U	Q
4	R1-1	RAB 1	1" cover plate with 3/4" fillet weld; CP fillet welded to col web and flanges	R	Q
5	R1-2	RAB 1	Same as for R1-1	R	Q
6	R1-3	RAB 1	Same as for R1-1	R	Q
11	R1-4	RAB 1	Same as for R1-1	R	D
12	R1-5	RAB 1	Same as for R1-1	R	D
8	R1-6	RAB 1	Same as for R1-1	U	Q
13	R2	RAB 2	Same as AB, plus 1/2" fillet weld transition from cover plate to flange	R	D
14	R3-1	RAB 3	Same as RAB 1, plus 1/2" fillet weld transition and repositioned continuity plates	R	D
17	R3-2	RAB 3	Same as for R3-2	R	D

10500

Footnotes for Table 1:

- Note 1: AB = As-Built Connection; RAB 1 = Revised As-Built Connection Type 1; RAB 2 = Revised As-Built Connection Type 2; RAB 3 = Revised As-Built Connection Type 3
- Note 2: R = rotary straightened; G = gag straightened; U = unstraightened
- Note 3: Q = quasi-static cyclic loading; D = dynamic (1 Hz) cyclic loading

and the other two (A6-A7) had gag straightened columns. The loading protocol was the same for all four (dynamic). It should be possible to assess the influence of the straightening protocol, if any, examining these results.

Further, one AB specimen (A8) had an unstraightened column; this was tested under quasi-static loading. The results for this test can be compared to those of tests A1-A3, which were otherwise identical, allowing for an assessment of the effects of rotary straightening versus no straightening.

Similarly, one RAB 1 specimen (R1-6) had an unstraightened column; the results can be evaluated against those of the otherwise identical tests R1-1 through R1-3 to assess the effects of rotary straightening versus no straightening.

- (iii) Influence of cover plate transition weld: One revised AB specimen, RAB 2 (test no. R2) had the 1/2 inch cover plate to column flange fillet weld transition as the only change from the AB specimens. R2 was tested under dynamic loading, and the column was rotary straightened. The effects of the transition weld, if any, can be assessed by comparing the results for R2 with those of A4 and A5.
- (iv) Influence of continuity plate position: Two revised AB specimens, RAB 3 (test

nos. R3-1 and R3-2) had the 1/2 inch cover plate transition weld as well as repositioned continuity plates. The column was rotary straightened and the loading was dynamic. The effect of the repositioned continuity plates can be determined by comparison with test R2, which was otherwise identical.

The results of the two RAB 3 tests can also be compared to those of RAB 1, numbers R1-4 and R1-5. Other than the cover plate transition weld, specimens R1-4/R1-5 and R3-1/R3-2 only differ in the position of the continuity plates.

The preceding discussion presents that rationale for the evaluation and comparison of the test results. The careful design of the specimens and the multiple samples of several of the tests allow for the assessment of key performance criteria, as well as the replication of individual, complex tests. It is believed that this program of testing represents a unique opportunity to determine the effects of straightening and loading protocols, as well as the design of connection details for improved seismic performance. Further, based on failure modes and rotation capacities, it is envisioned that questions about steel material performance and joint ductility and energy absorption capacities can be addressed conclusively.

3.3 Materials for the Test Specimens

The most common structural steel today is A572, Grade 50, a 50 ksi yield stress material. In the planning of the research program, this was the grade of steel that was chosen; it was also the steel used for the California structure where fabrication problems had arisen. For the last several years ASTM A572 (50) has been supplied in enhanced form, with tighter control on chemistry and mechanical properties; this is now described by ASTM Specification A992.

00503

The column and beam elements for the test specimens were supplied by the sponsor, Nucor-Yamato Steel. Since NYS does not produce steel in plate form, the materials for cover plates, beam web shear plates and column continuity plates were obtained from a San Antonio, Texas, steel service center. The plate steel met the requirements of ASTM A572 Grade 50.

A full program of materials testing was planned for the specimens of the connection testing program. Detailed data are given in Chapter 5.

3.4 Fabrication of Test Specimens

The test specimens were fabricated in San Antonio. Quality assurance plans were developed by the fabricator in close cooperation with Nucor-Yamato Steel (NYS), and the fabrication was overseen by fabricator personnel and a representative of NYS.

As a result of the original cracking problem in the California structure, for which it was eventually determined that hydrogen presence had been the root cause, strict QA/QC procedures were put in place for the fabrication of the test specimens. The Welding Procedure Specification (WPS) that had been developed by the fabricator for the California structure was adopted with minor modifications (5/64 inch welding wire in lieu of 7/64 wire), using criteria detailed by the AWS Structural Welding Code (4) and the Code of Standard Practice of the AISC (1).

Preheat requirements were developed in accordance with Appendix XI of the AWS Structural Welding Code, rather than using the minimum temperatures of Table 4.3 of AWS D1.1 (4). This was done specifically to eliminate fabrication issues as a parameter for the connection testing program. Assuming no hydrogen control and high joint restraint, AWS Appendix XI indicated a preheat and interpass temperature

00504

of 240°F for the thicknesses involved. During the fabrication 250°F was used, as an additional measure of conservatism. Torches were used for the heating, and heat indication crayons ensured that the correct preheat temperature had been reached before welding.

Self-shielded E70TG-K2 electrodes (Lincoln 311-Ni) with a specified minimum CVN toughness of 20 ft-lbs at - 20°F were used for the beam flange and cover plate complete joint penetration (CJP) welds, along with ceramic backing bars and runoff tabs. The runoff tabs were removed after the welding. The welds were deposited in the horizontal (downhand) position, and the specimen assembly then was turned over for the welding of the bottom cover plate. Following the CJP welding for the flanges and the cover plates, the fillet welds for the cover plate and the beam web shear tab were placed, using gas-shielded E70T-1 electrodes.

The continuity plate welds were made with gas shielded E70T-1 electrodes (Hobart RXR); these had a specified minimum CVN toughness of 20 ft-lbs at - 20°F. CJP-s were used for the as-built specimens (tests no. A1-A8) and the revised as-built specimen 2 (test no. R2), for a total of nine; fillet welds were used for the revised as-built specimens 1 and 3 (tests no. R1-1 through R1-6 and R3-1 and R3-2). All intermediate passes were made in the downhand position, and were chipped, ground and wire brushed as needed.

After the welds had cooled to ambient temperature, all were examined visually. The CJP-s were tested ultrasonically, in accordance with AWS D1.1; the findings showed that the welds met the AWS acceptance criteria. The inspection also showed that no cracking had occurred anywhere, including in the k-region of any of the columns in the test assemblies.

4. TESTING PROTOCOLS, COMPUTATIONS AND EQUIPMENT

4.1 General Description

To perform the beam-to-column connection tests, a suitable test frame was available at Southwest Research Institute (SwRI) in San Antonio, Texas. Other equipment was acquired by Nucor-Yamato Steel to have the tests performed as specified by the criteria of the Applied Technology Council (ATC) (6). In particular, the necessary load and displacement levels and testing protocols required hydraulic capacity significantly beyond what was available at SwRI at the time.

The first eight tests were planned for quasi-static loading conditions, i.e. slow cyclic loads to increasing displacement levels, in accordance with the recommendations of ATC (6). Subsequent evaluations by ATC and researchers in the United States and Japan indicated that fully dynamic loading conditions would afford closer similarity with actual seismic activity, especially in terms of strain rates. It was therefore decided to run the second group of nine tests with dynamic load input at a frequency of 1 Hz. The equipment that was installed would allow for such testing conditions. It is believed that the dynamic tests that were performed as part of this research program represent the only series of full-scale connection specimens that have been tested under such conditions in the United States.

Opinions continue to differ as to the necessity of dynamic testing. However, as described in Chapter 3 of this report, the research program was designed such that it would be possible to assess the influence of the loading protocol on the connection performance, since otherwise identical specimens were tested with both types of loading. This provides a unique and valuable opportunity for structural assessment.

4.2 Test Frame and Specimen Installation

Figure 6 shows the overall layout of the test (reaction) frame with an installed beam-to-column connection specimen, and Figs. 7 through 9 are photographs of the installation at Southwest Research Institute. Specifically, Fig. 7 shows one of the specimens in the loading frame, Fig. 8 shows the column detail at the base (pin), and Fig. 9 shows the end of the beam with the attached hydraulic actuator and load cell.

As indicated by Fig. 6, the intent of the specimen installation was to have pinned ends at the top and bottom of the column as well as for the load application point at the tip of the beam. Pins were selected in order to model beam and column inflection points at midheight and midspan of the column and the beam, as is experienced in actual moment frames. The test specimen therefore reflects a steel frame with a story height of 13'-7", modeling the structure in California that had experienced fabrication problems. The response of the specimens during testing confirmed the anticipated rotational behavior of the pins. However, to ensure that even minor restraint effects at the supports would be known and their effects quantified, LVDT-s were installed to measure any support movements. Additional discussion of these issues is given in Chapter 4.6.2.

It was decided to perform the test without an axial load applied to the column. Since the primary purpose of the tests was to determine the response characteristics of the connection and its surrounding region, including the steel material and the welded joints, it was believed that a column axial load would have no discernible effect on the results. Other connection tests of recent vintage have not utilized an axial load. It is also noted that the absence of an axial load significantly simplified the test setup and the testing itself.

4.3 Measurement Needs and Instrumentation

The following primary response parameters were needed to achieve a complete picture of the performance of the beam-to-column connections; these were to be measured during each test:

- (1) Applied load at beam tip
- (2) Magnitudes and directions of vertical and horizontal displacements at beam tip
- (3) Vertical and horizontal displacements at top, midheight and bottom of column
- (4) Horizontal displacements at the levels of the continuity plates of the connection
- (5) Diagonal displacements of the connection panel zone
- (6) Strains at a number of locations within the connection region (panel zone) and the adjacent beam and column portions

Among these measurements, the most important are items (1), (2) and (3). When combined with the computed moment at the column face and the actual (calculated) beam tip displacement, this allows for the computation of the elastic and plastic chord rotation angles of the connection. These, in turn, are used to establish the connection hysteresis loops for load vs. beam tip displacement and, most importantly, the hysteresis loops for moment vs. plastic rotation angles.

Items (4) through (6) are of interest for local material and member behavior. As such, the response of the connection panel zone was particularly important to the development of any cracking in this region, especially if such were to form along the column k-lines.

4.4 Loads and Hydraulic Load Application System

The beam tip load was measured with a calibrated load cell; this can be seen in Fig. 9. The load cell was calibrated for a maximum load range of plus or minus 150 kips. Beam tip and other displacements were measured with LVDT-s (linearly variable displacement transducers); these were used in pairs, to ensure that backup data would be available in case any one instrument were to fail. The hydraulic actuator was capable of delivering upwards and downwards displacements each of approximately 10 inches. This satisfied the maximum testing needs of ± 10 inches.

4.5 Testing and Loading Protocols

The loading was delivered to the beam tip by the hydraulic actuator and pumping system. This was a closed loop system, governed by the displacement of the rod of the actuator. The desired rod amplitude levels were programmed for the command computer of the control system, producing the necessary beam tip displacements.

4.5.1 Quasi-Static Loading Protocol: At the time of preparation of the first part of the research program, under which a total of eight beam-to-column connection tests were to be run, the ATC-24 loading protocol (6) recommended quasi-static loading to predetermined beam tip displacement levels. Initially, the specimen would be subjected to three completely elastic cycles under load control. This form of control was also used for the following three cycles, where loads near the proportional limit were applied. The elastic and proportional limit loads were computed before the test.

The remainder of each quasi-static test was conducted under displacement control. This was necessary since yielding would occur after the proportional limit load, with increasing plastic deformations in the connection and its elements. In the first part of this range, the specimen would be subjected to three cycles at a displacement which

caused "significant yielding" (6). This was defined by ATC-24 as the load causing a deflection equal to 1.33 times the proportional limit value. Subsequent cycles were applied as multiples of the proportional limit deflection, since it was felt that this would give more meaningful test data than using the ATC-recommended multiples of the yield displacement. The change from the ATC recommendation was also necessitated by the constraints of the test setup (9). The test was continued until actual failure or when a significant, sudden drop of the load occurred. For the second group of nine tests, a shutoff control mechanism was installed to allow for the immediate stopping of a test. This would also prevent damage to sensitive measurement gages and other elements of the testing system.

The typical loading sequence for the eight quasi-static tests (A1-A3, A8, R1-1 to R1-3 and R1-6) was:

- 3 cycles at \pm 35 kips beam tip load (load control)
- 3 cycles at \pm 55 kips beam tip load (load control)
- 3 cycles at \pm 2.5 inches beam tip displacement (displacement control)
- 3 cycles at \pm 3.8 inches beam tip displacement (displacement control)
- 3 cycles at \pm 5.7 inches beam tip displacement (displacement control)
- 3 cycles at \pm 7.6 inches beam tip displacement (displacement control)
- 3 cycles at \pm 9.5 inches beam tip displacement (displacement control)

4.5.2 Dynamic Loading Protocol: Based on updated considerations for connection testing, coming from ATC and other sources (6, 12), it was decided to run the second group of nine tests with a dynamic loading protocol. In addition to imposing displacement control for all stages of a test, the dynamic protocol chosen utilized a loading frequency of 1 Hz. Thus, each cycle consisted of a sinusoidally shaped beam

tip displacement progression of neutral-up-neutral-down-neutral movements of the hydraulic actuator rod; this was accomplished in one second. This is a very severe loading condition, going well beyond the demands of the quasi-static testing procedure. Figure 10 shows a schematic of the dynamic loading protocol, as expressed in the form of numbers of cycles and associated beam tip displacements.

The targeted beam tip displacements for the nine dynamic tests (A4-A7, R1-4 and R1-5, R2, R3-1 and R3-2) are shown below. It was recognized that the actual deflections might differ slightly from the theoretical values, although the testing itself showed good correlation.

- 3 cycles at \pm 0.75 inches beam tip displacement
- 3 cycles at \pm 1.50 inches beam tip displacement
- 3 cycles at \pm 2.00 inches beam tip displacement
- 3 cycles at \pm 4.00 inches beam tip displacement
- 3 cycles at \pm 6.00 inches beam tip displacement
- 3 cycles at \pm 8.00 inches beam tip displacement
- 3 cycles at \pm 10.00 inches beam tip displacement

With the exception of two of the tests (Revised As-Built Connection 3 (RAB 3), test nos. R3-1 and R3-2), the 21 cycles indicated above were sufficient to reach failure of the specimens. The command computer software had a built-in control that would shut down the test at the completion of the 21st cycle. However, when Specimen R3-1 was tested, no discernible failure had occurred after 21 cycles. The software was then modified to allow for a larger number of cycles, but continuing to use the 10.00 inch displacement level, since the actuator was not capable of delivering a larger stroke. As will be seen in Chapter 9, the last test to be run was no. R3-2. This

specimen underwent a total of 28 cycles, or 10 cycles at the 10.00 inch displacement, before overall failure occurred. (The actual failure was subsequently determined to have taken place after 26-1/2 cycles. Details are given in Chapter 9.)

The beam tip displacement amplitudes shown above were based on the ATC-24 recommendations (5), and results of a finite element (FE) analysis of the connection specimen. The FE model is illustrated in Fig. 11. Using a nonlinear analysis, it was determined that the end of the elastic range occurred at a load of 51.3 kips. By ATC terminology, this was defined as $0.75Q_y$, where Q_y is the yield force. On this basis, the yield force for the connection specimens was determined to be $Q_y = 68.3$ kips. Extrapolating linearly from the $0.75Q_y$ -value, it was found that the displacement for a beam tip load equal to Q_y was 2.00 inches. This deflection value was termed the yield displacement, δ_y .

ATC-24 recommends that the testing include at least six cycles with amplitudes less than δ_y , hence the choice of amplitudes of 0.75 and 1.50 inches, each for three cycles. It also recommends the use of three cycles with $\delta = \delta_y$, hence the use of the 2.00 inch case. Finally, the recommendations indicate that all load steps with displacements larger than δ_y should utilize constant amplitude increments, equal to δ_y . This produced the 3 cycle sequences at amplitudes of 4.00, 6.00, 8.00 and 10.00 inches. For the unique case of Test R3-2, it was necessary to continue the cycles at 10.00 inch displacements, since the actuator was limited to a stroke no larger than approximately ± 11 inches.

As will be discussed in the next section, a beam tip displacement of approximately 8.00 inches produces a plastic connection rotation of 0.030 radians.

4.6 Computation of Displacements and Rotations

4.6.1 Measure of Performance: The key measure for the performance of a connection is its plastic rotation capacity or angle, θ_p . This gages the ability of a connection to sustain plastic deformations prior to failure, and is therefore regarded as a criterion by which the connection can be evaluated for seismic performance and suitability.

In order to arrive at the plastic rotation angle for the connections, a number of computations have to be done on the basis of the measured performance parameters. The procedure that was used is outlined in the following; it is in agreement with the principles specified by the Applied Technology Council (6).

4.6.2 Key Assumptions: First, assuming that the test frame is infinitely stiff, the true beam tip displacement would be defined as the vertical deflection of the beam end, measured relative to its undeformed (original) horizontal position. However, the test frame is not rigid, and frame deformations of some magnitude therefore have to take place. If the specimen displacements are measured in relation to the test frame, the frame deformations would be added to the true specimen displacements in some fashion, resulting in incorrect beam tip and other deformations. To account for these effects during the tests, vertical and horizontal displacements were measured at the centers of the top and bottom column supports (pins), the center of the clevis pin at the beam end, and at the center of the column panel zone. These displacements were used to calculate the actual beam tip deflections and to eliminate effects of the frame flexibility.

4.6.3 Shakedown Test: A special ("shakedown") test of a separate as-built connection specimen that was not part of the testing program was performed to check the performance of the loading system, computer software and all measurement

00513

devices. It was also used to assess the test frame deformations, which formed the basis for the evaluation of the results for all of the connections.

The shakedown test showed that vertical translations occurred at the top and bottom column support pins as load was applied. The translations for both locations were less than ± 0.06 inches, and took place in the same direction as the applied load. They appeared to be a result of tolerances in the pins used for the column supports. In the subsequent computations it was assumed that the entire test specimen translated in the vertical direction; the magnitudes at each column end were measured during the test and averaged to give the value of the translation offset, δ_{off} . The offset was then subtracted from the measured beam tip deflection, δ_{end} , to obtain the beam tip displacement.

In addition to the vertical translations of the column end supports, horizontal movements occurred at both column ends as well as at the panel zone center. The sense of these displacements indicated that the entire test specimen rotated as a rigid body around a point on the column close to the bottom pin. It would not be realistic to expect the center of specimen rotation to be located at the center of the panel zone, due to shape of the test specimen and the unsymmetrical loading and stiffness distribution of the test frame.

The shakedown test showed that the top column pin moved horizontally, in direct proportion to the beam end deflection, with magnitudes up to ± 0.3 inches. The lower column pin also moved horizontally, but in the opposite direction; the magnitudes of this translation were never larger than ± 0.04 inches. It was decided to treat this deformation as insignificant, leading to the above conclusion that the entire specimen rotated as a rigid body about the bottom column pin support.

4.6.4 Computation of Rotations and Translations: Figure 12 illustrates the rigid body translations and flexural displacements of the test specimen. The figure also shows the column and beam lengths that are used in the following to demonstrate the theoretical background of the computations for the beam tip displacements and the plastic rotation angles.

With the specimen rotating about the bottom column pin, the horizontal displacement at the top of the column, δ_x , creates the column rotation, θ . This rigid body rotation is the same as the rotation of the beam, as shown in Fig. 12. The beam rotation creates the rigid body beam tip displacement, δ_r . The value of δ_r is arrived at as follows:

$$\sin \theta = \delta_x / L_c \quad (4.1)$$

and therefore

$$\sin \theta = \delta_r / L_b \quad (4.2)$$

where L_c = column length and L_b = beam length. Equations (4.1) and (4.2) are used to get the expression for δ_r in terms of the column top displacement and the member lengths, thus:

$$\delta_r = \delta_x (L_b / L_c) \quad (4.3)$$

On this basis, the actual beam tip displacement, Δ_r , is found from Eq. (4.4) as the measured deflection minus the sum of the vertical offset and the deflection due to the rigid body rotation of the entire test specimen:

$$\Delta_t = \delta_{\text{end}} - (\delta_{\text{off}} + \delta_g) \quad (4.4)$$

This equation has been used to calculate the actual beam tip displacements and subsequently the required rotation angles of the connection. The procedure is outlined in the following.

4.6.5 Plastic Rotations: During an earthquake, the deformation demand, as best exemplified by the interstory drift, is partly accommodated by the elastic displacements of the frame. The necessary additional deformations have to be provided by the structure in the form of plastic hinge rotations in the beams and by plastic deformations in the column panel zones. (This form of response assumes that the usual strong column-weak beam design philosophy has been used, thus avoiding plastic hinges in the columns. Column hinges might endanger the overall stability of the frame, hence the rationale for the design concept.)

The FEMA Interim Guidelines (7) that have been developed over the past several years as a result of the SAC research project recommend that new steel-framed construction should be able to accommodate plastic rotations of at least 0.030 radians in the connection regions. Minimum rotation capacities of 0.025 radians are recommended for retrofitted structures. Both of these criteria are regarded as sufficiently conservative.

For connection testing, either as proof of performance of existing construction or for the acceptance of new designs, the minimum plastic rotation capacities indicated above should be sustained for at least one full cycle of loading. It is noted that the FEMA guideline recommendations for connection testing are based on a quasi-static testing protocol; no criteria address the issues associated with dynamic testing.

00516

However, it is generally agreed that although the dynamic protocol is more severe, in the absence of specific criteria the quasi-static recommendations will be applied.

The plastic rotation angle for the test specimens in this research program was computed in accordance with accepted FEMA (7) and SEAOC (2) approaches. The procedure is outlined in the following.

The plastic rotation angle, θ_p , is defined by Eq. (4.5):

$$\theta_p = \Delta_p/L_b \quad (4.5)$$

where L_b is the distance from the load application point at the tip of the beam to the face of the column. For the tests of this research program L_b equals 170.75 inches, based on the specimen showed in Fig. 6.

The plastic displacement equals the total deformation minus the elastic deflection:

$$\Delta_p = \Delta_t - \Delta_e \quad (4.6)$$

and the elastic deformation is given by

$$\Delta_e = P/K \quad (4.7)$$

P is the applied load at the beam tip and K is the elastic stiffness of the test specimen, as determined from the initial slope of the load-displacement diagram for each test.

The equation for the plastic rotation then becomes

$$\theta_p = [\Delta_t - (P/K)]/L_b \quad (4.8)$$

4.6.6 Cumulative and Normalized Cumulative Plastic Rotations: Most research efforts dealing with connection testing have limited the presentation of the results to the requisite plastic rotations and the accompanying number of cycles. The reports typically also include hysteresis loops, observations of failure modes and whether the FEMA acceptance criterion were met. However, beyond the appearance of the hysteresis loops there is nothing provided to permit an analysis of the important measure of *energy absorption capacity* of a connection. For seismic performance this is a key measure of suitability.

For the past few years Japanese research reports have included data on cumulative plastic rotations and normalized cumulative plastic rotations (8). The former is simply the sum of the plastic rotations associated with each cycle of loading until failure occurs; the latter is a relative measure of the same. However, it is evident that the cumulative plastic rotation for a connection in large measure reflects its energy absorption capacity, and therefore provides key information on its true performance ability. Clearly, the survival of a connection for one or more cycles at a certain plastic rotation level says very little about its potential response under sustained seismic activity.

For the above reasons it was decided to incorporate data on the cumulative plastic rotations and their normalized value for the connections tested in this program.

The cumulative plastic rotation, $\Theta_p = \Sigma\theta_p$, is defined as the sum of the individual plastic rotations occurring during each complete half cycle of the test (7). The quantity also includes the excursion amount occurring at failure.

00518

The normalized cumulative plastic rotation, η , is defined as

$$\eta = \Theta_p / \theta_y = (\Sigma \theta_p) / \theta_y \quad (4.9)$$

The term θ_y is defined as the elastic rotation of the beam cross section for a moment equal to the fully plastic moment. The normalized plastic rotation capacity may be described as similar in nature to the amount of plastic rotation a compact beam cross section is capable of reaching before local buckling or strain hardening takes place, i.e. it is the length of the plastic moment plateau.

5. MATERIALS TESTING

5.1 General Observations

A full complement of material property tests was performed for the column shapes used in the beam-to-column connection specimens. Only the column shapes were tested, since these were the members being subjected to the greatest stress and strain demands. The tests included tensile properties, Charpy V-Notch impact tests for toughness at various locations, hardness, chemistry, and grain size. The test specimens were taken from the locations specified by the governing ASTM standards where such was dictated; in other cases additional tests were performed to acquire a complete picture of the variation of the properties within given regions of the shapes. Details are provided in each of the following sections of this report.

5.2 Tensile Properties

The tensile properties of the material were determined with 0.505 inch diameter round coupons, in accordance with the requirements of ASTM A370. The specimens were taken from the column flanges, as dictated by ASTM A6 (3), and also from the web

and the k-region of the shapes. Figure 13 shows the sampling locations within each shape and in the regions of the test specimen assembly.

5.2.1 Tensile Properties of Material in Initial Eight Specimens: The average tensile properties of the material in the different regions of the column shapes for the first eight tests are shown in Tables 2A and 2B. The different reporting of the results for tests A1-A3 and R1-1 to R1-3 and tests A8 and R1-6 is important since the first six utilized rotary straightened columns; the last two used unstraightened column shapes. The data in Table 2A are based on 11 tests; the data in Table 2B are based on 3 tests.

The tensile properties for the flange and web specimens illustrate nothing unexpected. The values are within reasonable ranges, and certify that the material met the requirements of ASTM A572 Grade 50; they also meet the requirements of the recently added ASTM standard A992. The yield and tensile stresses of the flange material are somewhat lower than those of the web, but entirely within the same statistical population. Elongations and reduction-of-area (RA) values are also as would be expected, and show excellent uniaxial ductility. The yield-to-tensile ratios are also good, with no values higher than 0.85.

As expected, the yield and tensile strengths for the k-region are significantly higher than those of the flange and web specimens. The elongation and RA-values are acceptable (the smallest value of the elongation at rupture is 15.5 percent), although the elongation is well below those of the flange and the web.

Comparing the data for the rotary straightened and the unstraightened shapes offers some interesting results. All of the tensile properties for the flange and the web are close, indicating that the straightening has no measurable influence on these

00570

and the k-region of the shapes. Figure 13 shows the sampling locations within each shape and in the regions of the test specimen assembly.

5.2.1 Tensile Properties of Material in Test Specimens A1-A8: The average tensile properties of the material in the different regions of the column shapes for the first eight tests are shown in Tables 2A and 2B. The different reporting of the results for tests A1-A6 and tests A7-A8 is important in view of the fact that the first six utilized rotary straightened columns; the last two used unstraightened column shapes. The data in Table 2A are based on 11 tests; the data in Table 2B are based on 3 tests.

The tensile properties for the flange and web specimens illustrate nothing unexpected. The values are within reasonable ranges, and certify that the material met the requirements of ASTM A572 Grade 50; they also meet the requirements of the recently added ASTM standard A992. The yield and tensile stresses of the flange material are somewhat lower than those of the web, but entirely within the same statistical population. Elongations and reduction-of-area (RA) values are also as would be expected, and show excellent uniaxial ductility. The yield-to-tensile ratios are also good, with no values higher than 0.85.

As expected, the yield and tensile strengths for the k-region are significantly higher than those of the flange and web specimens. The elongation and RA-values are acceptable (the smallest value of the elongation at rupture is 15.5 percent), although the elongation is well below those of the flange and the web.

Comparing the data for the rotary straightened and the unstraightened shapes offers some interesting results. All of the tensile properties for the flange and the web are close, indicating that the straightening has no measurable influence on these

characteristics. As expected, the k-area shows lower yield and tensile stresses for the unstraightened shape and about the same as those of the web area.

Additional details regarding the above test results are given in the report by Strybos et al. (9).

Table 2A

**Average Tensile Properties for Material
in Rotary Straightened Column Shapes
for Tests A1-A3 and R1-1 to R1-3**

Loc. in Shape	Yield Stress (ksi)	Tensile Strength (ksi)	Yield Ratio	Elongation (%)	Reduction of Area (%)
Flange	53.2	75.1	0.71	28.5	71.6
Web	68.7	80.4	0.85	22.5	68.1
k-area	83.1	89.5	0.93	15.5	64.7

Table 2B

**Average Tensile Properties for Material
in Unstraightened Column Shapes for Tests A8 and R1-6**

Loc. in Shape	Yield Stress (ksi)	Tensile Strength (ksi)	Yield Ratio	Elongation (%)	Reduction of Area (%)
Flange	50.6	73.1	0.69	27.1	72.1
Web	67.6	79.4	0.85	20.3	67.4
k-area	69.5	79.8	0.87	21.2	66.2

5.2.2 Tensile Properties of Material in the Final Group of Nine Test Specimens: These test specimens included four of the as-built connections (tests A4-A7), with the A4-A5 having rotary straightened columns and A6-A7 gag straightened columns. The group also included five revised connections (tests R1-4 and R1-5, R2, and R3-1 and R3-2). These five specimens utilized rotary straightened columns. The average properties for the nine specimens are shown in Tables 3A and 3B.

The tensile properties for the flange and web tests exhibit the same characteristics as was found for the steel from the first eight connection specimens. As expected, the yield stress in the web is higher than that of the flange, by about 10 percent. The yield to tensile ratios, elongations at rupture and reductions of area are also in conformance with the requirements of the ASTM standard. The k-area values for the rotary straightened specimens are comparable to the data for the earlier eight connection tests, including yield ratios between 0.9 and 0.99. However, it is emphasized that the tensile property tests are uniaxial, and therefore not representative of the conditions in the structure. The three-dimensional restraint conditions in the structure act to raise the available strength of the material, in consonance with the Bridgman Effect (13). In other words, steel under three-dimensional restraint will not exhibit the same yielding and fracture behavior as uniaxial specimens.

The k-area data for the gag straightened columns are interesting. The numbers are directly comparable to those of the web tensile properties, as should be expected, since this form of straightening involves only the application of discrete load, i.e. the gag load.

5.2.3 Testing for Material Properties Before and After the Connection Tests: Several of the tensile tests for the group of nine connections were taken from the assemblies before and after the connection tests. These data are included with the results shown in Tables 3A and 3B. In general, no discernible differences could be found for the

Table 3A

**Average Tensile Properties for Material
in Rotary Straightened Column Shapes
for Tests A4, A5, R1-4, R1-5, R2, R3-1 and R3-2**

Loc. in Shape	Yield Stress (ksi)	Tensile Strength (ksi)	Yield Ratio	Elongation (%)	Reduction of Area (%)
Flange	58.5	76.6	0.76	26.6	72.5
Web	65.4	79.5	0.82	23.3	69.7
k-area	88.5	90.4	0.94	16.2	66.4

Table 3B

**Average Tensile Properties for Material
in Gag Straightened Column Shapes
for Tests A6 and A7**

Loc. in Shape	Yield Stress (ksi)	Tensile Strength (ksi)	Yield Ratio	Elongation (%)	Reduction of Area (%)
Flange	57.6	76.4	0.76	26.5	72.3
Web	63.4	78.5	0.80	24.5	71.8
k-area	62.9	78.4	0.80	24.1	71.2

flange material. The web material exhibited post-test average strength values on the order of 5 to 10 percent higher than the pre-test data, and were similar for the rotary straightened and gag straightened columns. The k-area material showed smaller differences; the average post-strength was about 2 percent higher. Such differences would be expected, considering the significant local strain demands that were imposed on the specimens in the connection region proper during the testing. In other words, the material in the connections experienced strain hardening during the tests. It is not believed that these differences are important for the performance of the connections, but rather emphasize the redundancy and redistribution characteristic of steel in complex joints. Removing the load and then reloading, the response of the structure would tend to approach elastic conditions.

5.3 Charpy Impact Testing

5.3.1 Testing Locations and Rationale: Extensive toughness examinations of the column material were conducted, in accordance with the requirements of ASTM A370 for Charpy V-Notch (CVN) impact testing. CVN samples were taken from the ASTM A673-specified location within the shapes; a large number of additional specimens were also prepared from other areas of the cross section. In particular, the toughness data for material within the k-region (see. Fig. 13) and the core of the shapes were needed, considering the types of details that are used for beam-to-column connections and the weld metal that will be deposited close to these areas.

The locations within the k-area and the core were also to be examined for hardness. Since the hardness testing was done before the tests for toughness properties, it afforded an opportunity to re-assess the locations for the CVN samples. The intent was to be able to find the "hardest" locations. Figure 14 shows the hardness testing locations within the portion of the cross section that includes the k-area and the core;

00525

CVN samples were taken from the web, core and k-region. As will be noted in the next section of this report, the highest hardness locations tended to vary from shape to shape, but they were all within the same general area.

5.3.2 Charpy V-Notch Tests: CVN tests were conducted at the ambient (76°F) as well as a number of other temperatures. All specimens were taken in the longitudinal-transverse (LT) orientation, to gain information on the toughness of the steel in the most likely crack initiation and propagation direction. This would also give data for impact energy (CVN toughness) vs. temperature curves, which might provide adequate information on the ductile-to-brittle transition temperatures (DBTT) for the steel in the test areas. Further, to gain an assessment of the influence of the connection testing itself, pre- and post-test CVN values were also obtained.

5.3.3 Straightening Protocols: The straightening protocol that had been used for the W14x176 column of the connection test specimens was another major consideration. Specifically, rotary straightening affects the material in the k-region, as demonstrated by the tensile test results. It might be expected that the toughness (and hardness) in this area would also be influenced by the straightening method. The data base of 17 connection tests, from which such information could be obtained, is believed to be the only one where the effects of the straightening protocol can be determined conclusively.

Of the 17 connection tests, 13 used rotary straightened columns, 2 columns had been gag straightened, and 2 were unstraightened. It is emphasized again that the rotary straightening was done to the maximum extent possible, to force as much cold working in the k-areas as possible. "Maximum straightening" is defined as the effort needed to reach a straightness that is such that any additional loading will lead to a

straightening-induced crack in the shape (which would make the shape a reject under normal production procedures). Finally, it is also re-emphasized that the unstraightened members represent unique samples, provided only for the purposes of the connection research program. Unstraightened shapes are not commercially available, and cannot be obtained from the steel mills.

5.3.4 CVN Toughness Data: Table 4A gives the average CVN toughness data for pre-test samples and Table 4B the post-test numbers, both at the ambient temperature (76°F).

The data in Tables 4A and 4B show nothing that was unexpected or otherwise surprising. As is common with CVN testing, the variability of the individual results was significant, but for the flange, web and core specimens from all 17 connection assemblies the lowest pre-test CVN value was 42.7 ft-lbs. The lowest individual post-test value was 21.0 ft-lbs.

Due to the inherent variability of CVN testing, there are no significant differences between the flange, web and core data that can be attributed to rotary versus gag straightening, neither for the pre-test nor the post-test results. Similarly, there are no obvious differences between pre- and post-test data, with the possible exception of the web results. It also appears that the results for the unstraightened member display the same characteristics, again with the possible exception of the web data.

As expected, the k-line CVN results for the rotary straightened shapes are significantly below the properties of the other locations within the cross section. The lowest individual value was 5.0 ft-lbs, and the highest was 105.7. The latter number may indicate a shape that was originally very straight, for which the amount of cold

00527

working during the rotary straightening process would have been low. On the whole, the k-line toughness properties are well below those of the other areas of the shape,

Table 4A

**Average Pre-Connection-Test CVN Values
at 76°F Ambient Temperature (ft-lbs)**

Straightening Protocol	Flange	Web	Core	k-line
Rotary	88.5	127.8	124.9	26.9
Gag	94.7	125.3	110.5	97.0
Not straightened	76.3	145.0	134.0	130.0

Table 4B

**Average Post-Connection-Test CVN Values
at 76°F Ambient Temperature (ft-lbs)**

Straightening Protocol	Flange	Web	Core	k-line
Rotary	84.7	92.7	126.5	13.8
Gag	93.5	97.2	139.8	57.0
Not straightened	99.5	64.0	146.0	110.0

although in many cases they would satisfy the ASTM material standard requirements.

The gag straightened results show no significantly lower CVN data for the k-line than for other locations, with the possible exception of the post-test result. This may have been caused by cold working during the connection test. The unstraightened members exhibit no such tendencies, again with the possible exception of the web results.

5.3.5 Impact Energy vs. Temperature Data: Based on the ambient and a range of other temperature CVN test results, impact energy vs. temperature diagrams were developed for the materials. Focusing on the k-region for rotary straightened vs. unstraightened shapes, Fig. 15 shows the data obtained from the material of the first eight connection tests (nos. A1-A3, A8, R1-1 to R1-3 and R1-6). The curves have not been statistically determined, but the trends are fairly clear and as expected. The ductile-to-brittle transition temperature (DBTT) was estimated on the basis of identifying the 50 percent shear fracture appearance from the CVN specimens. The core area material has a significantly lower DBTT than the k-line material.

In similar fashion, Fig. 16 shows the same type of results for one of the rotary straightened columns, comparing the core and the k-region. The contrast between the materials from the two locations is as was shown above.

Figures 17 and 18 show the CVN results for the core and k-region for another rotary straightened vs. a gag straightened shape. The shapes of the transition regions are significantly different, although the great variability of the toughness values is similar to the data presented for the other shapes.

5.4 Hardness

5.4.1 Test Method and Locations: Extensive Rockwell B hardness testing was

performed at numerous locations at the T-shaped flange-to-web intersections of all of the column material samples that were taken. Figure 14 shows the typical cross section of an area that was to be tested, indicating the sampling points throughout the web and the flange, including the core and the k-region. The same locations were used for rotary straightened, gag straightened and unstraightened shapes.

5.4.2 Hardness Results: Tables 5A, 5B and 5C give representative Rockwell B hardness results for three shapes with the three types of straightening protocol. The tests run for other shapes with the same treatment gave very similar data. These and other results from the same types of shape and straightening show that:

- (i) The hardness values and distribution within top and bottom flange T-shapes for rotary straightened shapes are consistent and very similar. The values also are very similar for different locations along the length of the column, as would be expected for a rotary straightened member.
- (ii) The hardness values and distribution within top and bottom flange T-shapes for gag straightened shapes are consistent and very similar. The HRB values varied within the T-section by 0.5 to 1.0. These shapes did not have definitive maximum hardness locations, as would be expected.
- (iii) As shown in Tables 5A and 5B, the hardness at the k-line of rotary straightened shapes is significantly higher than those for the same location in the gag straightened shapes. The HRB values for the former are typically 10 higher than those for the latter.
- (iv) The area of higher hardness, i.e. the k-area, is consistently located

between hardness drop points 4 and 8. This means that for the W14x176

Table 5A

**Rockwell B Hardness (HRB) Results for the
Top Flange of a Rotary Straightened Shape**

Hardness Drop No.	Position A	Position B	Position C
1	80.4	82.4	82.6
2 (core)	82.1	82.3	83.9
3	86.2	84.0	84.0
4	89.5	89.7	89.0
5 (k-line)	92.8	92.7	92.7
6	91.4	92.0	91.2
7	90.3	90.6	90.3
8	89.3	89.5	89.9
9	87.7	85.8	87.7
10	85.9	83.3	86.0
11 (web)	84.7	82.7	84.8

shapes used as columns in this research program, the k-area extends approximately 1 inch from the middle of the flange-to-web transition fillet into the web. Since the AISC k-value is 2.00 inches, as given in the steel construction manual (1), this translates into a k-area that goes 3/4 inch beyond the fillet, into the web.

- 18500
- (v) The hardness profiles for the unstraightened shapes are significantly different from those of the rotary straightened ones. For all of the tests,

Table 5B

**Rockwell B Hardness (HRB) Results for the
Top Flange of a Gag Straightened Shape**

Hardness Drop No.	Position A	Position B	Position C
1	80.6	83.0	82.5
2 (core)	82.3	84.6	83.5
3	82.5	83.2	83.0
4	83.0	82.3	83.0
5 (k-line)	82.6	82.4	83.1
6	82.7	83.2	85.1
7	83.4	83.0	84.8
8	83.6	82.4	82.9
9	82.4	82.3	82.7
10	82.5	82.4	82.5
11 (web)	82.7	83.2	82.7

the HRB values were no more than 80 to 84; for the shape whose data are shown in Table 5C the minimum HRB is 78.6 and the maximum is 81.2.

- (vi) The hardness profiles for the unstraightened shapes are not significantly

different from those of the gag straightened ones. The HRB values for both are mostly in the low 80-s, and the differences are generally around 2 HRB. Considering the inherent variability of hardness testing, some of the difference of 2 may be attributed to local hardness variations.

Table 5C

**Rockwell B Hardness (HRB) Results for the
Top Flange of an Unstraightened Shape**

Hardness Drop No.	Position A	Position B	Position C
1	78.7	80.2	79.4
2 (core)	78.6	81.2	79.8
3	80.2	81.0	78.6
4	79.9	79.0	79.2
5 (k-line)	80.1	80.3	79.1
6	81.0	80.3	79.6
7	81.2	80.1	79.7
8	81.2	80.9	80.0
9	80.9	80.2	80.1
10	81.2	80.2	79.7
11 (web)	81.1	79.8	80.1

- (vii) On the average, the hardness of rotary straightened columns in the k-area is approximately 15 to 18 percent higher than the same location within the unstraightened shape. Comparing rotary and gag straightened

columns, the k-area average is about 10 to 12 HRB higher. However, for the gaged column the hardness distribution along the length is close to the unstraightened member. This is because the gag load is a force applied at discrete locations. At the same time it is important to bear in mind that the k-area is small, and only occupies a fraction of the full W-shape cross section. Its impact on the in-structure performance is likely to be very limited, if any.

5.5 Grain Size and Chemistry

5.5.1 Grain Size Measurements: T-sections from each of the columns were examined for ferritic grain size and structure in accordance with ASTM E112. The prime purpose of these tests was to determine whether straightening had any effect on the microstructure of the steel. Detailed results are presented in References 9 through 11; only the key findings will be given here.

Overall, the grain sizes ranged from 8.0 to 10.0. In the interior (center) locations, both rotary and gag straightened columns had grain sizes between 8.0 and 9.0; the surface typically had grains 0.5 size finer than the center. The unstraightened shapes had grain sizes ranging from 7.5 in the interior and 8.0 to 9.0 at the surface. There appeared to be some banding (preferential alignment) of pearlite colonies in the straightened sections, but this is unlikely to be related to the straightening action.

5.5.2 Chemistry: Normal chemistry tests were used to ascertain that the steel satisfied the requirements of ASTM A572 (50). This was done in addition to the mill certification that accompanies each heat of steel. All chemical components were in agreement with the ASTM criteria for A572, Grade 50, as well as A992.

6. PERFORMANCE OF AS-BUILT CONNECTIONS WITH ROTARY STRAIGHTENED COLUMNS

6.1 Connection Design and Materials

The as-built connections with rotary straightened columns were tested as Specimens A1 through A5. Figure 1 shows the appearance of the as-built connection, and Chapter 3 gives all details regarding materials, detailing, individual elements and fastening methods. Data regarding testing protocols, instrumentation, etc. are provided in Chapter 4. Tests A1 to A3 were run with quasi-static loading; tests A4 and A5 were tested dynamically.

6.2 Quasi-Static Tests

6.2.1 Specimen Test Performance: Figures 19 through 21 show the beam tip load ("load") vs. displacement and moment vs. plastic rotation hysteresis loops for Tests A1 through A3, and Figs. 22 through 24 are pairs of photographs of the connections after failure.

In the early loading stages all three connections exhibited the same response. Initial yielding occurred at approximately 60 kips. Significant yielding had taken place by the time the load reached 70 kips, for an applied moment of 12,000 k-in. This is consistent with the calculated panel zone strength. All three specimens exceeded the required strength level, and none suffered any appreciable strength or stiffness degradation until failure took place.

6.2.2 Plastic Rotations: As illustrated by Figs. 19 and 20, tests A1 and A2 behaved almost identically through failure. Both specimens achieved three full cycles of plastic rotation at 0.017 radians and between one and two full cycles at 0.0275 radians.

0105335

Since both were as-built specimens, they met the FEMA minimum rotation requirement for such connections of at least one full cycle of a plastic rotation equal to or greater than 0.025 radians (7). Figure 21 shows that specimen A3 did not meet the FEMA requirement, since it was only able to achieve one full cycle of a plastic rotation equal to 0.017 radians.

6.2.3 Failure Characteristics: Most of the deformation associated with the failure of each of these specimens was concentrated within the panel zone of the connection. The assemblies even exhibited a certain amount of "kinking" in the column; this appeared to have contributed to the failure modes through the development of displacement-induced (secondary) stresses between the beam and column flanges. This was especially demonstrated by Test A3, a photograph of which is shown in Fig. 24.

Examination of the fracture surfaces for Specimens A1-A3 indicated the following characteristics for all three failures:

- (i) Crack initiation occurred in a slightly undercut (but acceptable by AWS standards) region in the cover plate to column flange CJP weld.
- (ii) The crack propagated through the heat affected zone (HAZ) of the weld and then into and through the flange of the column.
- (iii) A microcrack appeared to have occurred in the cover plate to column flange CJP weld in specimen A3, adjacent to the fracture location. It is very likely that this was a pre-existing shrinkage crack that was too small to be detected during the weld inspection after fabrication. Clearly the

microcrack would have been a contributing source to the crack that eventually fractured the specimen, and may be the reason A3 performed relatively poorly, compared to the identical specimens A1 and A2.

- (iv) The microcrack and undercut of A3 was not found in tests A1 and A2, emphasizing the statements made above regarding the failure mode and the contributing influences for A3.

Since the fracture modes were similar for A1 through A3, and A3 failed earlier than the other two, a detailed fractographic analysis of A3 was performed. Figure 25 is a photograph of the fracture surface for A3, showing the crack initiation point A; this is primarily in the weld metal. Once initiated, the crack propagated parallel to the weld on both sides, towards the column flange to web transition fillet. Once the fillet region was reached, the crack extended along the length of the column within the fillet region. This is further illustrated in Fig. 23. The crack propagated in a brittle manner. However, there was no indication that the crack initiation took place in the fillet region, which includes the k-area.

6.3 Dynamic Tests

6.3.1 Specimen Test Performance: As an illustration of the dynamic loading protocol, Fig. 26 shows the beam tip displacement vs. time trace and Fig. 27 shows the beam tip load vs. time trace for the test of Specimen A4. It is seen that the 1 Hz cycle is maintained very closely during the entire testing sequence; this was experienced for all of the dynamically tested connection assemblies. Fig. 27 also reflects the behavior of the specimen once the first indication of local failure has occurred, noting the maximum applied load and its subsequent degradation as the failure progressed. Since the tests were displacement controlled, Fig. 26 does not record the initiation and

00537

propagation of the failure. Finally, these and other measurements were recorded through the computer software; readings were made at a rate of 100 per second.

Figures 28 and 29 show the beam tip load vs. displacement and moment vs. plastic rotation hysteresis loops, respectively, for Test A4. The somewhat "ragged" nature of the curves is a result of the dynamic testing, as well as the very high rate of data recording. In fact, Figs. 28 and 29 reflect three-point moving average curves; without such data averaging the curves are even more ragged. Figure 30 shows the moment vs. plastic rotation hysteresis loops for Test A5, and Fig. 31 is a photograph of the cracking region for specimen A4.

Test A4 reached a maximum positive (upstroke of actuator) load of 110.1 kips and a maximum negative load of 115.1 kips. Both occurred during the first 8 inch amplitude cycle, which was the 16th. Failure took place as a crack at the intersection between the bottom flange cover plate and the column flange. Full specimen stiffness was maintained for one complete cycle at the 8 inch amplitude.

Test A5 reached a maximum positive load of 113.9 kips and a maximum negative load of 106.4 kips. As in test A4, both occurred during the first 8 inch amplitude cycle. Failure took place as a crack at the intersection between the top flange cover plate and the column flange. Full specimen stiffness was maintained for three complete cycles at the 6 inch amplitude and one half cycle at the 8 inch amplitude.

6.3.2 Plastic Rotations: Figures 29 and 30 show the moment vs. plastic rotation hysteresis loops for tests A4 and A5. As already noted, connection A4 was able to sustain one complete cycle at the 8 inch amplitude level; this corresponded to plastic rotations of +0.029 radians and -0.027 radians. This satisfies the FEMA requirement

00538

for as-built construction.

Connection A5 underwent 3 complete cycles at the 6 inch amplitude level; the corresponding maximum (+) and minimum (-) plastic rotations were +0.016 and -0.018 radians. It was only able to undergo one half complete cycle at the 8 inch amplitude level for a plastic rotation of 0.027 radians. Since A5 could not sustain a complete cycle with plastic rotations larger than or equal to 0.025 radians, this connection test did not meet the FEMA requirement.

6.3.3 Failure Characteristics: Specimens A4 and A5 failed in very similar manner, although one had the major crack and failure occur from the bottom flange and the other from the top flange. Bottom or top is not believed to be a significant failure consideration. Figure 32 is a photograph of specimen A5, showing the crack at the toe of the cover plate to column flange weld, and Fig. 33 show the fracture surfaces for A4, including the origin and the shear lip.

Figure 34 is a schematic illustration of specimens A4 and A5, showing the location and propagation of the initial cracks, including through the column flange. For both, once the crack had extended through the column flange, it began moving into the k-region of the column. However, it changed direction and eventually extended through the web and along the continuity plate. Although the change of direction occurred in the vicinity of the weld access hole, fractographic analyses did not indicate that the access hole played a significant role. Finally, the crack that extended into the column web appeared to be ductile, as exemplified by the fracture surfaces of specimen A4; this is illustrated by the photograph in Fig. 35.

6.4 Assessment of Performance

Table 6 summarizes the key points of the test results for specimens A1 through A5. Additional evaluations are provided in the following.

Table 6
Summary of Performance Data for Tests of
As-Built Connections with Rotary Straightened Columns

Test No.	Load. Prot ¹ .	Plastic Rot θ_p (max./min.) (radians)	Cumul. Plastic Rotat. Θ_p	Norm. Plastic Rot. η	Full cycles at θ_p	FEMA Crit ² . Met ?
A1	Q	0.027 0.027	0.471	46.1	1	Yes
A2	Q	0.027 0.027	0.528	51.7	1	Yes
A3	Q	0.017 0.017	0.219	21.5	1	No
A4	D	0.029 0.027	0.389	35.0	1	Yes
A5	D	0.016 0.018	0.336	30.3	3	No

Notes for Table 6

Note 1 Q = quasi-static testing; D = dynamic testing

Note 2 FEMA requirement for as-built connections: minimum one full cycle at plastic rotation 0.025 radians

Apart from the loading protocol, specimens A1 to A5 were identical and were tested under identical conditions. Three of the five specimens met the FEMA minimum

00540

requirement, although one of the two that did not (A5) was able to rotate one half cycle at 0.027 radians.

The results in Table 6 do not indicate a clear effect of the quasi-static versus the dynamic testing protocols. However, the average cumulative plastic rotation capacity for the two Q-specimens that passed the FEMA requirement is 48.9 versus the 35.0 for the one D-specimen that passed. If nothing else, this indicates that the dynamic testing protocol is a more severe condition, but that was known beforehand. The specimens that were tested dynamically and passed the FEMA criterion are clearly acceptable.

Of the two tests that failed the FEMA requirement, only the Q-specimen failed prematurely. It was not able to undergo more than one cycle of plastic rotation at 0.017 radians. The D-specimen was very close to passing the FEMA requirement, since it underwent 3 complete cycles at 0.017 radians and one half cycle at 0.027 radians.

7. PERFORMANCE OF AS-BUILT CONNECTIONS WITH GAG STRAIGHTENED COLUMNS

7.1 Connection Design and Materials

The as-built connections with gag straightened columns were tested as Specimens A6 and A7. Figure 1 shows the appearance of the as-built connection, and Chapter 3 gives all details regarding materials, detailing, individual elements and fastening methods. Data regarding testing protocols, instrumentation, etc. are provided in Chapter 4. The dynamic loading protocol was used for both of these specimens.

7.2 Test Results

7.2.1 Specimen Test Performance: Figures 36 and 37 show the moment vs. plastic rotation hysteresis loops for Tests A6 and A7, respectively. The maximum and minimum loads for A6 were +108.8 kips and -111.8 kips; for A7 these loads were +111.0 kips and -110.9 kips.

Specimen A6 went through the first complete cycle at the 8 inch amplitude (cycle 16); significant loss of stiffness as a result of top region cracking took place during the first half of the following cycle. Specimen A7 behaved exactly the same as A6, including the complete 16th cycle and the top region failure during the first half of the 17th cycle.

7.2.2 Plastic Rotations: Both connections A6 and A7 underwent ± 0.028 radians during the 16th cycle, for which the amplitude of 8 inches controlled the load input. The first half of the 17th cycle also gave a plastic rotation of 0.028 radians; however, the specimens failed during the second half of this cycle. In view of the fact that these were as-built connections and that they were able to sustain plastic rotations larger than 0.025 radians for at least one full cycle, both specimens met the FEMA rotation requirement.

7.2.3 Failure Characteristics: Connection A6 failed through a crack that initiated at the toe of the top cover plate to column flange weld. The crack subsequently extended through the flange, and then along the k-region towards the bottom continuity plate (about 15 inches long).

A7 failed in much the same way as A6, in that the initiating crack and propagation were the same. However, once the crack had gone through the column flange, it

propagated across the k-region and then through the web, away from the continuity plate for a total length of approximately 9.5 inches. Figure 38 shows details of the fractures in specimen A6, and Fig. 39 indicates crack initiation and propagation details for this specimen. The appearance of the mechanisms for A7 are closely similar.

7.3 Assessment of Performance

Table 7 summarizes the key points of the test results for specimens A6 and A7. For comparison with otherwise identical connections with rotary straightened columns, the results for specimens A4 and A5 are also included in the table. Additional evaluations are provided in the following.

Table 7

**Summary of Performance Data for Tests of
As-Built Connections with Gag Straightened Columns (A6-A7)
with Data for Rotary Straightened Columns (A4-A5)**

Test No.	Load. Prot.	Plastic Rot θ_p (max./min.) (radians)	Cumul. Plastic Rotat. Θ_p	Norm. Plastic Rot. η	Full cycles at θ_p	FEMA Crit'. Met ?
A6	D	0.028 0.028	0.416	40.4	1	Yes
A7	D	0.028 0.028	0.442	42.9	1	Yes
A4	D	0.029 0.027	0.389	35.0	1	Yes
A5	D	0.016 0.018	0.336	30.3	3	No

Note for Table 7

Note 1 FEMA requirement for as-built connections: minimum one full cycle at plastic rotation 0.025 radians

The two connections with gag straightened columns both satisfied the FEMA plastic rotation requirement. So did one of the tests with a rotary straightened column (A4), but the other one did not, although it was close to being satisfactory, as noted in Chapter 6. The cumulative and especially the normalized cumulative plastic rotations are somewhat larger for the specimens using gag straightened columns. However, the differences are not large enough to warrant an unequivocal statement to the effect that gag straightened assemblies perform better. The number of parameters that play a role in the performance of beam-to-column connections is so large that any more definitive statements cannot be made. This observation only applies to as-built connections of the type that was tested under this program, although it is reasonable to expect similar results for other types of connections.

8. PERFORMANCE OF AS-BUILT CONNECTION WITH UNSTRAIGHTENED COLUMN

8.1 Connection Design and Materials

The single as-built connection with an unstraightened column was tested as Specimen A8. Figure 1 shows the appearance of the as-built connection, and Chapter 3 gives all details regarding materials, detailing, individual elements and fastening methods. Data regarding testing protocols, instrumentation, etc. are provided in Chapter 4. The quasi-static loading protocol was used for this specimen.

00544

8.2 Straightening Protocol

Although unstraightened shapes cannot be obtained commercially, for practical production reasons, it was decided to run two connection tests with such columns. It was reasoned that this would allow for a direct comparison with the performances of tests with rotary straightened and gag straightened members. The columns that were used were literally lifted off the cooling bed in the steel mill before entering the normal straightening sequence.

Following their removal from the cooling bed, the out-of-straightness of the unstraightened shapes was measured. It was found that both members met the requirements of ASTM A6 (3).

8.3 Test Results

Figure 40 shows the load-displacement and moment-plastic rotation hysteresis loops for Test A8. The behavior and the load and deformation levels were very similar to the specimens with rotary straightened and gag straightened columns. A8 was able to undergo 1 complete cycle at 8 inch, with maximum and minimum plastic rotations of $+0.028$ and -0.028 radians, for a cumulative plastic rotation of 0.768 radians. The normalized cumulative plastic rotation was 75.3 , evidencing significant ductility. The failure of the connection was initiated by a crack at the toe of the cover plate to column flange weld; a crack also developed at the edge of the cover plate close to the edge of the column flange.

8.4 Assessment of Performance

Table 8 summarizes the test data for specimen A8. The as-built connection using an unstraightened column behaved similarly to the specimens using rotary straightened and gag straightened columns. The rotation capacity was good, and the FEMA

requirement was met. However, the specimen showed no clear evidence of any improvement in behavior or load-carrying and plastic rotation capacity as compared to the specimens with rotary straightened columns.

Table 8

Summary of Performance Data for Test of an
As-Built Connection with an Unstraightened Column

Test No.	Load. Prot.	Plastic Rot θ_p (max./min.) (radians)	Cumul. Plastic Rotat. Θ_p	Norm. Plastic Rot. η	Full cycles at θ_p	FEMA Crit ¹ . Met ?
A8	Q	0.028 0.028	0.768	75.3	1	Yes

Note for Table 8

Note 1 FEMA requirement for as-built connections: minimum one full cycle at plastic rotation 0.025 radians

9. PERFORMANCE OF REVISED AS-BUILT CONNECTION TYPE 1

9.1 Connection Design and Materials

The revised as-built connections Type 1 were tested as Specimens R1-1 through R1-6. Figure 3 shows the appearance of this connection, and Chapter 3 gives all details regarding materials, detailing, individual elements and fastening methods. Of particular interest are the smaller thickness cover plate and the use of fillet welds for the continuity plates. Data regarding testing protocols, instrumentation, etc. are provided

00546

in Chapter 4. Specimens R1-1 through R1-3 and R1-6 were tested quasi-statically; R1-4 and R1-5 were tested dynamically. The reason for the different testing protocols is that four of these specimens were tested during the first phase of the research program; tests R1-4 and R1-5 were done during the second phase.

9.2 Straightening Protocol

Specimens R1-1 through R1-5 had rotary straightened columns; specimen R1-6 used an unstraightened column.

9.3 Quasi-Static Tests

9.3.1 Specimen Test Performance: Figures 41 through 43 show the load vs. displacement and the moment vs. plastic rotation hysteresis loops for Tests R1-1 through R1-3, respectively, and Fig. 44 gives a photographic example of the failure appearance of these tests. The strength requirement was satisfied for all of these connections, and the plastic rotation capacity was similar to the as-built connections A1 through A3.

Figure 45 shows the load vs. displacement and the moment vs. plastic rotation hysteresis loops for connection R1-6. This specimen used an unstraightened column. The behavior of this assembly was similar in all respects to that of specimens R1-1 through R1-3, although it did not reach the rotation level of R1-1.

9.3.2 Plastic Rotations: Connections R1-2 and R1-3 were able to achieve one full cycle of plastic rotation of ± 0.027 radians, and both failed during the second half of the second 0.027 radian cycle. Since these were revised connections (i.e. new construction, in accordance with FEMA (7)), they did not meet the 0.03 radians requirement.

Connection R1-1 underwent 3 complete cycles at the 0.027 radian plastic rotation level and also one full cycle with plastic rotations of ± 0.043 radians. This specimen met the FEMA requirement.

Connection R1-6 was able to achieve one full cycle of plastic rotation of ± 0.027 radians. It failed during the second half of the second 0.027 radian cycle. Since this also was a revised connection, it did not meet the 0.03 radians FEMA requirement.

9.3.3 Failure Characteristics: All four specimens R1-1 through R1-3 and R1-6 failed in very similar manner, although the much better performance of R1-1 can clearly be attributed to the initial cracking and the subsequent response of the connection. First, the failure of specimens R1-2, R1-3 and R1-6 was initiated by a crack at the toe of the cover plate to column flange weld. There appeared to be a limited lack of fusion in the fillet weld between the flange and the continuity plate. The fracture extended in a fashion similar to that of the as-built configuration of specimens A1 through A3. The use of an unstraightened column for R1-6 did not make any difference to the performance of this connection.

Specimen R1-1 also had an initiating crack at the toe of the cover plate to column flange weld. In addition, the lack of fusion (LOF) that was found in the other two specimens in the fillet weld between the continuity plates and the column flange was also found for specimen R1-1, but the LOF was more extensive in this case. As a result, R1-1 was able to allow the continuity plates to move during the cycling, removing much of the strain demand that otherwise would have been concentrated in the flange and subsequently the web area. This explains the excellent performance of this connection.

00548

9.4 Dynamic Tests

9.4.1 Specimen Test Performance: Figures 46 and 47 show the moment vs. plastic rotation hysteresis loops for Tests R1-4 and R1-5, respectively, and Figs. 48 and 49 are photographs of the specimens after failure.

The maximum and minimum loads for specimen R1-4 were +104.1 kips and -104.8 kips, respectively, and it maintained full stiffness during three 8 inch displacement cycles. The connection failed during the second half of the first 10 inch amplitude cycle through a crack that developed between the top cover plate and column flange weld.

The maximum and minimum loads for specimen R1-5 were +104.5 kips and -100.4 kips, respectively, and it maintained full stiffness during two and a half of the 8 inch displacement cycles. The load started decreasing during the second half of the third 8 inch amplitude cycle, although the stiffness was maintained. The connection failed during the second half of the first 10 inch amplitude cycle through a crack that developed between the top cover plate and column flange weld.

9.4.2 Plastic Rotations: Connection R1-4 achieved three full cycles of plastic rotation of +0.031 radians and -0.030 radians. For the following one half cycle the plastic rotation reached +0.039 radians. Since this was a revised connection, met the 0.03 radians FEMA requirement.

The performance of connection R1-5 was identical to R1-4 for all practical purposes. It achieved three full cycles of plastic rotation of +0.031 radians and -0.030 radians. For the following one half cycle the plastic rotation reached +0.039 radians. Since this was a revised connection, met the 0.03 radians FEMA requirement.

9.5 Assessment of Performance

Table 9 summarizes the key points of the results for specimens R1-1 through R1-6. Additional evaluations are provided in the following. Of the six revised Type 1 connections, three met the FEMA plastic rotation requirement. The three that did not were among the quasi-statically tested specimens. The two dynamically tested specimens behaved and failed in identical fashion, with crack initiation and propagation as further illustrated by Fig. 50.

Table 9

Summary of Performance Data for Tests of
Revised As-Built Connections Type 1'

Test No.	Load. Prot ² .	Plastic Rot θ_p (max./min.) (radians)	Cumul. Plastic Rotat. Θ_p	Norm. Plastic Rot. η	Full cycles at θ_p	FEMA Crit ³ . Met ?
R1-1	Q	0.043 0.043	0.825	80.8	1	Yes
R1-2	Q	0.027 0.027	0.544	53.4	1	No
R1-3	Q	0.027 0.027	0.540	52.9	1	No
R1-4	D	0.031 0.030	0.736	66.3	1	Yes
R1-5	D	0.031 0.030	0.598	53.9	3	Yes
R1-6	Q	0.027 0.027	0.618	60.5	1	No

Notes for Table 9

- Note 1 The column for specimen R1-6 was unstraightened, all others were rotary straightened.
- Note 2 Q = quasi-static testing; D = dynamic testing
- Note 3 FEMA requirement for new construction: a minimum of one full cycle at plastic rotation 0.030 radians

The use of fillet welds for the continuity plates represented a major change from as-built connection design and fabrication practice. It had been felt that such details would not be able to perform, especially under the very demanding conditions of the dynamic tests. This was proven to be incorrect, as will particularly be shown for the remaining specimens in the research program.

10. PERFORMANCE OF REVISED AS-BUILT CONNECTION TYPE 2

10.1 Connection Design and Materials

The single specimen of the revised as-built connection Type 2 was tested as Specimen R2. Figure 4 shows the appearance of this connection, and Chapter 3 gives all details regarding materials, detailing, individual elements and fastening methods. The column had been rotary straightened. Of particular interest is the use of a 1/2 inch transition fillet weld between the cover plate and the column flange; this was used both at the top and the bottom of the beam. Data for testing protocols, instrumentation, etc. are provided in Chapter 4. The specimen was tested dynamically.

10.2 Test Results

10.2.1 Specimen Test Performance: Figure 51 shows the moment vs. plastic rotation hysteresis loops for the connection. The maximum and minimum loads for

08551

the specimen were +110.7 kips and -115.6 kips, respectively, and it maintained full stiffness during three 8 inch displacement cycles. During the first half of the first 10 inch displacement cycle (cycle 19), the load continued increasing but with a slight reduction in assembly stiffness, until the maximum load was reached at a displacement of approximately 8.5 inches. The stiffness was maintained during the second half of the cycle, and the final failure occurred in the form of cracking in the bottom cover plate to column flange region.

10.2.2 Plastic Rotations: Figure 51 shows that ± 0.028 radians of plastic rotation were achieved for three full cycles (nos. 16-18). Although there was a slight drop in the connection load during cycles 19 and 20, the stiffness was maintained, and plastic rotations of ± 0.038 radians were achieved. It was therefore determined that the FEMA new construction requirement of ± 0.030 radians was met.

The cumulative plastic rotation for Specimen R2 was 0.612 radians, and the normalized cumulative plastic rotation was 59.4. The overall performance of this connection therefore must be judged as excellent.

10.2.3 Failure Characteristics: The initiating crack occurred at the bottom cover plate to column flange weld. This is also a location of the 1/2 inch transition fillet weld. The fracture extended through the column flange, across the k-region and then along the web. There was no crack extension along the k-region. A small crack was found between the cover plate and the beam flange. The top cover plate did not fracture, although small cracks were observed at the toe of the transition weld.

A crack was also found at the weld access hole at the edge of the continuity plate weld. As noted in Chapter 2.5 of this report, using the same detail as was specified

00552

for the California structure where the original fabrication cracks had occurred, the continuity plates had corners cropped by 1 inch. This was done to allow for the welding of the plates to the column web and flanges, and to avoid the flange to web fillet. With a flange thickness of 1.31 inches and a k-distance of 2.00 inches for the W14x176 column shape, this placed the ends of the continuity plate welds within the k-area of the shape. Larger cropping of the plates has since been recommended for improved detailing and fabrication.

10.3 Comparison of Performance with Other Connections

Figure 52 shows the locations of the initiating and through-column flange cracks for Connections R2, A6 and A7. The latter two used gag straightened columns, as noted in Chapter 7. *The failure appearances are similar, although Specimen R2 was able to achieve a significantly higher cumulative and normalized cumulative plastic rotations.* Since the performances of as-built connections with rotary and gag straightened columns are identical for all practical purposes, the improved response of R2 must be attributed to the presence of the 1/2 inch transition fillet weld.

Figure 52 emphasizes the different fracture path appearance for R2, as compared to A6 and A7; this is especially apparent in the horizontal crack of R2. Instead of going into the k-region, as was the case for A6 and A7, the R2 crack propagated along the continuity plate weld in a ductile fashion. Subsequent examinations of the fracture area for R2 did not reveal any anomalies that might explain the change in direction. However, it is noted that the crack direction change occurred in the vicinity of the access hole for the continuity plate.

Table 10 summarizes the performance data for connection specimen R2.

Table 10

Summary of Performance Data for Test of the
Revised As-Built Connection Type 2

Test No.	Load. Prot.	Plastic Rot θ_p (max./min.) (radians)	Cumul. Plastic Rotat. Θ_p	Norm. Plastic Rot. η	Full cycles at θ_p	FEMA Crit'. Met ?
R2	Q	0.038 0.038	0.612	59.4	2	Yes

Note for Table 10

Note 1 FEMA requirement for revised connections: minimum one full cycle at plastic rotation 0.030 radians

11. PERFORMANCE OF REVISED AS-BUILT CONNECTIONS TYPE 3

11.1 Connection Design and Materials

Two revised as-built connections Type 3 were tested as Specimens R3-1 and R3-2. Figure 5 shows the appearance of this connection, and Chapter 3 gives all details regarding materials, detailing, individual elements and fastening methods. The column had been rotary straightened. Of particular interest are (1) the smaller thickness cover plate; (2) the use of a 1/2 inch transition fillet weld between the top and bottom cover plates and column flanges; (3) the fillet welded continuity plates (CP); and (4) the repositioned continuity plates. Data regarding testing protocols, instrumentation, etc. are provided in Chapter 4. The specimens were tested dynamically.

00554

It was decided that a repositioning of the continuity plates would allow for an improved fracture path following crack initiation, based on the knowledge gained during the testing of the other specimens in the research program. The CP-s were thus placed with their outside edges in line with the interface between the beam cover plate and the beam flange, as illustrated in Fig. 5. The other 15 connections of the research program utilized the plates in the traditional location, with the mid-thickness line of the CP-s in the same location as the cover plate to beam flange interface.

As for specimens A6, A7, R1-4, R1-5 and R2, the continuity plate (CP) welds were deposited in the sequence (1) CP to column flange 1, (2) CP to column flange 2, and (3) CP to column web. It was felt that this would minimize the weld contraction strain *impact on the material in the column flanges.*

The original research program called for only one test of the revised as-built type 3 connection. However, following the test of R3-1 it was decided that another, identical specimen needed to be tested. This was done because of the unusually good response of R3-1, to ensure that the first test was not an anomaly.

11.2 Test Results

11.2.1 Specimen Test Performances: Figures 53 and 54 show the moment vs. plastic rotation hysteresis loops for connections R3-1 and R3-2. The maximum and minimum loads for Specimen R3-1 were +106.5 kips and -106.0 kips, respectively; this occurred during second cycle of the 8 inch displacement amplitude. The connection maintained full stiffness for all three of the 8 inch cycles (nos. 16-18) as well as the three 10 inch displacement cycles. *At the time of the testing of R3-1, it was the only one of the 16 connections that had been tested so far that was able to sustain more than one complete 10 inch amplitude cycle.* The test of R3-1 continued

with constant amplitudes of 10 inches until the test system computer software took control and exercised the preprogrammed test shutoff after 21 complete cycles. *No visible cracking or overall connection failure had taken place at the end of the test.*

The above description of test R3-1 explains why it was decided to run one additional test of the revised as-built connection Type 3. The performance was so unusual and good that it was felt necessary to run another, presumably confirmatory test. The computer software was revised to allow an indefinite number of cycles with 10 inch displacement.

The maximum and minimum loads for Specimen R3-2 were +106.6 kips and -108.3 kips, respectively. The maximum load was recorded during the first cycle (no. 16) of the 8 inch displacement amplitude; the minimum load occurred during the first cycle of the 10 inch amplitude (cycle 19). The peak loads remained essentially constant for all cycles through no. 21, which was the third with a 10 inch amplitude. The connection maintained full stiffness and integrity for all of the 8 inch cycles as well as the three first 10 inch displacement cycles. The stiffness and beam tip load decreased slightly and uniformly for each cycle after no. 21, although the connection continued to maintain its integrity, with no observed cracking.

The test of R3-2 continued with constant amplitudes of 10 inches and with complete integrity during 26-1/2 cycles. Any test specimen was considered to have maintained its structural integrity if, within each cycle, the beam tip loads were constantly increasing during the upstroke and downstroke portions of the cycle. Specimen R3-2 maintained this response characteristic through the first half of cycle 27. The load then started dropping off when the displacement reached approximately 6-1/2 inches, which was defined as the initiation of failure. Specimen R3-2 eventually failed due to

fracture (cracking) in the top flange cover plate to column flange region. Local buckling did not occur.

11.2.2 Plastic Rotations: By the end of the 21 cycles of the test of Specimen R3-1, plastic rotations of +0.037 and -0.038 radians were recorded. By the end of the 26 first cycles of test R3-2 the maximum and minimum plastic rotations were +0.038 and -0.040 radians; during the first half of the 27th cycle the plastic rotation was +0.039 radians. Both connections easily met the FEMA plastic rotation requirement.

Comparing the results for connection R3-2 after 21 cycles with those of R3-1, R3-2 had undergone cumulative plastic rotations of +0.986 and -0.985 radians. These compare very closely with the cumulative plastic rotation for specimen R3-1 after 21 cycles of 1.004 radians.

11.2.3 Failure Characteristics: For connection R3-1, cracks initiated at the weld root between the top and bottom cover plates and the beam flange. The crack in the top connection extended about 1-1/2 inches through the column flange. Overall failure had not taken place at the end of 21 cycles of loading.

For connection R3-2, a crack initiated at the weld root between the top cover plate and the beam flange. This crack eventually extended through the column flange and intersected with a secondary crack that had initiated at the weld access hole adjacent to the toe of the continuity plate weld. The crack at the access hole had the appearance of stable growth, before it intersected with the flange crack. Following intersection of the cracks, the fracture extended from the top continuity plate towards the bottom continuity plate.

00557

Figures 55 through 58 show various views of the cracks that were found during the post-test evaluation of specimen R3-1, and Figs. 59 through 65 give similar data for specimen R3-2.

Specifically, Figs. 55 and 56 show the cover plate to beam flange interface crack for R3-1. Figure 57 shows the sectioned top cover plate location for R3-1, including the interface crack (A). Arrow B shows a small crack that was found in the fillet weld for the continuity plate. *This demonstrates that the crack arrested and never went completely through the flange, which explains why this connection did not fail.* There were no welding anomalies. Figure 58 shows the exposed crack in R3-1, with arrows indicating the origin of the crack along the root of the weld. The dashed line separates the flange and weld materials.

Figures 59 through 65 show a variety of views of specimen R3-2 after failure. Specifically, Fig. 59 illustrates the fractured cover plate and flange of this connection, Fig. 60 shows the fracture path along the k-region of the connection, and Fig. 61 shows the cracked locations at the bottom cover plate and the bottom continuity plate.

Figures 62 and 63 show that the location of the secondary crack initiation for R3-2 was at the continuity plate weld that coincided with the k-region. The fracture markings indicate that the crack started at the intersection of the continuity plate fillet weld and the k-region, as shown in Fig. 62. Additional fractographic evaluation shows that there were numerous (7 in total) crack arrest marks; these are delineated in Fig. 62 and especially in Fig. 63. This indicates that the crack had been propagating for at least 7 cycles, meaning that the initiation occurred before the 20th cycle. This is consistent with the results for specimens R2 and R3-1, for which crack initiation

occurred after 10 cycles. These results also indicate that the k-region cracking at the weld for the continuity plate is a secondary fracture, and therefore not a primary failure location. *Finally, although the crack was propagating in the k-region, the arrest marks demonstrate that this was a slow and ductile cracking phenomenon.*

Additional fracture data are illustrated in the photographs of Figs. 64 and 65. Both show clear crack arrest marks. Figure 66 is a schematic illustration of the crack locations, crack depths and crack lengths for connections R3-1 and R3-2.

11.3 Assessment of Performance

Table 11 summarizes the test performance data for the revised as-built connections Type 3. Additional comments are given in the following.

Table 11

Summary of Performance Data for Tests of Revised As-Built Connections Type 3¹

Test No.	Load. Prot.	Plastic Rot θ_p (max./min.) (radians)	Cumul. Plastic Rotat. Θ_p	Norm. Plastic Rot. η	Full cycles at θ_p	FEMA Crit ² . Met ?
R3-1	D	0.038 0.037	1.004	97.4	3 ³	Yes
R3-2	D	0.038 0.040	1.840 ⁴	178.7	8	Yes

6509

Notes for Table 11

- Note 1 The columns for Specimens R3-1 and R3-2 were rotary straightened.
- Note 2 FEMA requirement for new construction: a minimum of one full cycle at plastic rotation 0.030 radians
- Note 3 The test of specimen R3-1 was terminated after 21 complete cycles without connection failure
- Note 4 In comparison with the test data for Specimen R3-1, Specimen R3-2 had cumulative plastic rotations of +0.985 and -0.986 after 21 cycles. This correlates closely with the results for R3-1.

The excellent performance of Connections R3-1 and R3-2 point to a number of significant observations. Primary among these is the fact that crack initiation did not occur in the k-region, but at the toe of the cover plate weld. A secondary crack did initiate in the k-region, but this propagated in a stable manner until it intersected with the crack from the toe of the cover plate weld. The stable crack growth in the k-region negates the perceived problem that the k-region and its high hardness and low toughness will always result in unstable brittle fracture. Further, some of the cracking initiated in the near vicinity of the continuity plate access holes. It is therefore clear that enlarging these access holes to move the weld termination farther away from the k-region will offer additional performance benefits. In other words, detailing continues to be a major issue for connections.

The effect of the slight relocation of the continuity plates further emphasizes the critical nature of the connection detailing. By providing for improved load paths in the connection, the rotation capacity and endurance of the assembly were increased very significantly.

Finally, two identical and very complex assemblies were tested, for which a large

number of parameters could influence the final results. The close correlation between the two tests is further testament to the quality of the materials and the connection design and fabrication as a whole.

12. REVIEW OF OVERALL TEST PROGRAM AND CONNECTION PERFORMANCE: CONCLUSIONS AND RECOMMENDATIONS

12.1 Connection Testing Program

An extensive series of 17 full-scale beam-to-column connection tests were conducted. Using a strong beam, weak column panel zone design concept, the intent of the research program was to examine the performance of the steel in the columns in a *variety of connection types. Further, the effects of steel mill straightening practices* were evaluated through the use of rotary straightened, gag straightened and unstraightened columns.

The specimens included flange and cover-plate complete joint penetration (CJP) welded beam to column joints with bolted web connections, and CJP-welded continuity plates. One such connection also had a fillet welded transition between the cover plate and the column flange. Other specimens used thinner cover plates and fillet welded continuity plates. Finally, two specimens used the thinner cover plates and fillet welded continuity plates, in addition to the transition fillet weld, and the continuity plates were repositioned.

Eight of the 17 connection specimens in the program were tested under quasi-static, displacement-controlled loading conditions. The other nine specimens were tested under 1 Hz dynamic loading, also using displacement-controlled amplitudes. The results show that dynamic loading is a more severe condition, but the differences in

performance between otherwise identical specimens are not significant. Since dynamic testing is more difficult to perform and also demands testing equipment of much higher hydraulic capacity, quasi-static testing appears to be the most practical approach for full-scale connection testing.

12.2 Measurements of Plastic Rotation Capacity

Current practice among researchers in the United States is to assess the seismic performance of a steel beam-to-column connection by its ability to undergo certain amounts of plastic rotation during cyclic testing. Further, the recommendations differentiate between the response of as-built or rehabilitated connections and new construction. The governing criteria focus on the ability of a connection to sustain the required minimum plastic rotation in one complete cycle of loading.

Whereas the single cycle plastic rotation certainly is one measure of ductility and deformation capacity, it does not reflect the energy absorption characteristics of a connection. The cumulative and normalized cumulative plastic rotation capacities are significantly better and more realistic measures of performance. Such data have been determined for all of the connections in this research program. It is recommended that future connection tests should report these data, for improved connection performance assessment.

12.3 Performance of As-Built Connections

The as-built connection design allows for adequate performance under most circumstances. However, detailing and fabrication are very critical for these connections, especially the use of heavy cover plates and continuity plates, and complete joint penetration welds for the continuity plates. These are neither structurally efficient nor economically fabricated connections. On the whole, the

rigidity of the assembly and the strain demands that are placed on the cover plate welds in particular make this solution less than ideal.

12.4 Performance of Revised Connections

Among the revised as-built connections, it is clear that Type 2 but especially Type 3 offer numerous performance and construction advantages. The tests of the Type 3 specimens demonstrated excellent plastic rotation and energy absorption capacities under the most demanding of testing conditions; their performance outpaced that of all other connections by significant margins.

Fabrication is much easier with the thinner cover plates and fillet welded and repositioned continuity plates. The cropping of the continuity plates appears to be important, to the effect that the ends of the welds should be moved away from the k-area of the column web. Further, suitable preheat and weld sequencing facilitate the shop operations. Overall, fabrication and construction economies are likely to be substantial when the revised Type 3 connections are used.

12.5 Influence of Straightening Protocol

Among the 17 full-scale connection tests that were run under this research program, 13 used columns that had been rotary straightened to the maximum extent possible. Two assemblies utilized gag straightened members, and another two used unstraightened columns. The results show conclusively that the manner of column straightening has no effect on connection performance.

13. REFERENCES

1. American Institute of Steel Construction (AISC) (1994), "Manual of Steel Construction - Load and Resistance Factor Design", Vol. 1, 2nd Edition. AISC, Chicago, Illinois.
2. Structural Engineers Association of California (SEAOC) (1996), "Recommended Lateral Force Requirements and Commentary", 6th Edition. SEAOC, Sacramento, California.
3. American Society for Testing and Materials (ASTM) (1998), "Specification for General Requirements for Rolled Structural Steel Bars, Plates, Shapes and Sheet Piling", ASTM Standard A6. ASTM, Conshohocken, Pennsylvania.
4. American Welding Society (AWS) (1998), "Structural Welding Code", AWS D1.1-98. AWS, Miami, Florida.
5. American Institute of Steel Construction (AISC) (1997), "Seismic Provisions for Structural Steel Buildings", and "Supplement 1 to the 1997 Seismic Provisions" (1999), AISC, Chicago, Illinois.
6. Applied Technology Council (ATC) (1992), "Guidelines for Cyclic Seismic Testing of Components of Steel Structures", ATC Guideline No. ATC-24. ATC, Redwood City, California.
7. Federal Emergency Management Agency (FEMA) (1995), "Interim Guidelines: Evaluation, Repair, Modification and Design of Steel Moment Frames", FEMA Report No. FEMA-267. FEMA, Washington, D.C.
8. Nakashima, M., Suita, K., Morisako, K. and Maruoka, Y. (1998), "Tests of Welded Beam-Column Assemblies. I: Global Behavior", *Journal of Structural Engineering*, ASCE, Vol. 124, No. 11, November (pp. 1236-1244).
9. Strybos, J. W., Ferrell, M., and Benac, D. J. (1997), "Full-Scale Testing of Beam to Column Connections", Report No. 06-8107, Southwest Research Institute, San Antonio, Texas.

- 00564
10. Goland, L. J., Redding, C. D., and Benac, D. J. (1999), "Full-Scale Testing of Beam to Column Connections (Test Specimen Nos. 9-12)", Report No. 18-8540, Southwest Research Institute, San Antonio, Texas.
 11. Goland, L. J., Page, R. A., Redding, C. D., and Benac, D. J. (1999), "Full-Scale Testing of Beam to Column Connections (Test Specimen Nos. 13-17)", Report No. 18-2669, Southwest Research Institute, San Antonio, Texas.
 12. Uang, C. M., and Bondad, D. (1995), "Progress Report on Cyclic Testing of Three Repaired UCSD Specimens", Technical Report, SAC Joint Venture, San Francisco, California.
 13. Dieter, G. E. (1986), "Mechanical Metallurgy", 3rd Edition. McGraw-Hill Book Company, New York, New York.

14. FIGURES

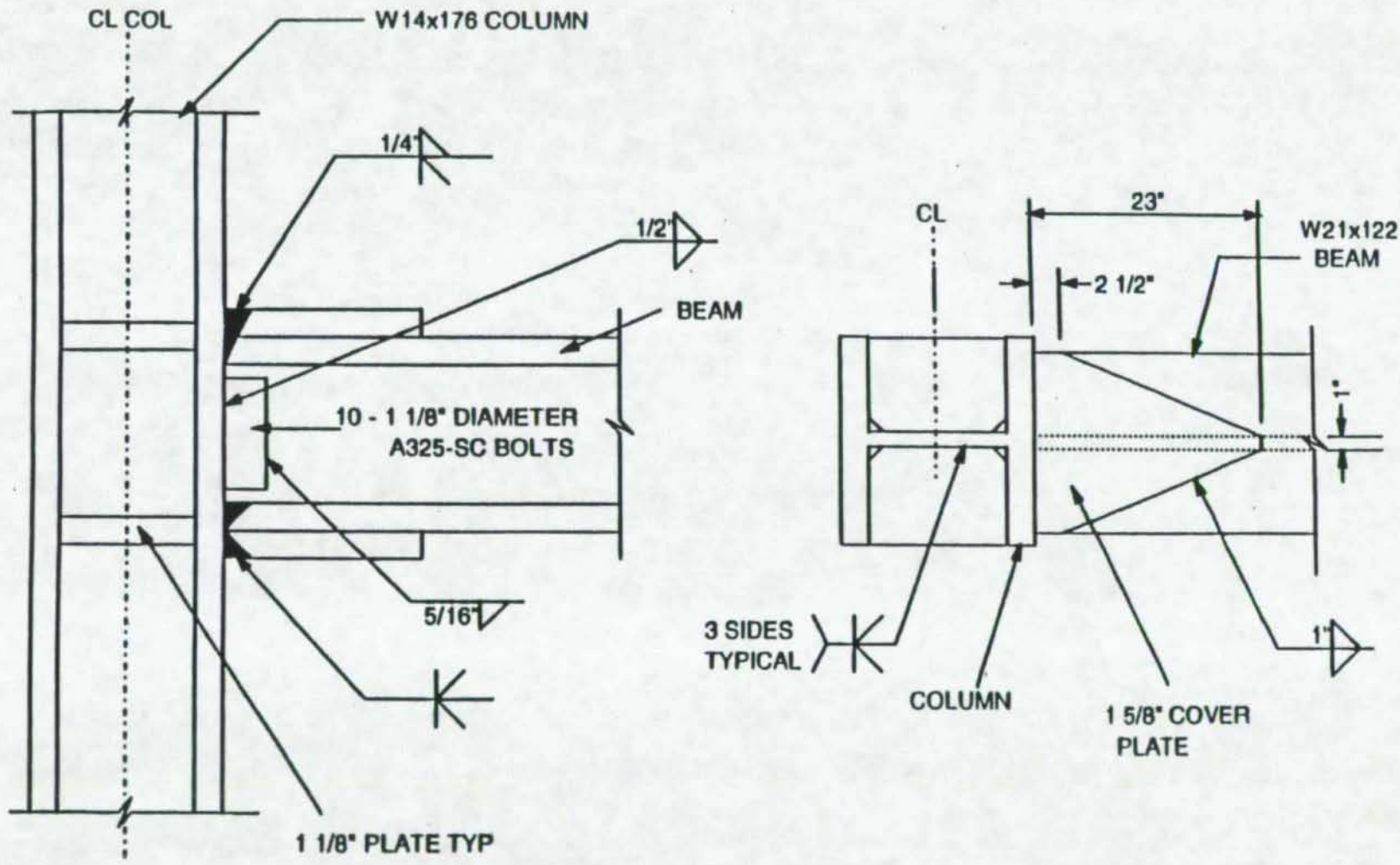
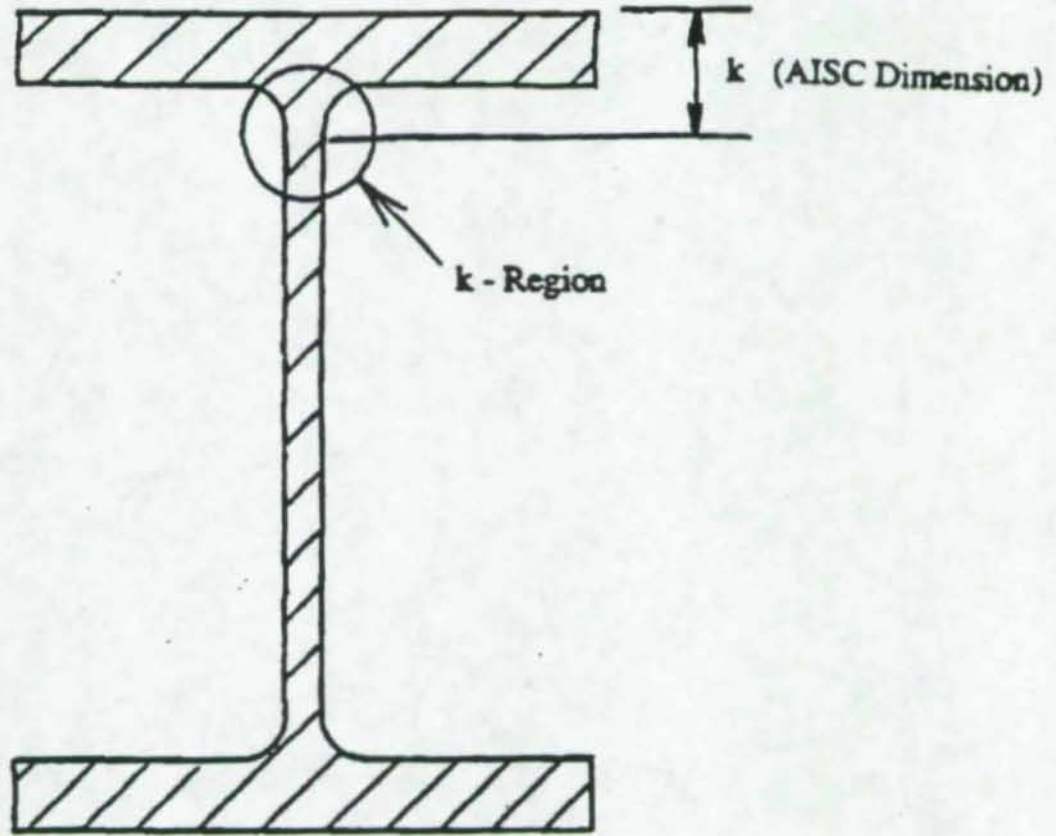


Figure 1 As-Built Connection



I - Beam Cross Section

Figure 2 Location of k-region in W-Shape

- 81 -

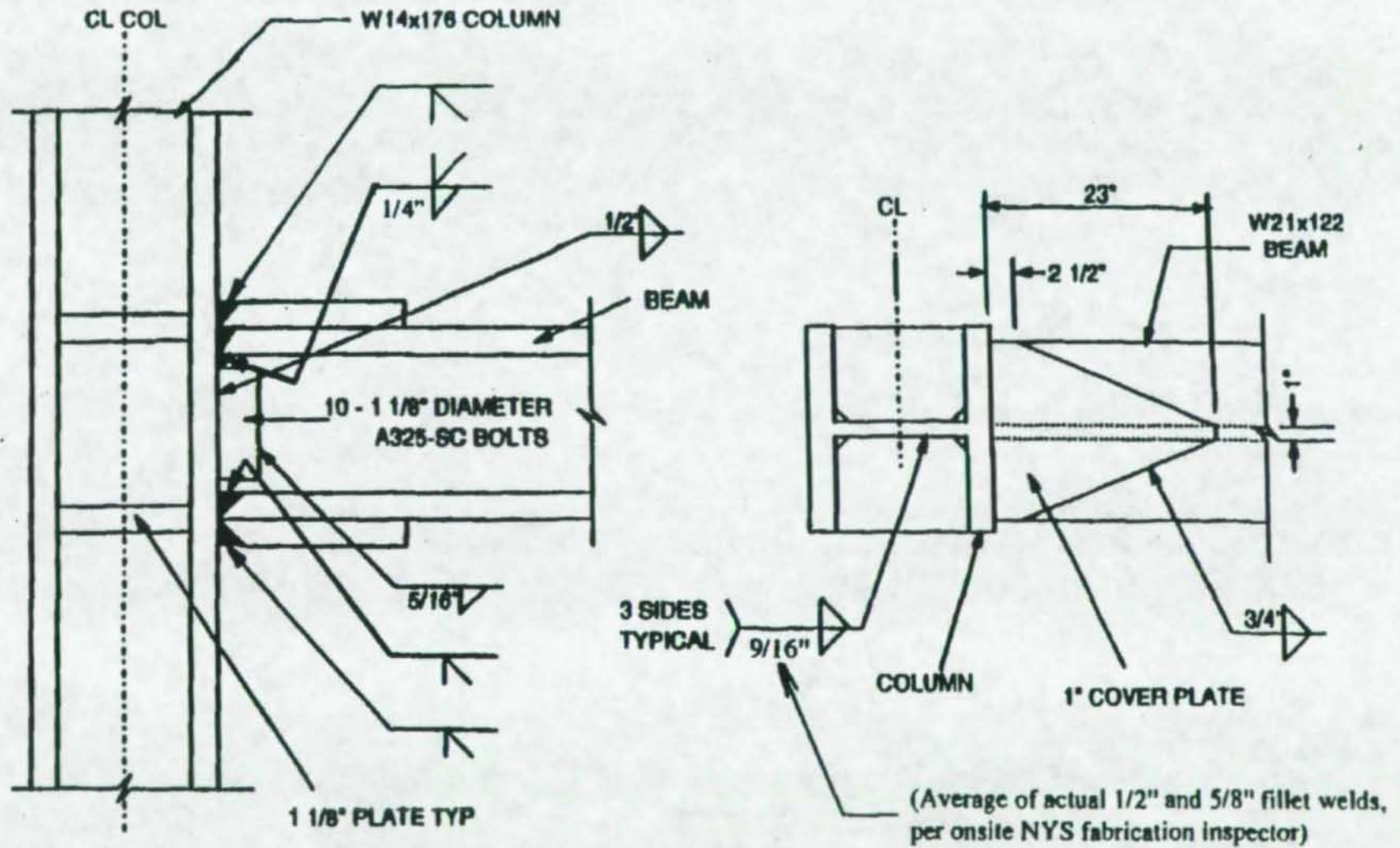


Figure 3 Revised As-Built Connection Type 1

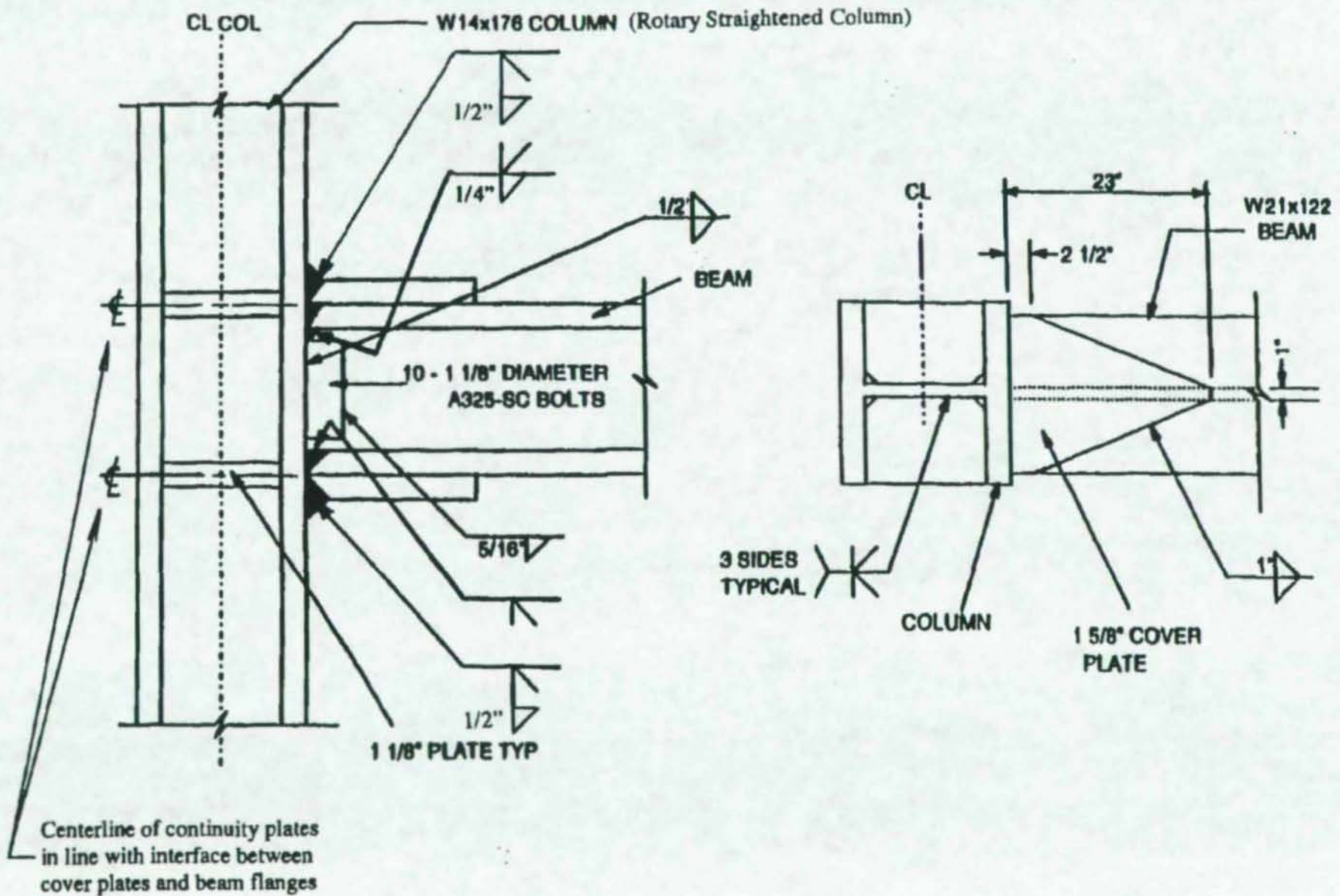


Figure 4 Revised As-Built Connection Type 2

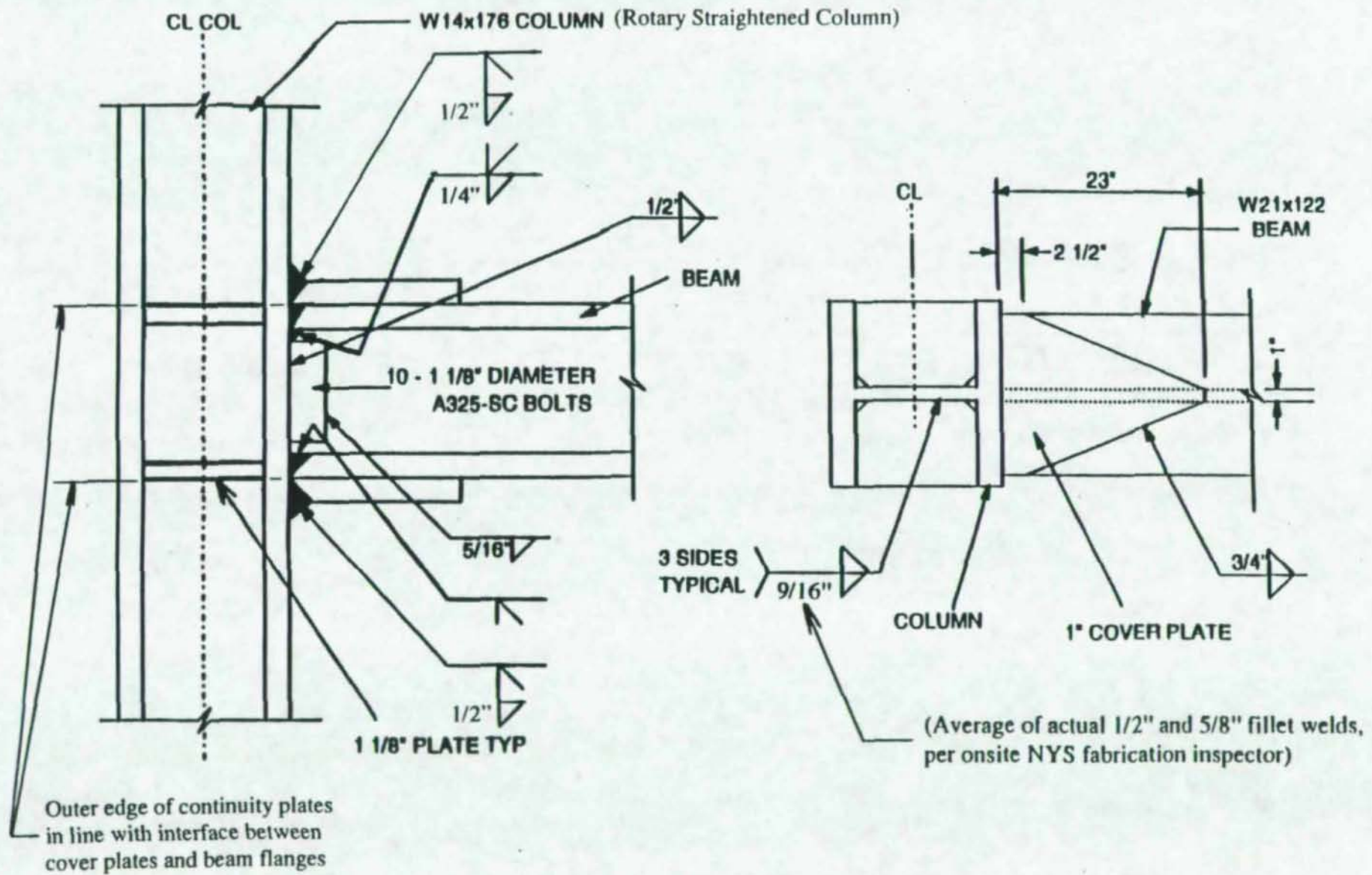


Figure 5 Revised As-Built Connection Type 3

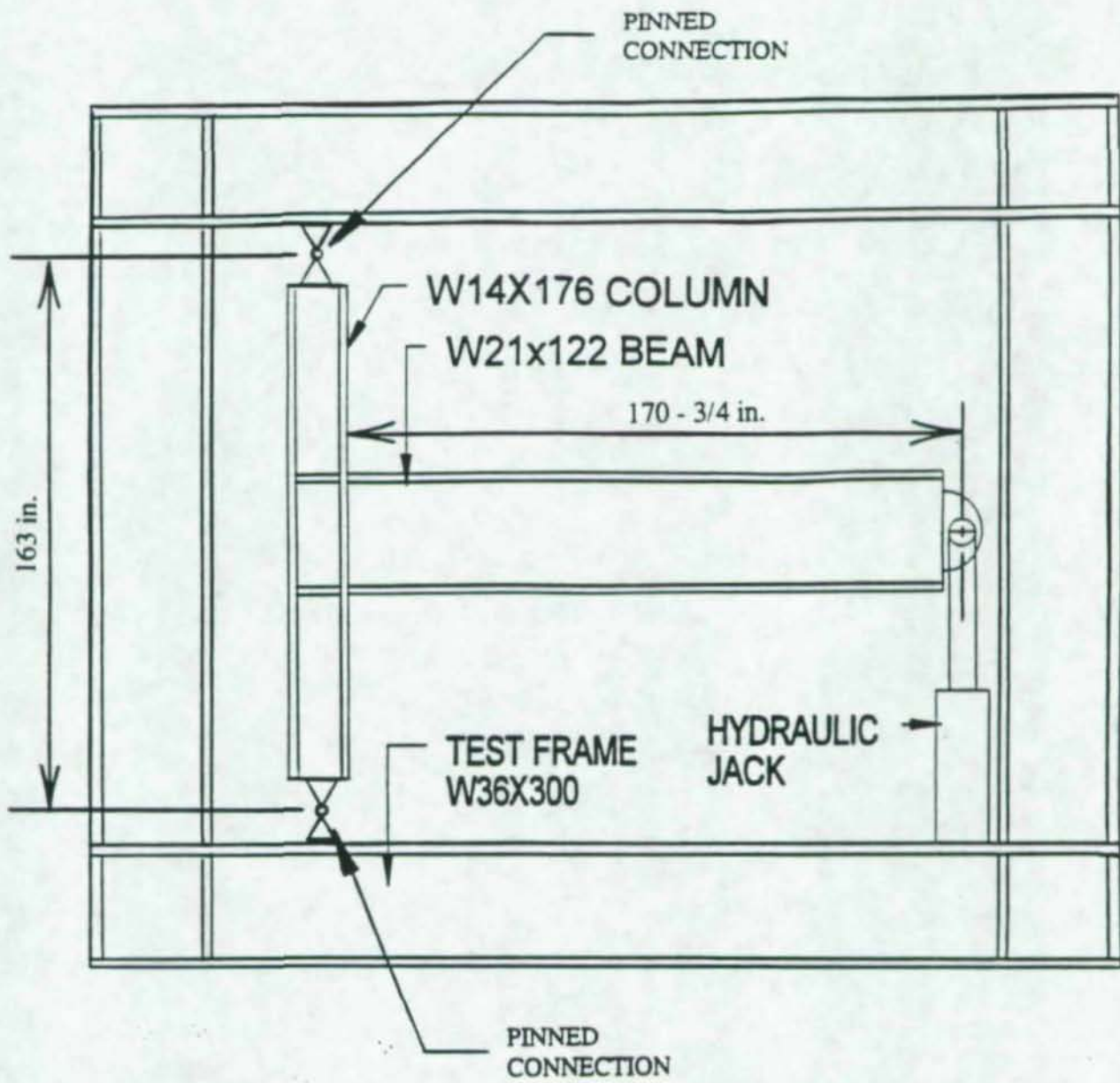


Figure 6 Configuration of Test Frame and Installed Specimen



Figure 7 Photograph of Installed Specimen

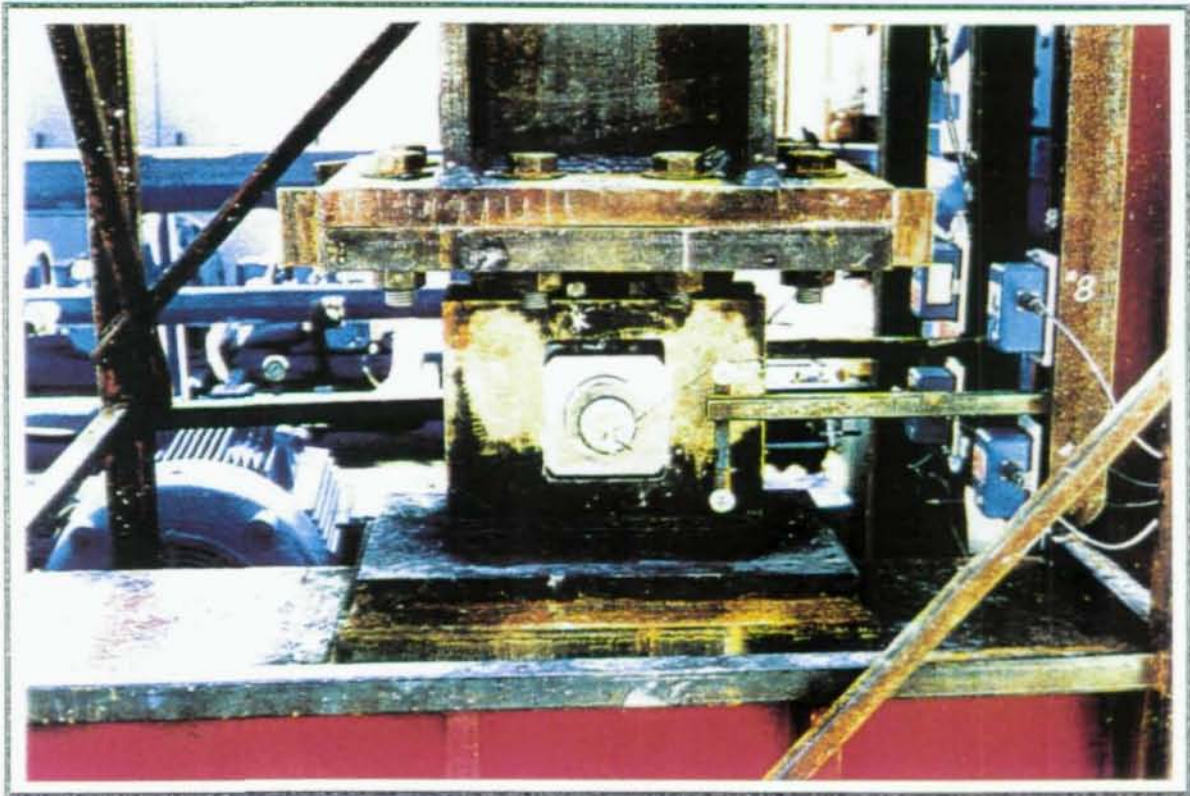
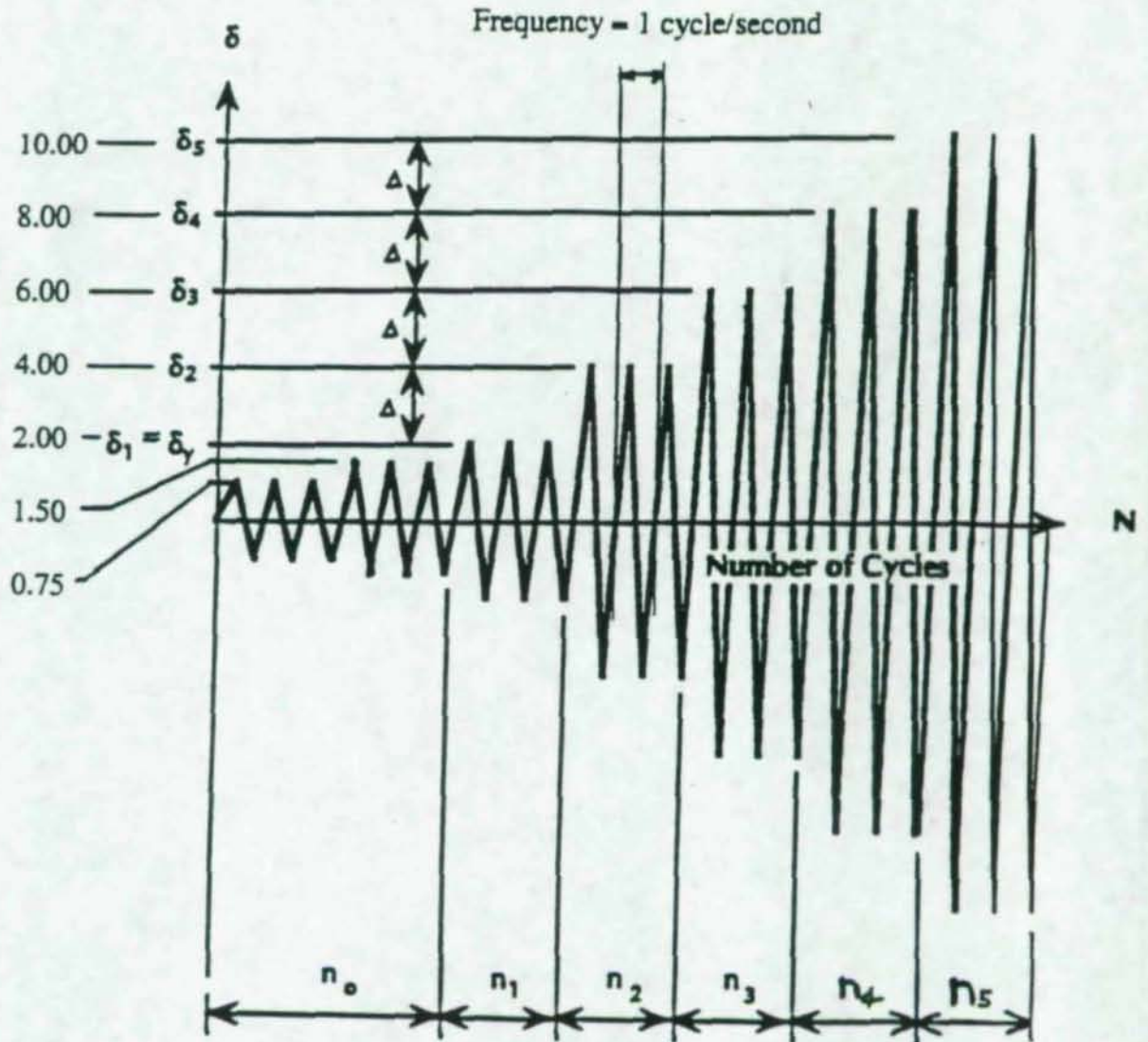


Figure 8 Photograph of Column Pinned Base



Figure 9 Photograph of Actuator and Beam End

Deformation Control Parameter
(Beam Tip Displacement, in.)



Note: 3 cycles at each beam tip displacement.

Figure 10 Beam Tip Cyclic Displacement Profile

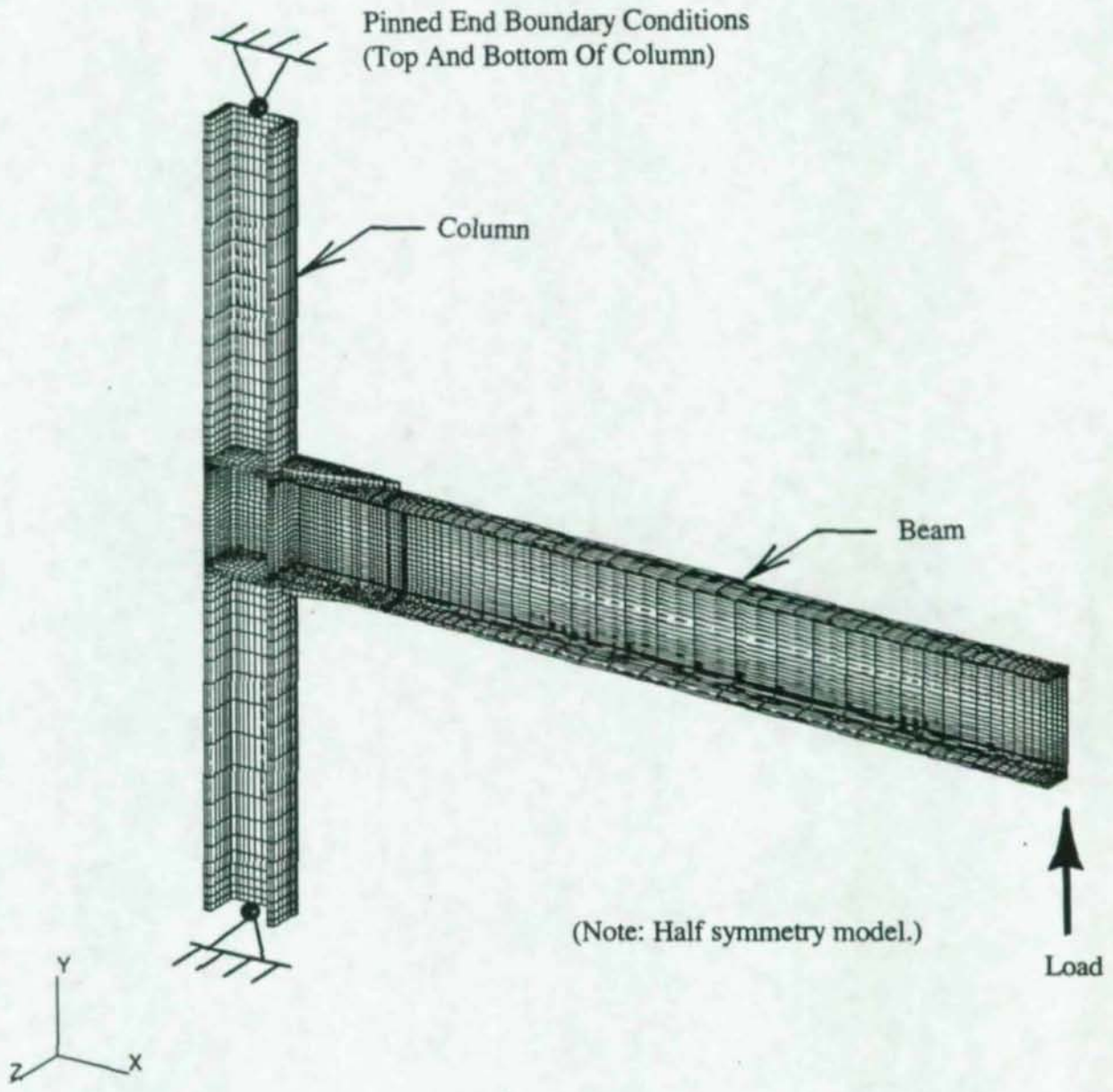


Figure 11 Finite Element Model of Test Specimen

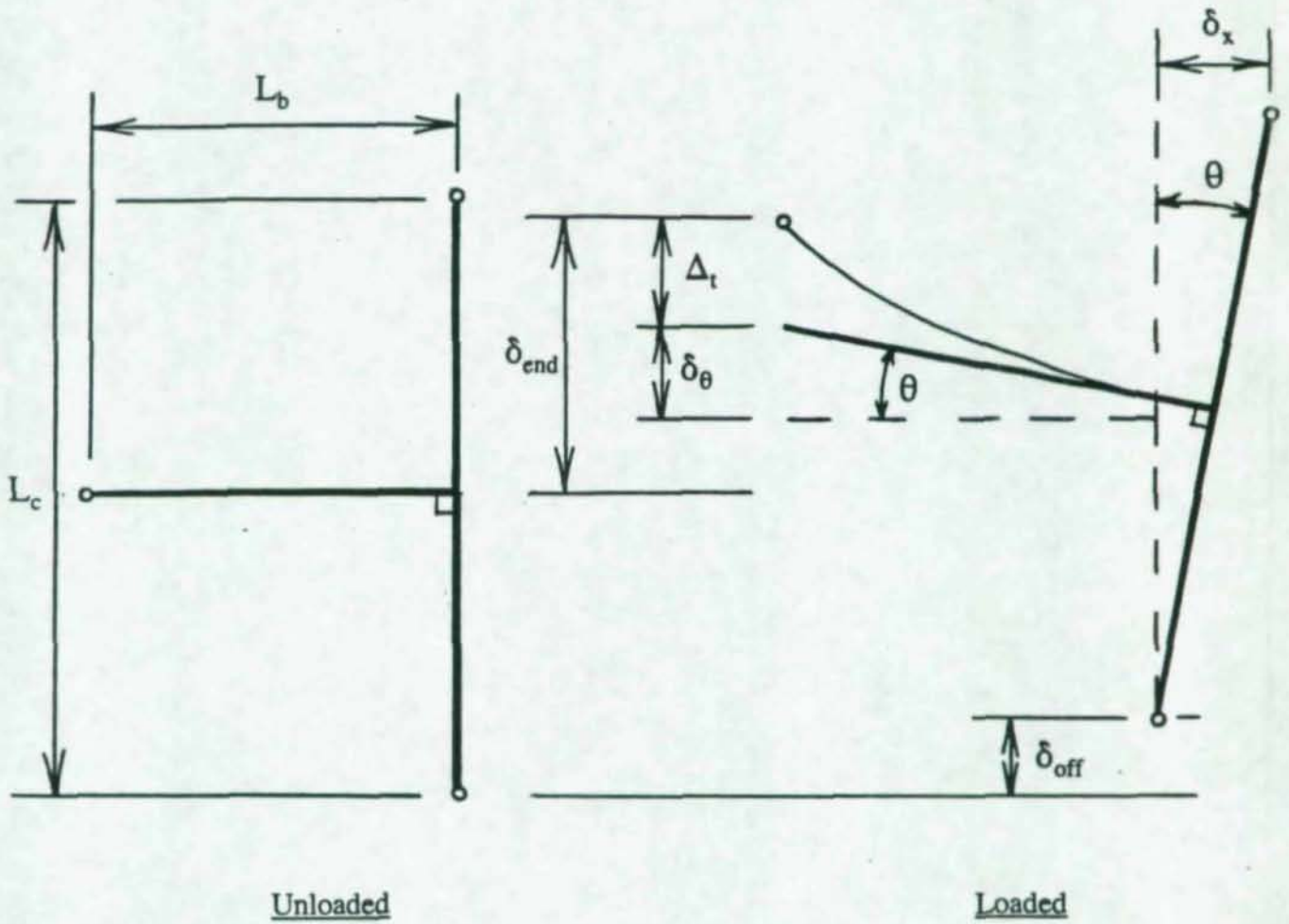


Figure 12 Nomenclature for Beam Tip Displacement Calculations

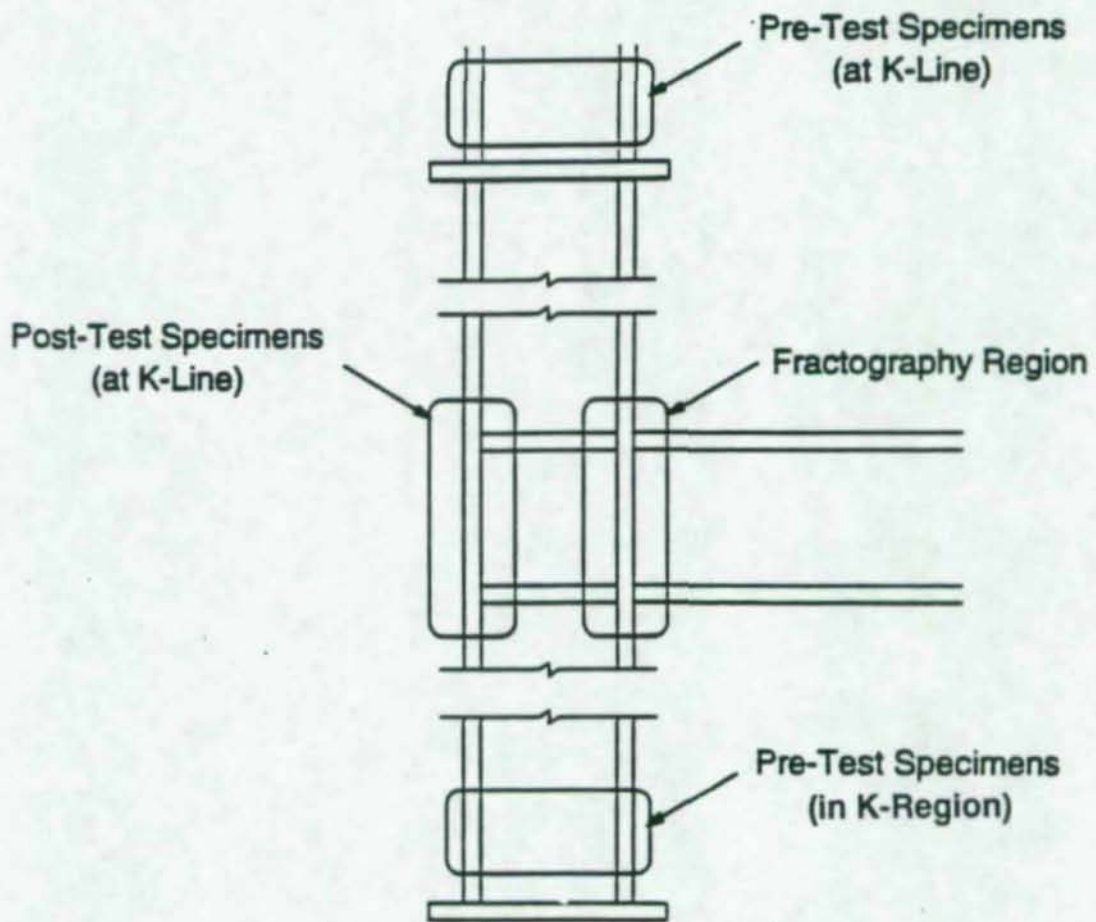
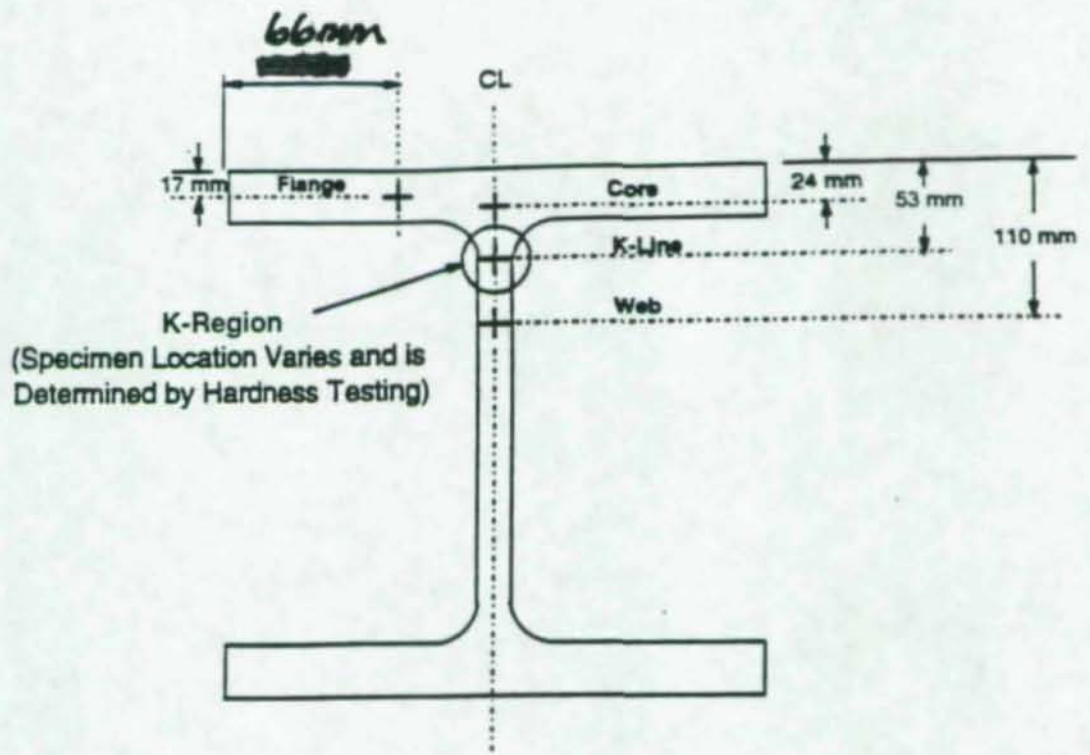
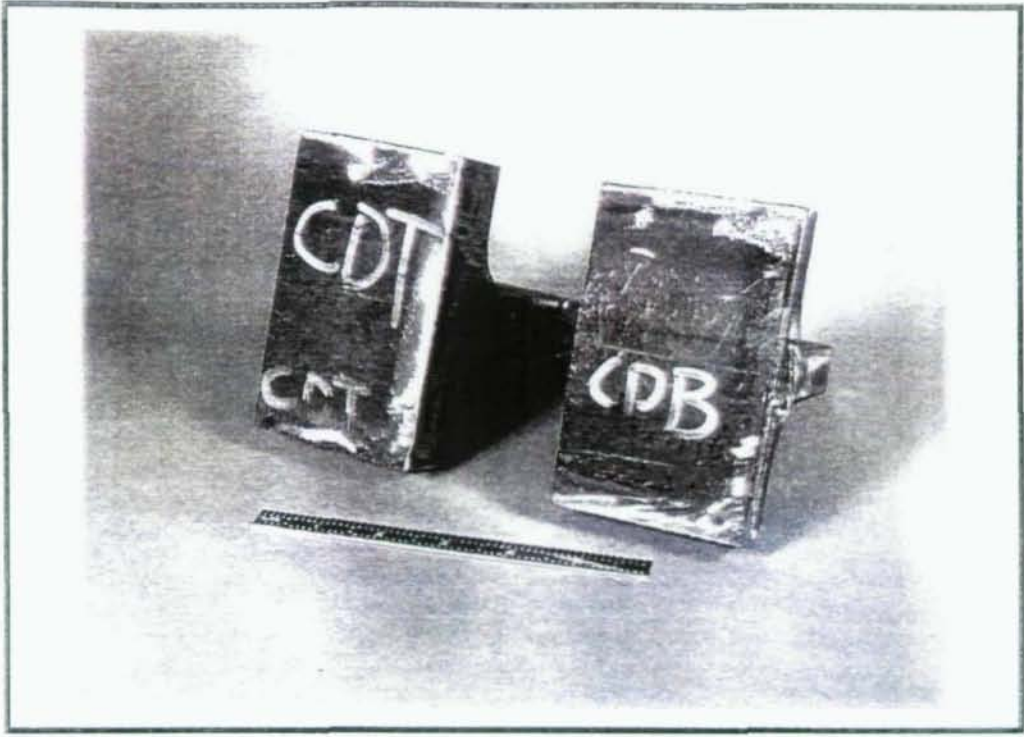
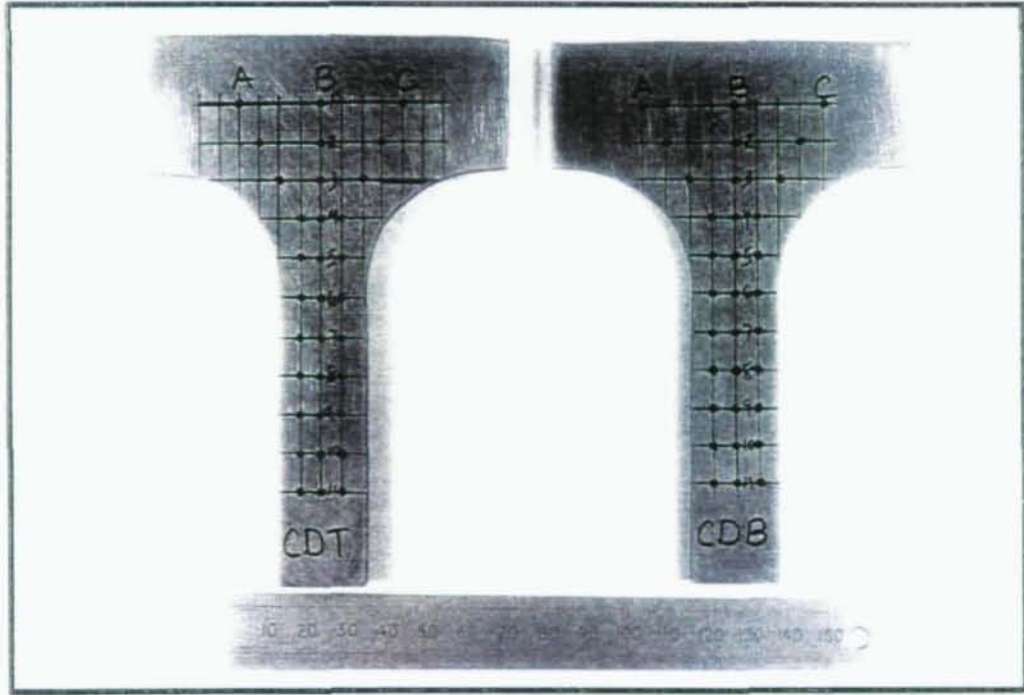


Figure 13 Material Property Specimen Locations in Column



Neg.No.93788

a). *AS-SECTIONED*

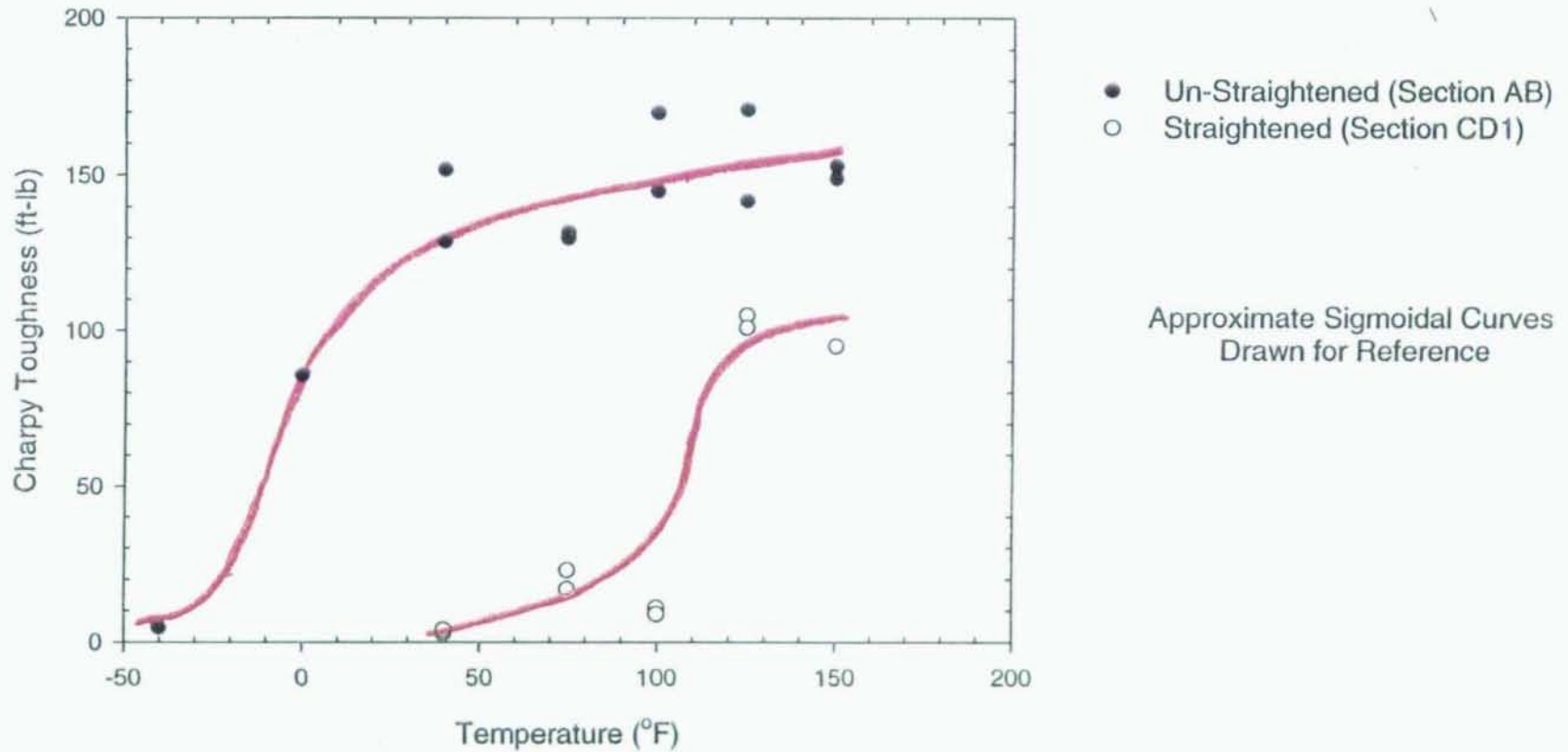


Neg.No.94033

b). *AS. POLISHED*

Figure 14 Photographs of Samples for Hardness Testing

Toughness vs. Temperature in "K-Region" of Column (W14x176)



- 93 -

Figure 15 Toughness vs. Temperature for k-Region of Straightened and Unstraightened Columns

Charpy Transition Curve for the Core and K-line

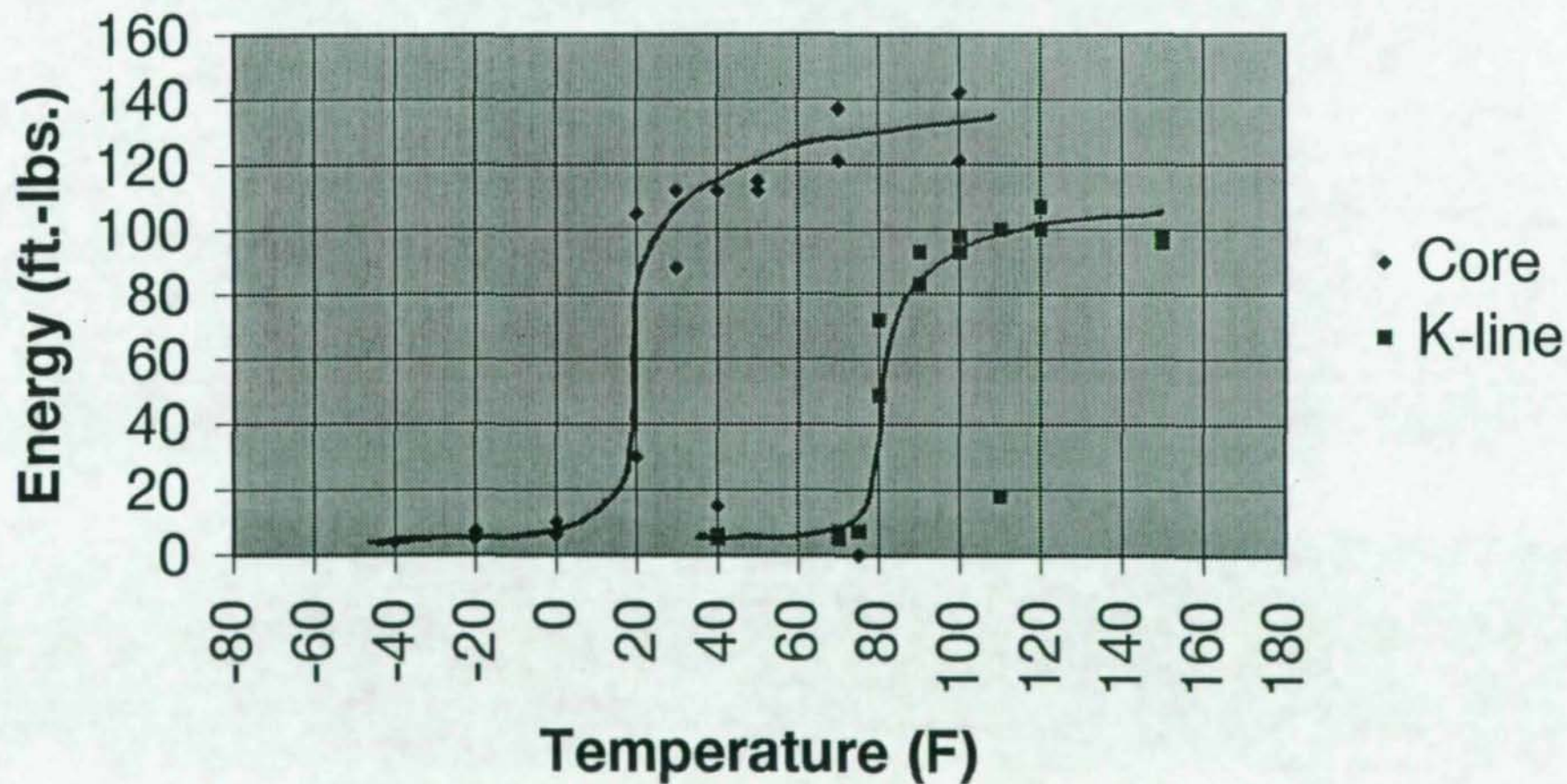


Figure 16 Toughness vs. Temperature for Core and k-Region

Charpy Transition Curves for the Core and k-Region for Section ABR, Rotary-Straightened

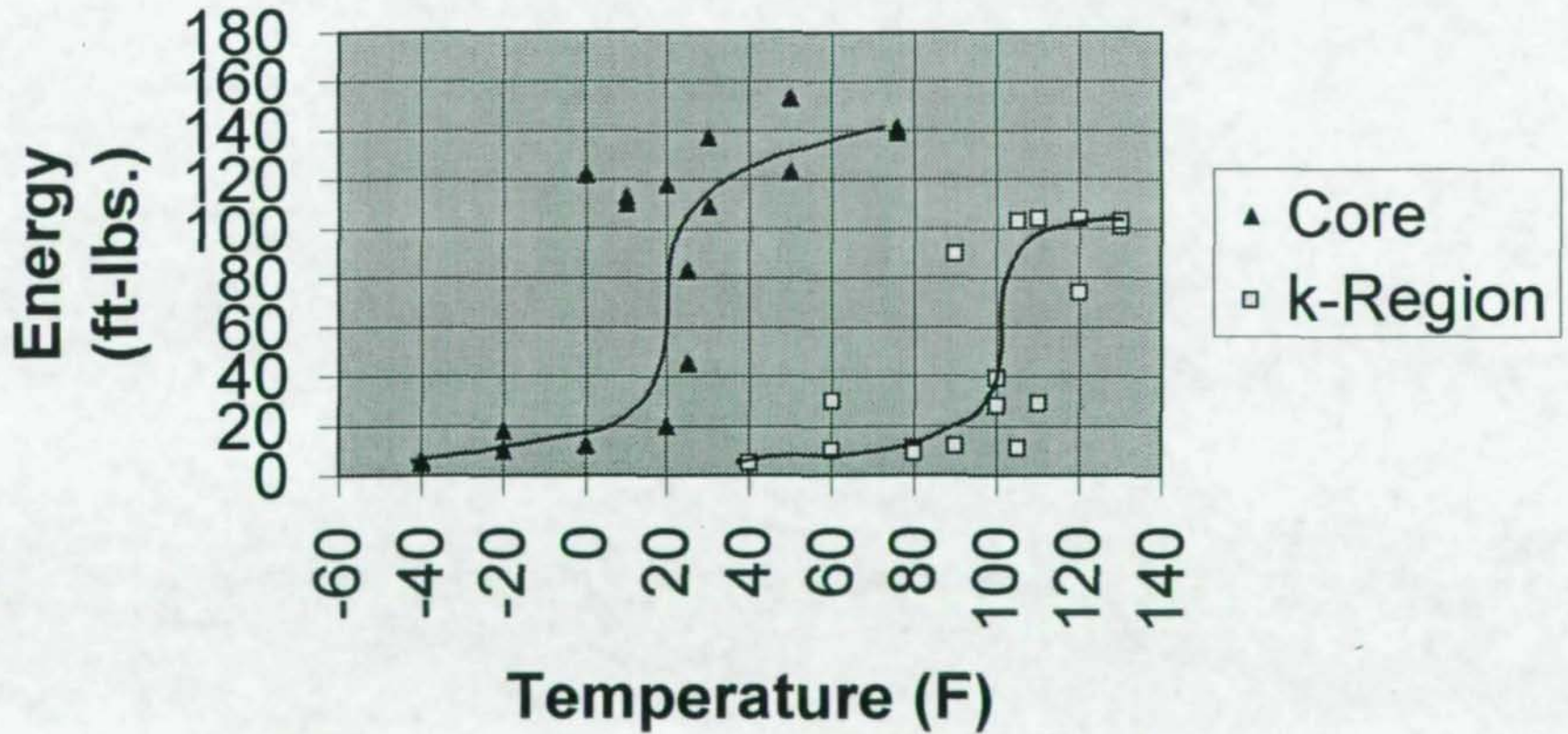


Figure 17 Toughness vs. Temperature for Core and k-Region of Rotary Straightened Column

Charpy Transition Curves for the Core and k-Region for Section ABG, Gag-Straightened

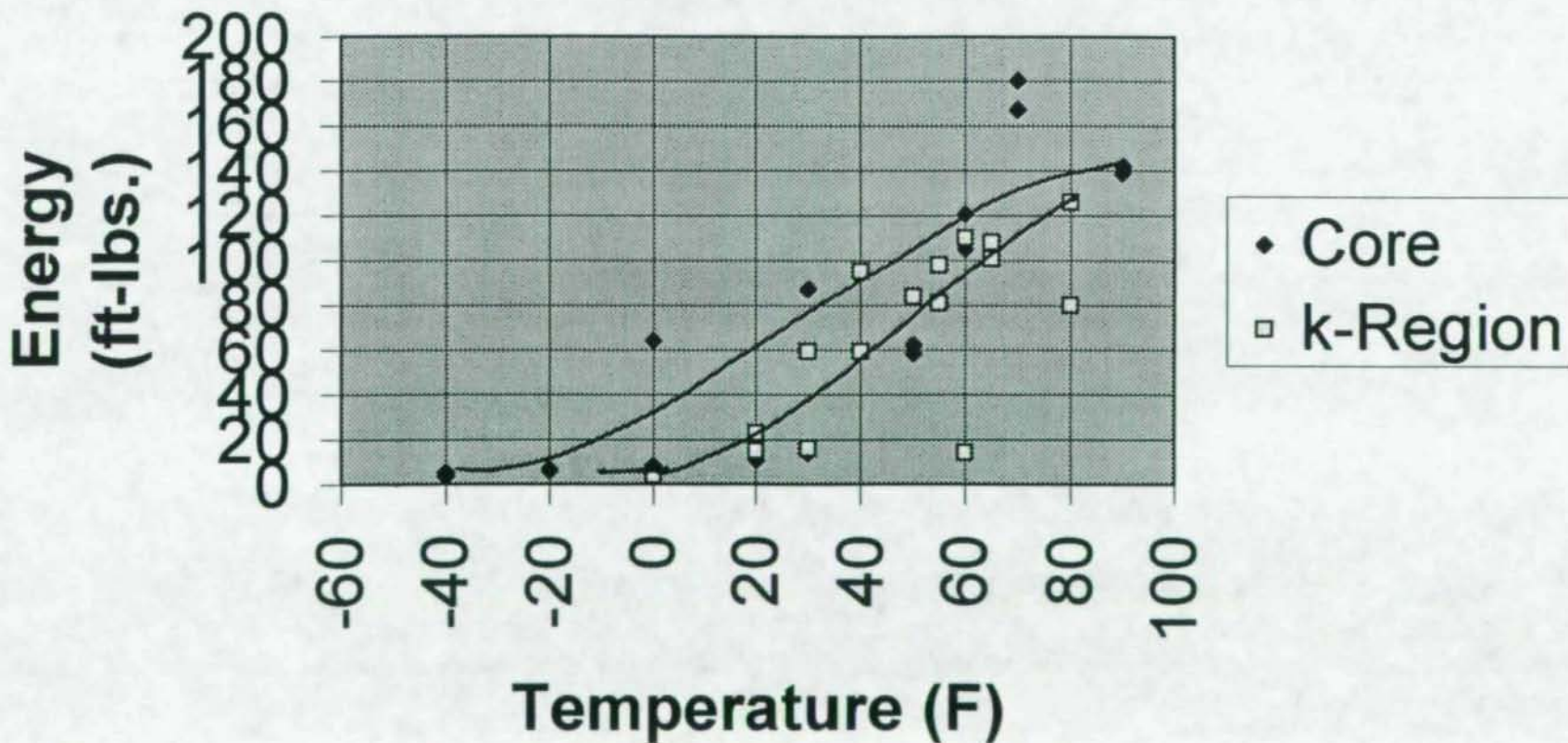
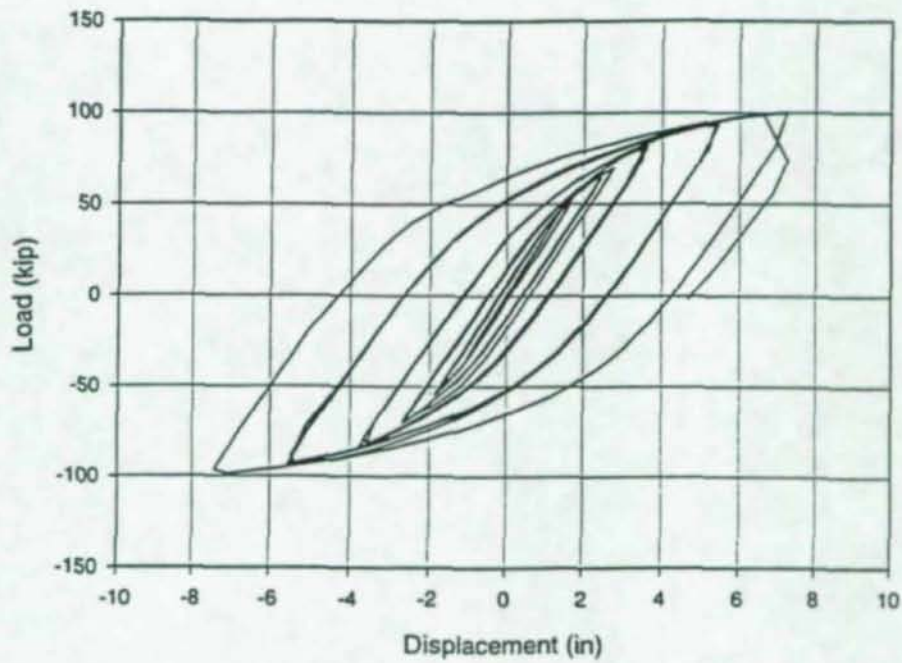
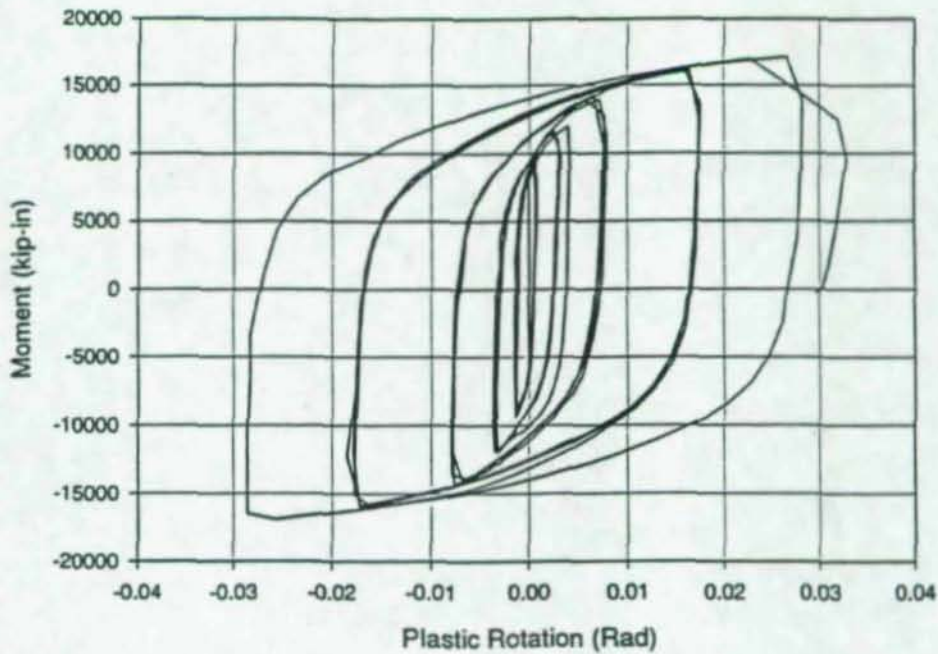


Figure 18 Toughness vs. Temperature for Core and k-Region of Gag Straightened Column

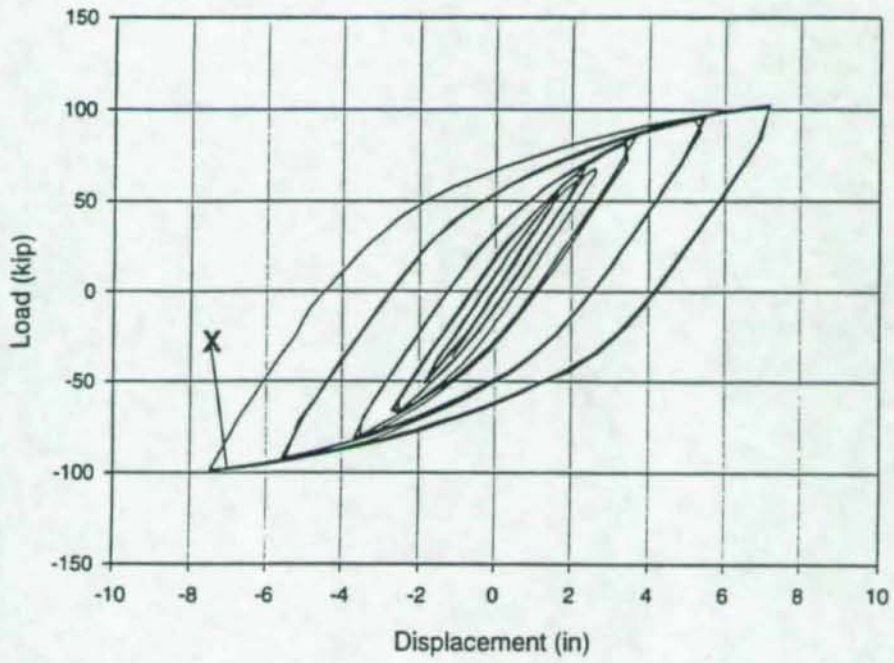


(a)

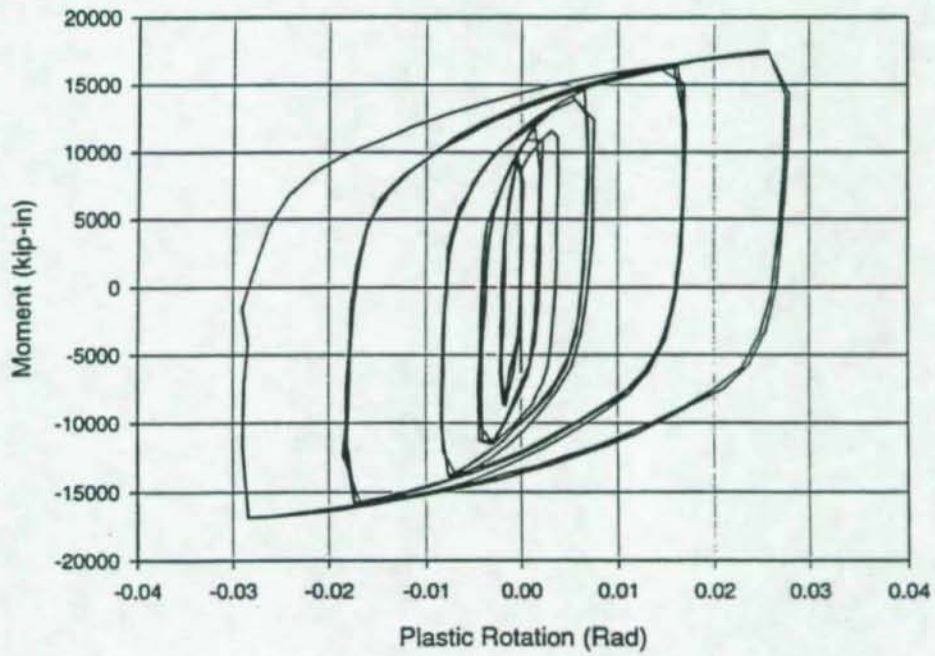


(b)

Figure 19 Load-Displacement and Moment-Plastic Rotation Hysteresis Curves for Specimen A1

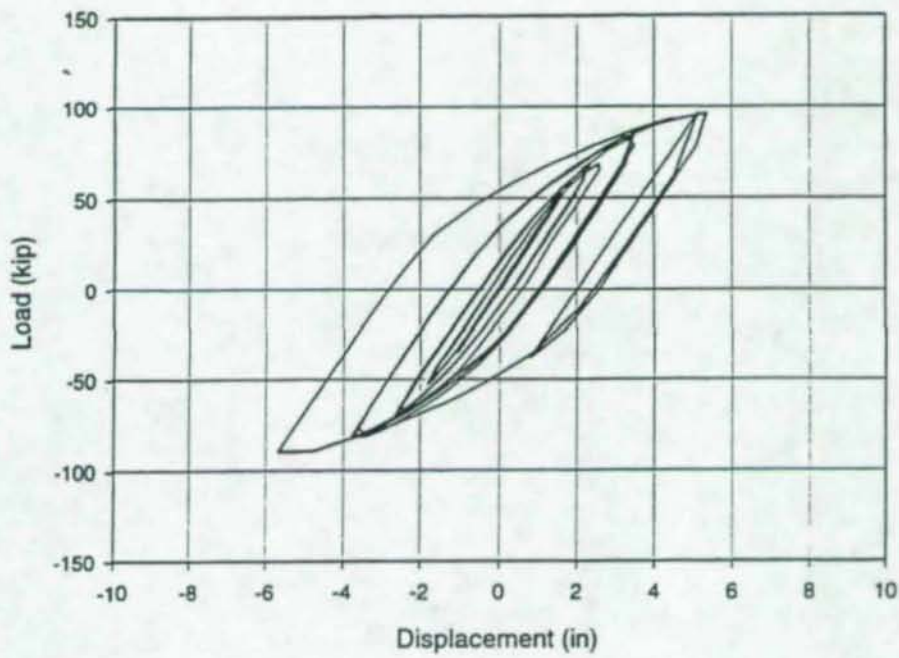


(a)

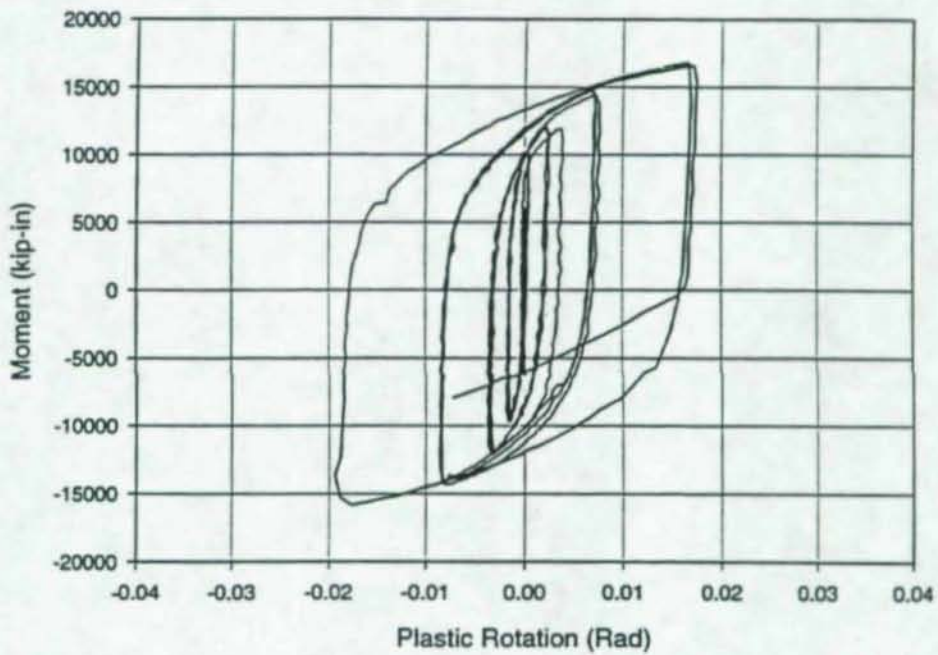


(b)

Figure 20 Load-Displacement and Moment-Plastic Rotation Hysteresis Curves for Specimen A2



(a)



(b)

Figure 21 Load-Displacement and Moment-Plastic Rotation Hysteresis Curves for Specimen A3

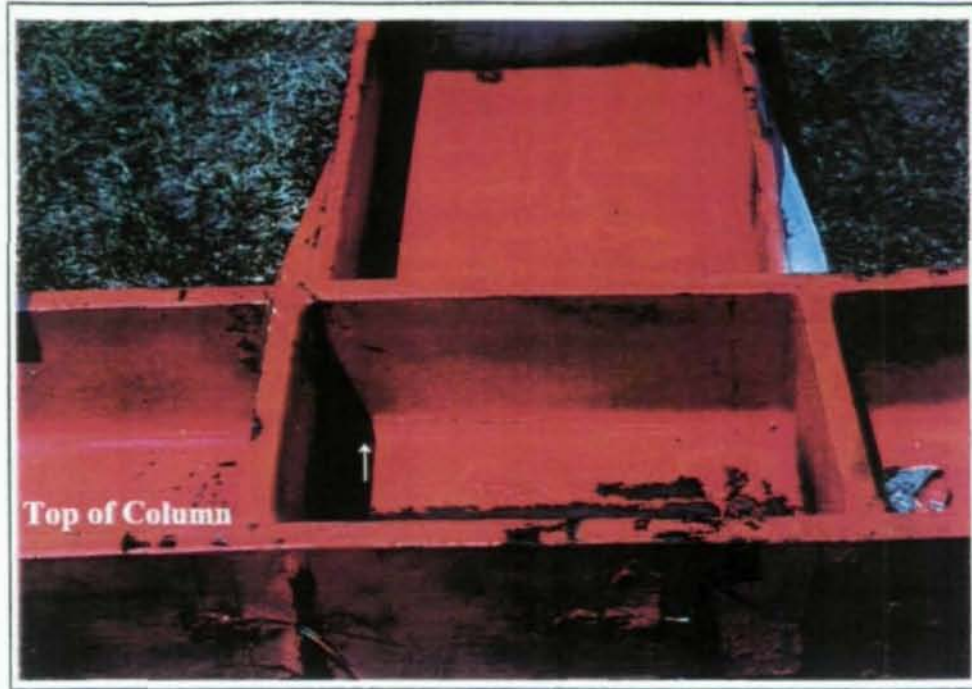


(a)



(b)

Figure 22 Photographs of Cracks in Specimen A1

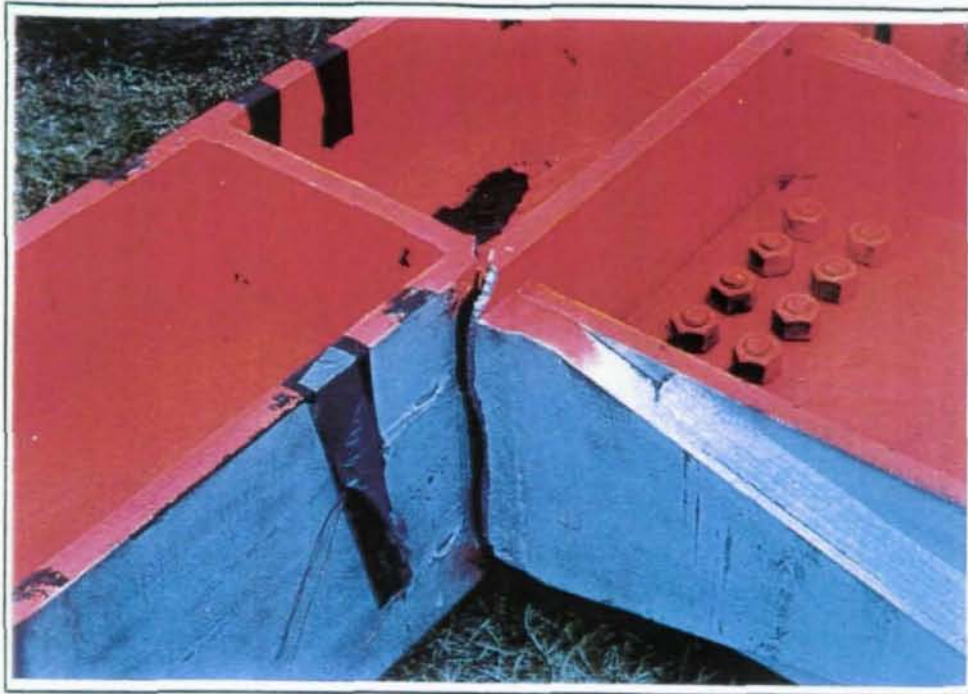


(a)

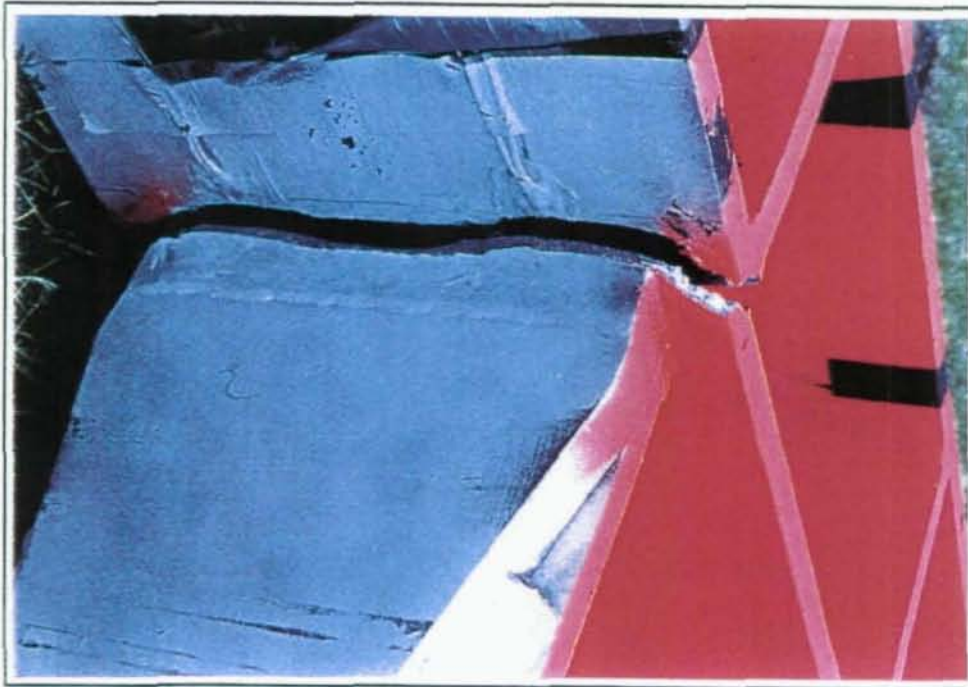


(b)

Figure 23 Photographs of Fractured Specimen A2



(a)



(b)

Figure 24 Photographs of Crack Adjacent to Weld in Specimen A3

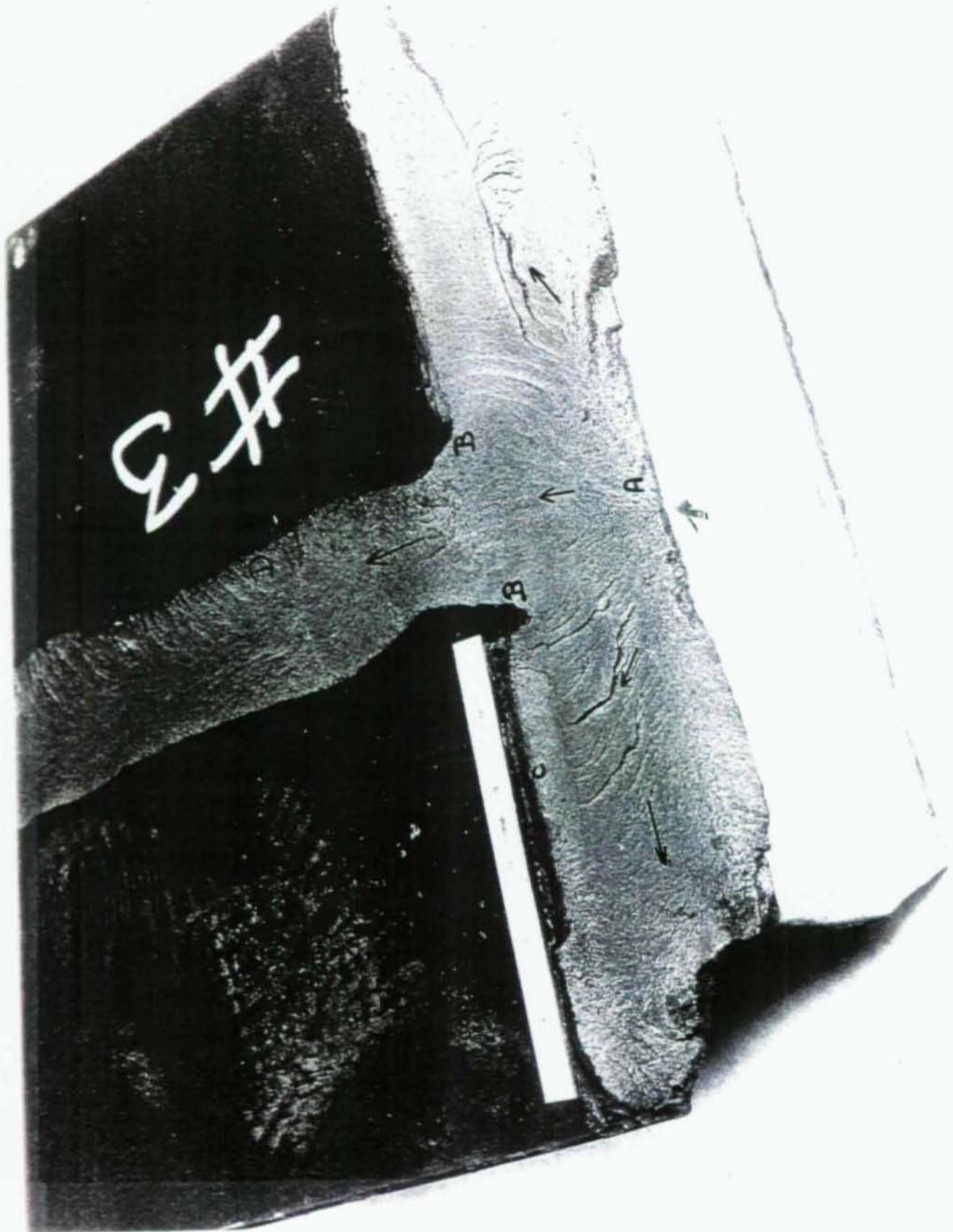
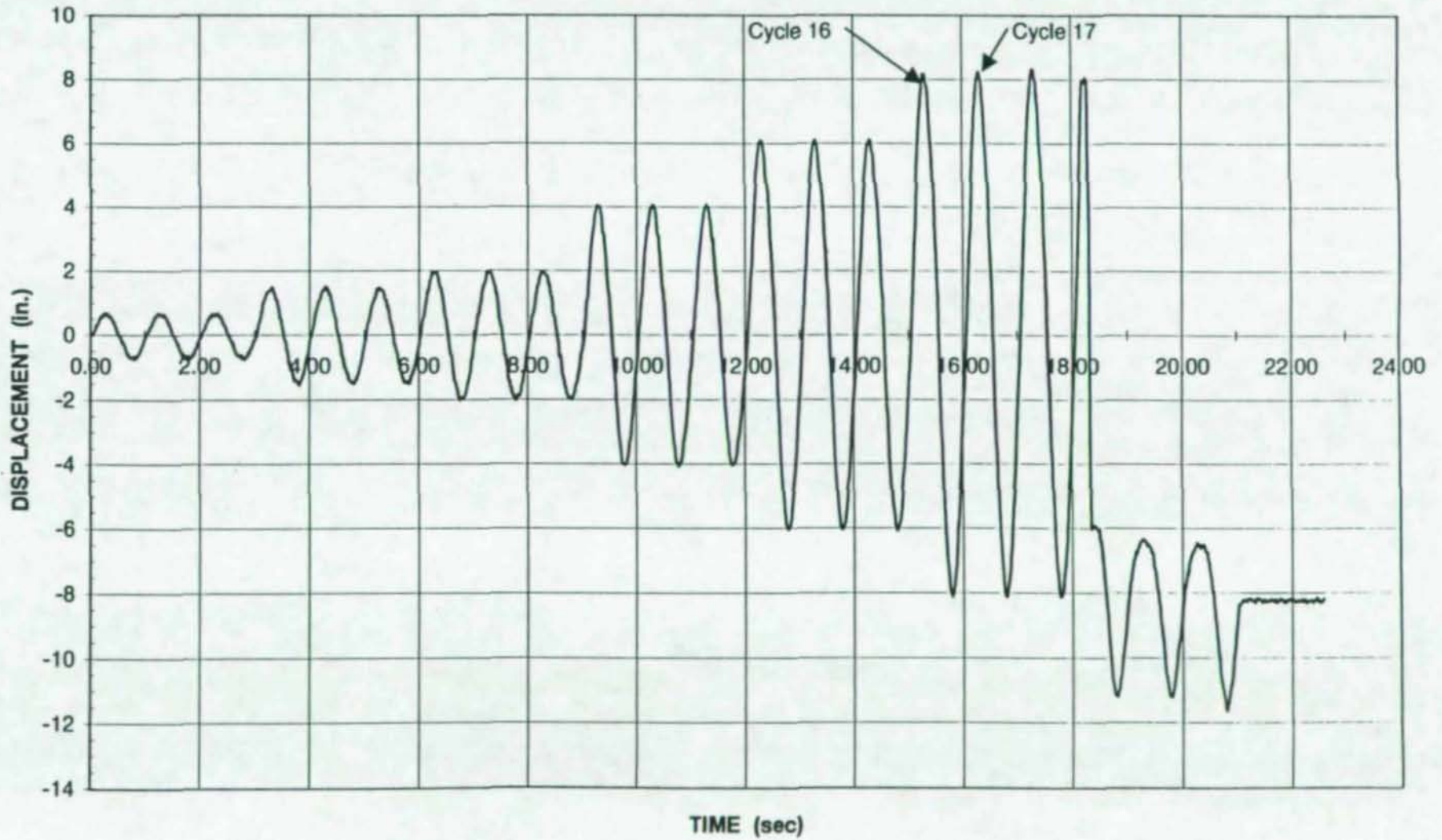


Figure 25 Photograph of Fracture Surface for Specimen A3

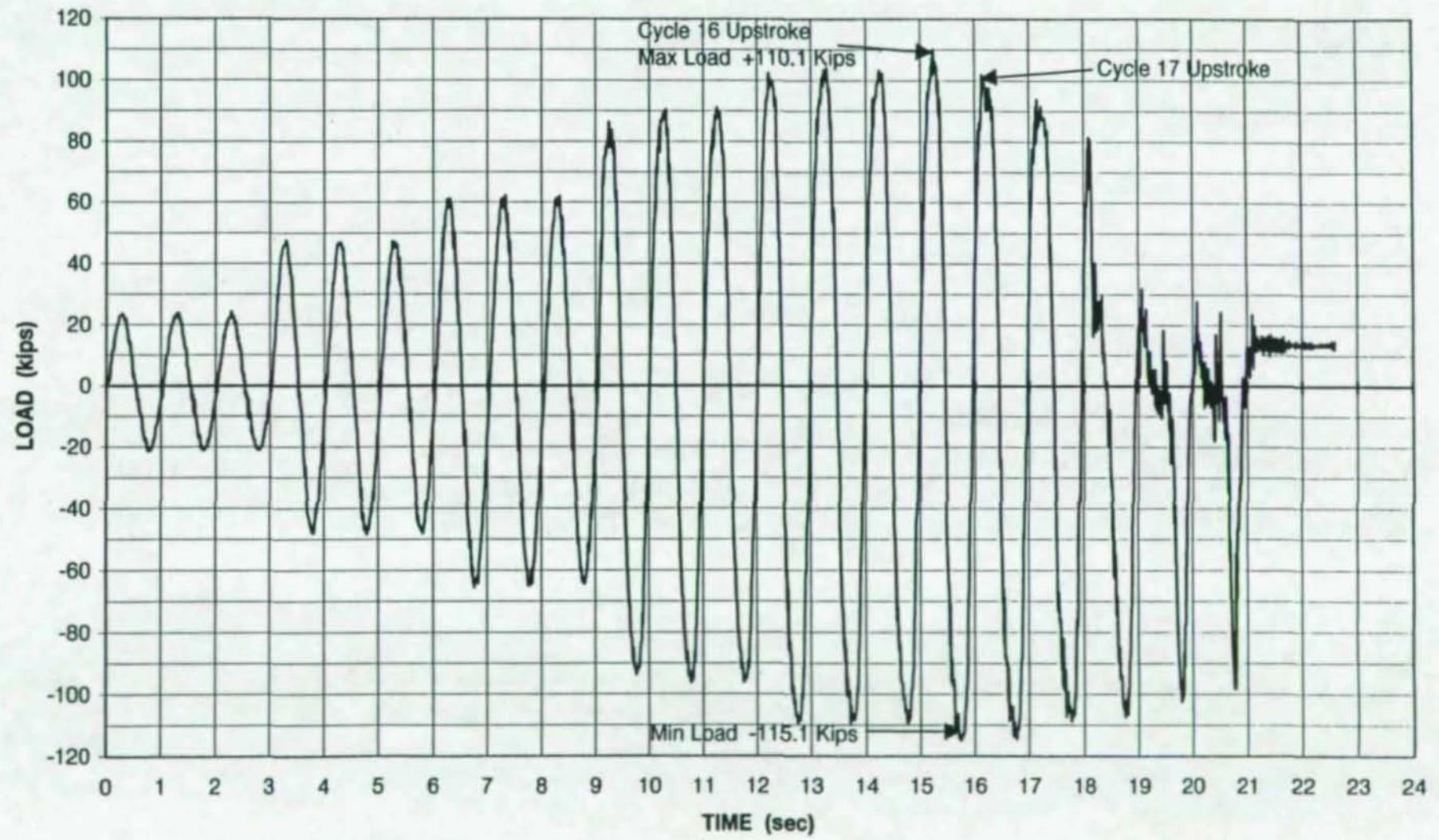
BEAM TIP DISPLACEMENT vs. TIME SPECIMEN NO. 9



- 104 -

Figure 26 Beam Tip Displacement vs. Time for Specimen A4

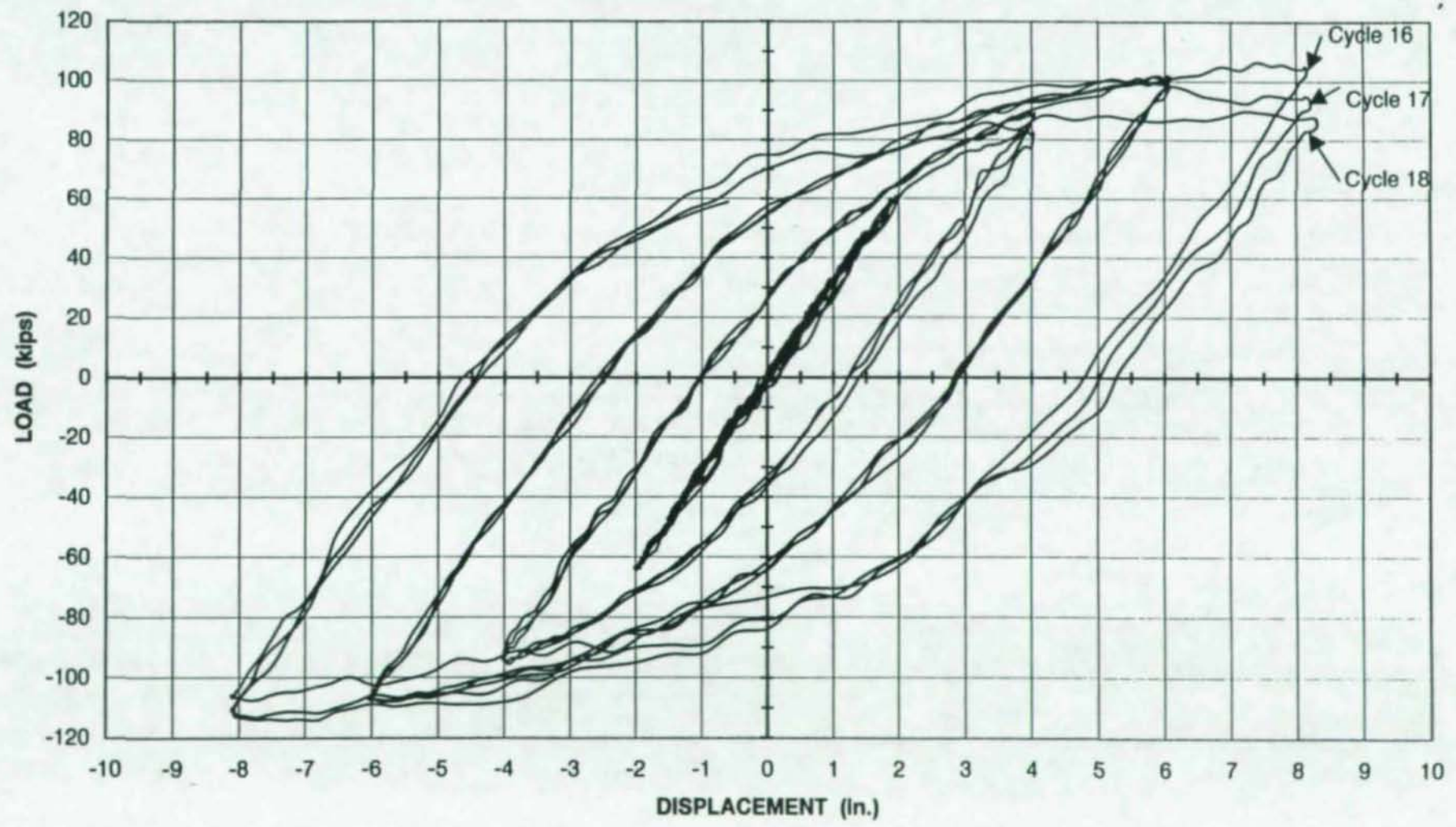
BEAM TIP LOAD vs. TIME SPECIMEN NO. 9



- 105 -

Figure 27 Beam Tip Load vs. Time for Specimen A4

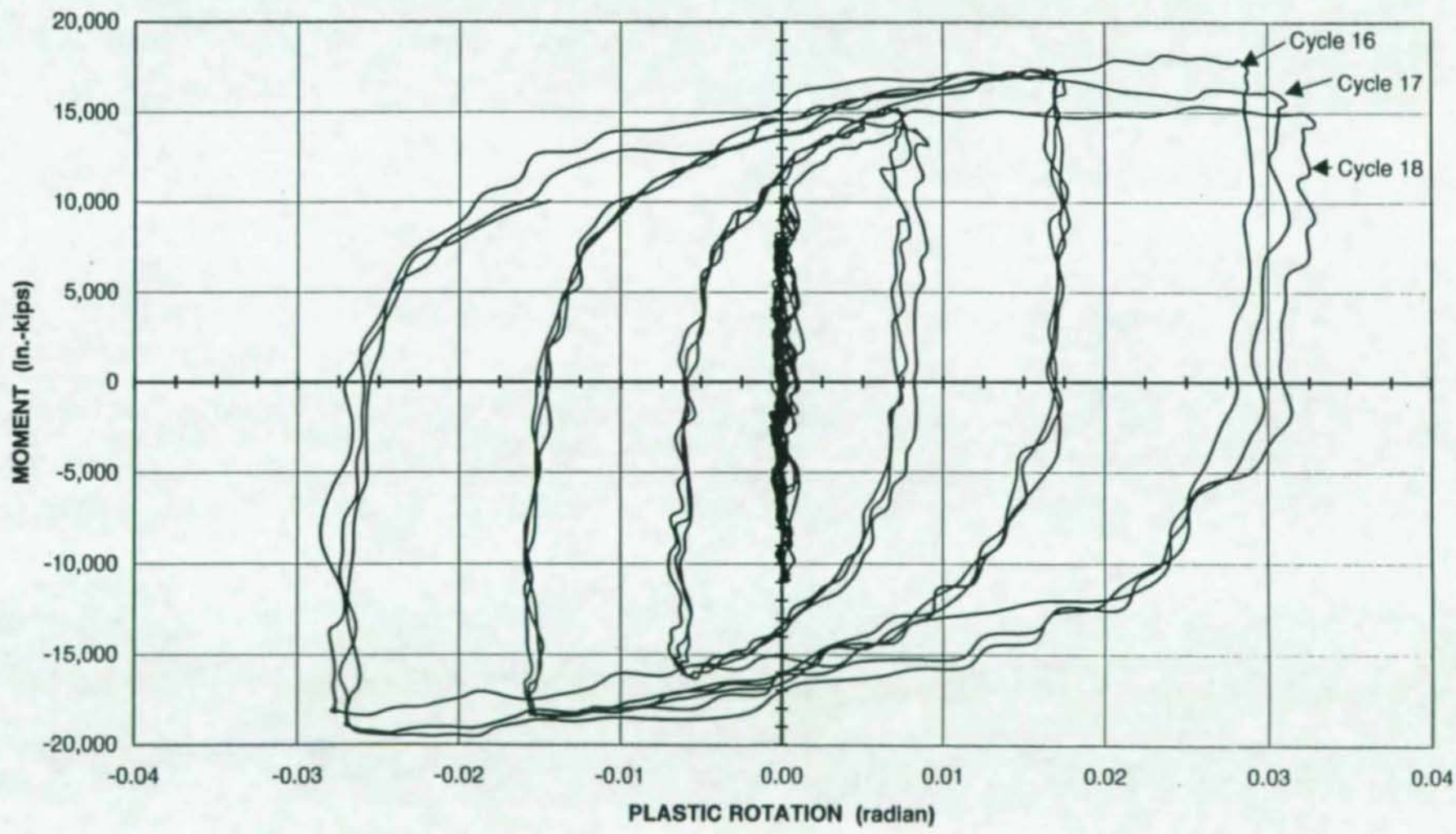
BEAM TIP LOAD vs. BEAM TIP DISPLACEMENT
SPECIMEN NO. 9
(3-POINT MOVING AVERAGE)



- 106 -

Figure 28 Beam Tip Load vs. Displacement Hysteresis Curves for Specimen A4

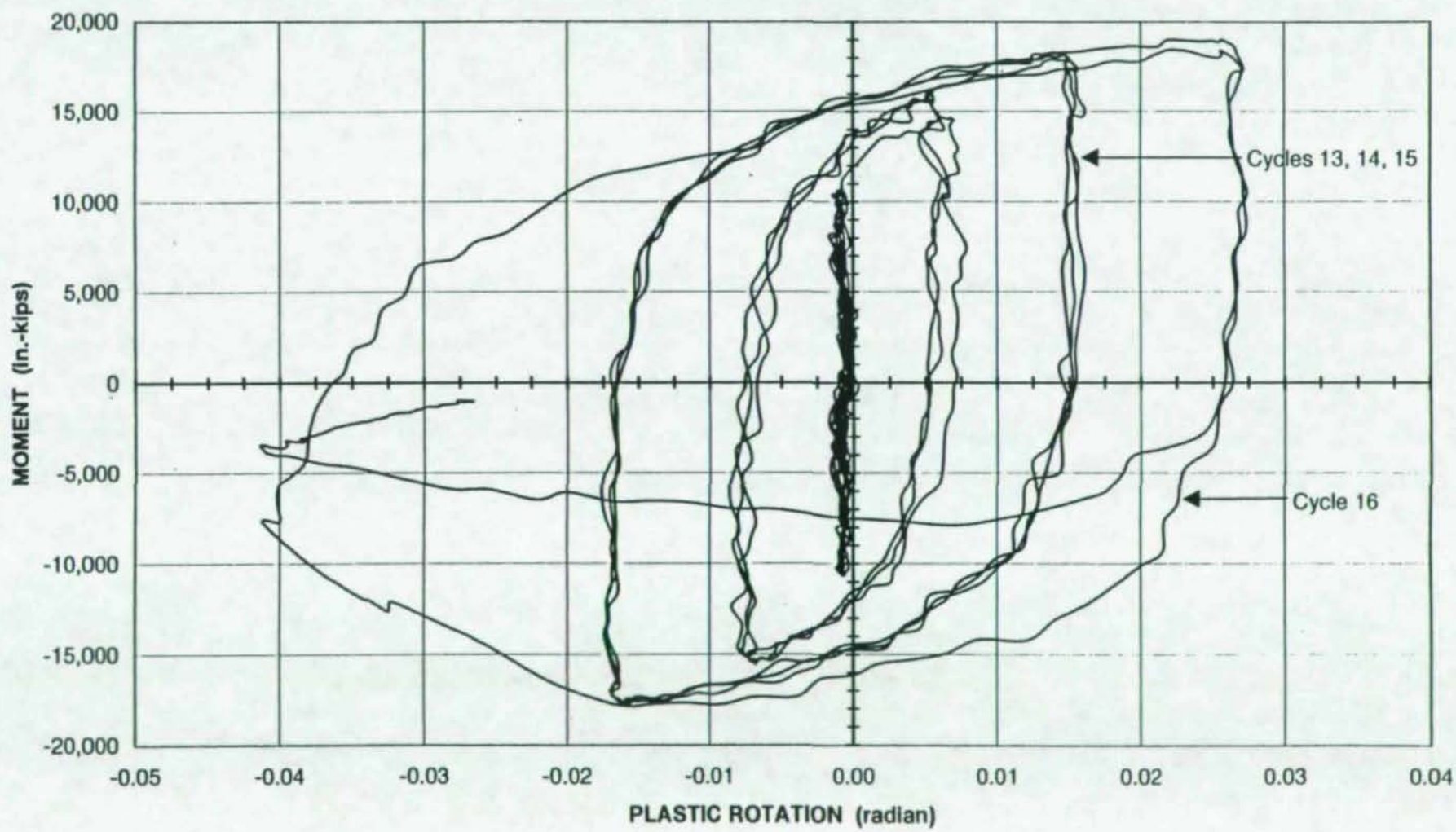
MOMENT vs. PLASTIC ROTATION
SPECIMEN NO. 9
(3-POINT MOVING AVERAGE)



- 107 -

Figure 29 Moment vs. Plastic Rotation Hysteresis Curves for Specimen A4

MOMENT vs. PLASTIC ROTATION
SPECIMEN NO. 10
(3-POINT MOVING AVERAGE)



- 108 -

Figure 30 Moment vs. Plastic Rotation Hysteresis Curves for Specimen A5



Neg.No.4596-12a

a). Top



Neg.No.3982-1a

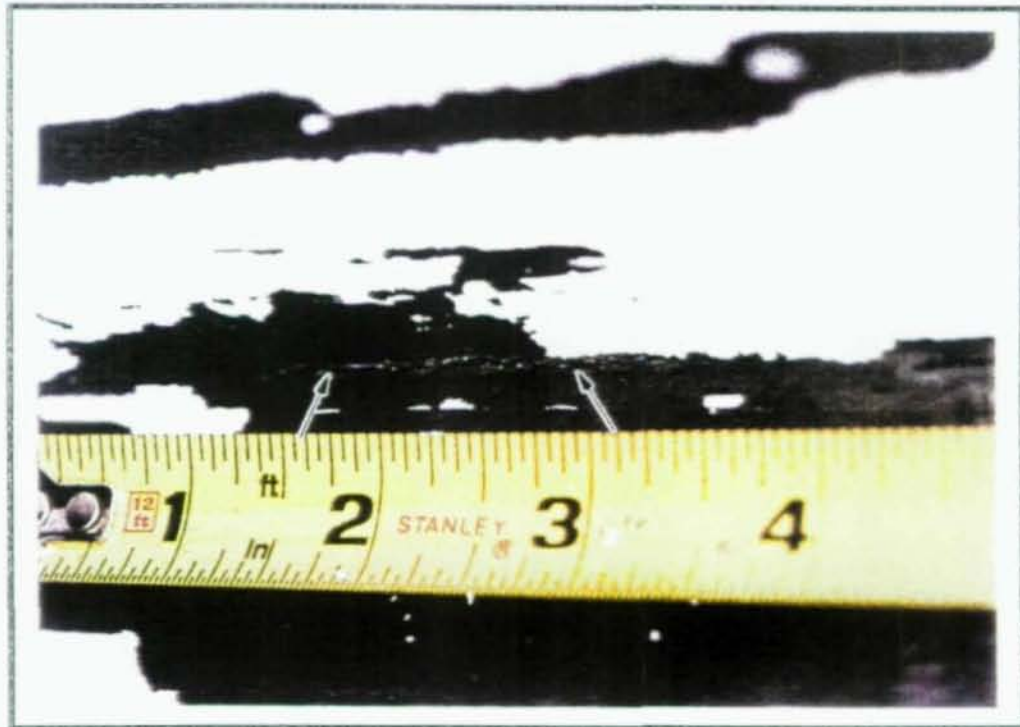
b). Bottom

Figure 31 Photographs of Top and Bottom Fracture Locations for Specimen A4



Neg.No.4328-14a

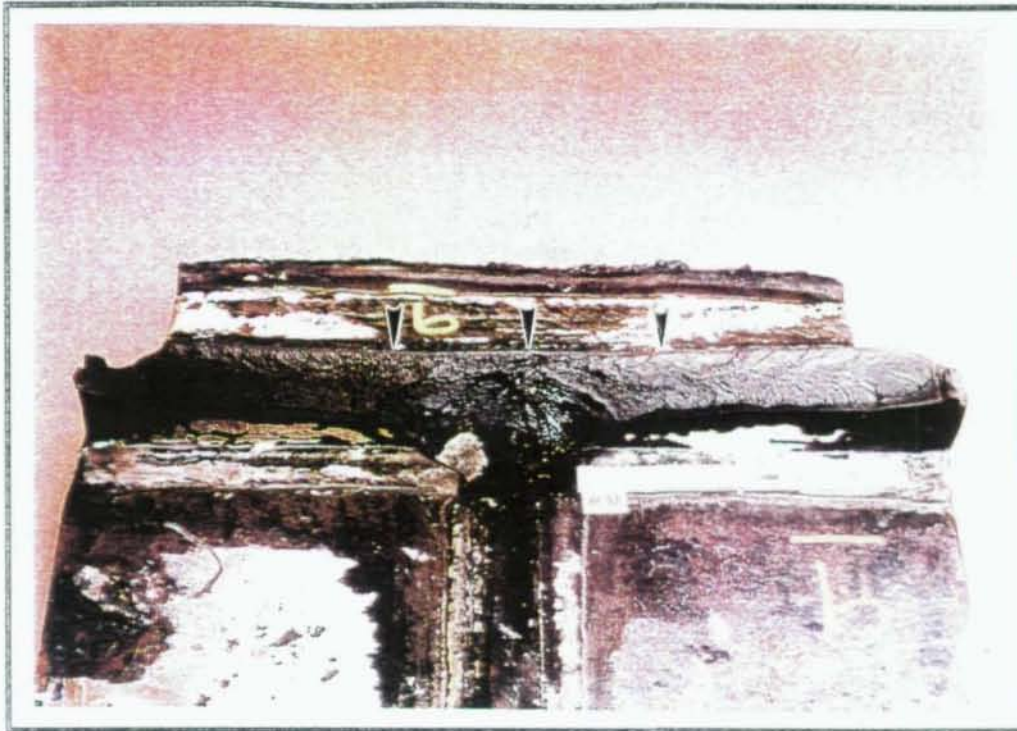
a).



Neg.No.4328-13a

b).

Figure 32 Photographs of Bottom Location for Specimen A5, Showing Crack at Toe of Cover Plate to Column Weld



Neg.No.4467-15

a).



Neg.No.4467-14

b).

Figure 33 Photographs of Fracture Origin with Shear Lip at Cover Plate to Column Weld for Specimen A4

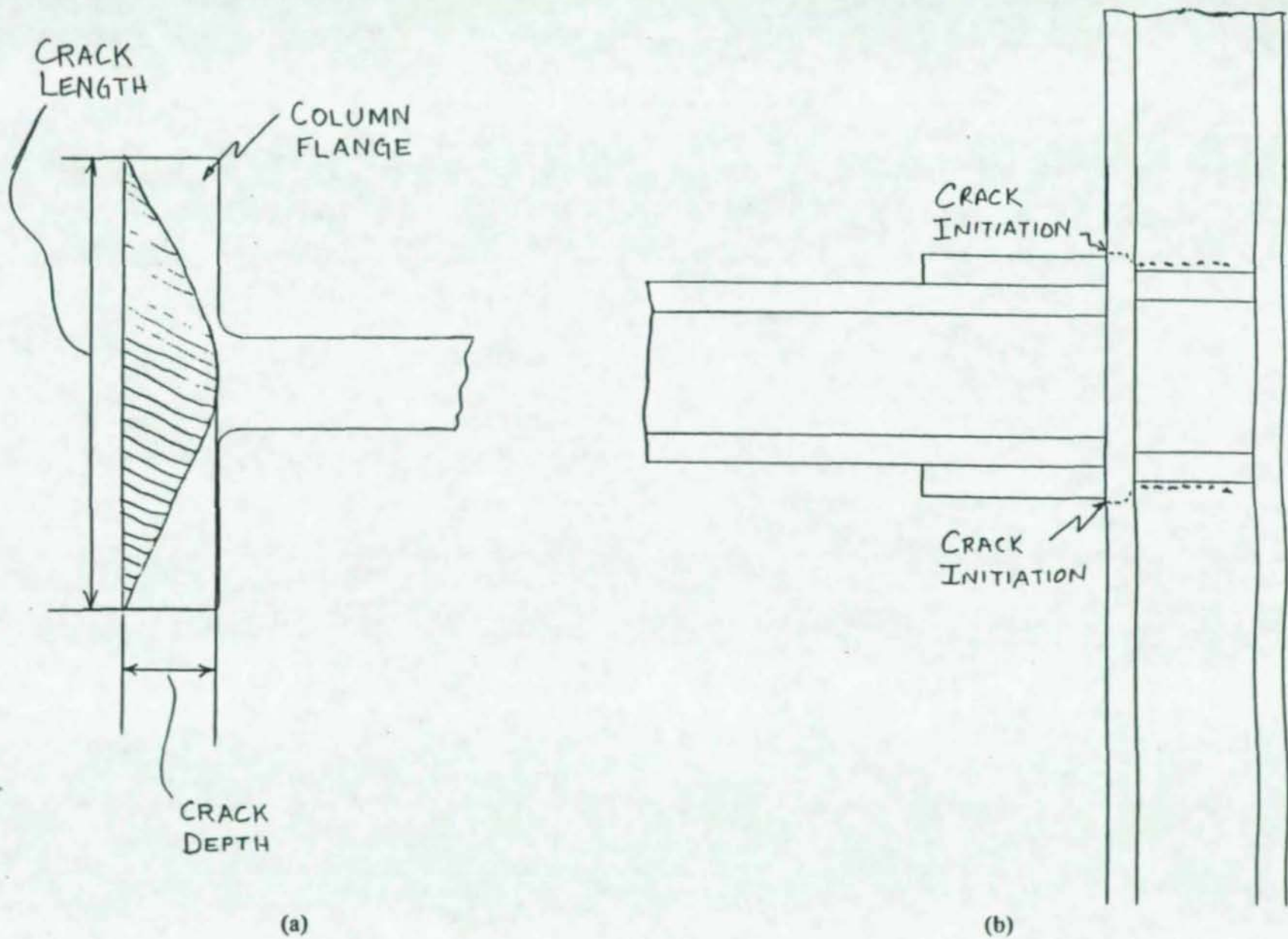
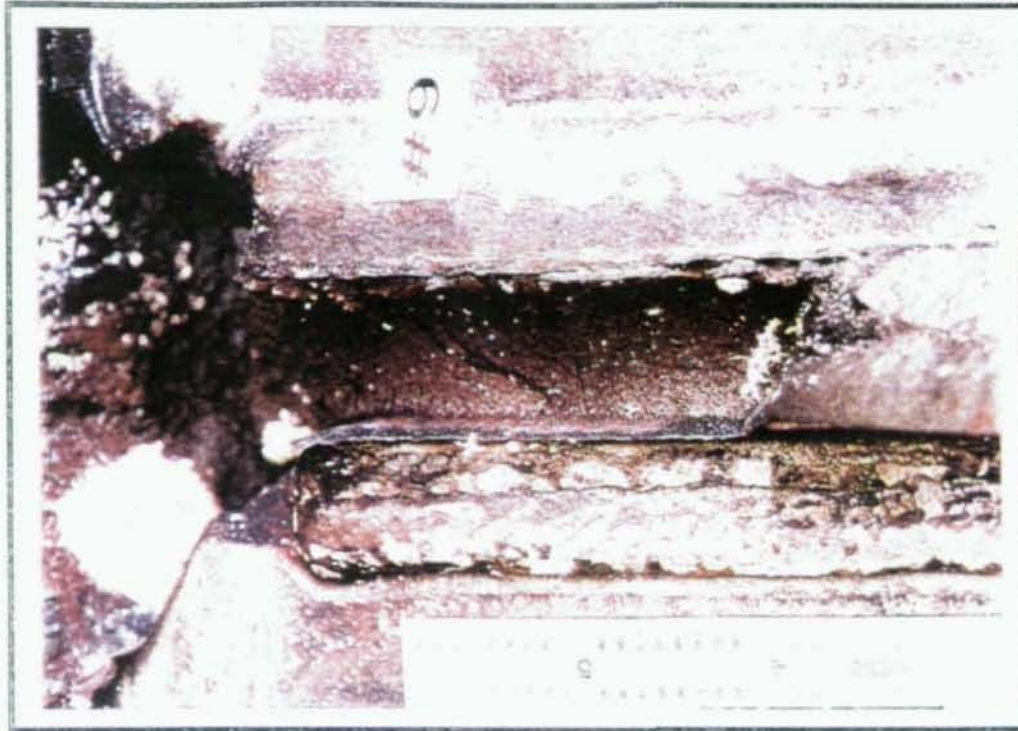


Figure 34 Schematic Illustration of Crack Locations, Depths and Lengths for Specimens A4 and A5



Neg.No.4474-11

a).

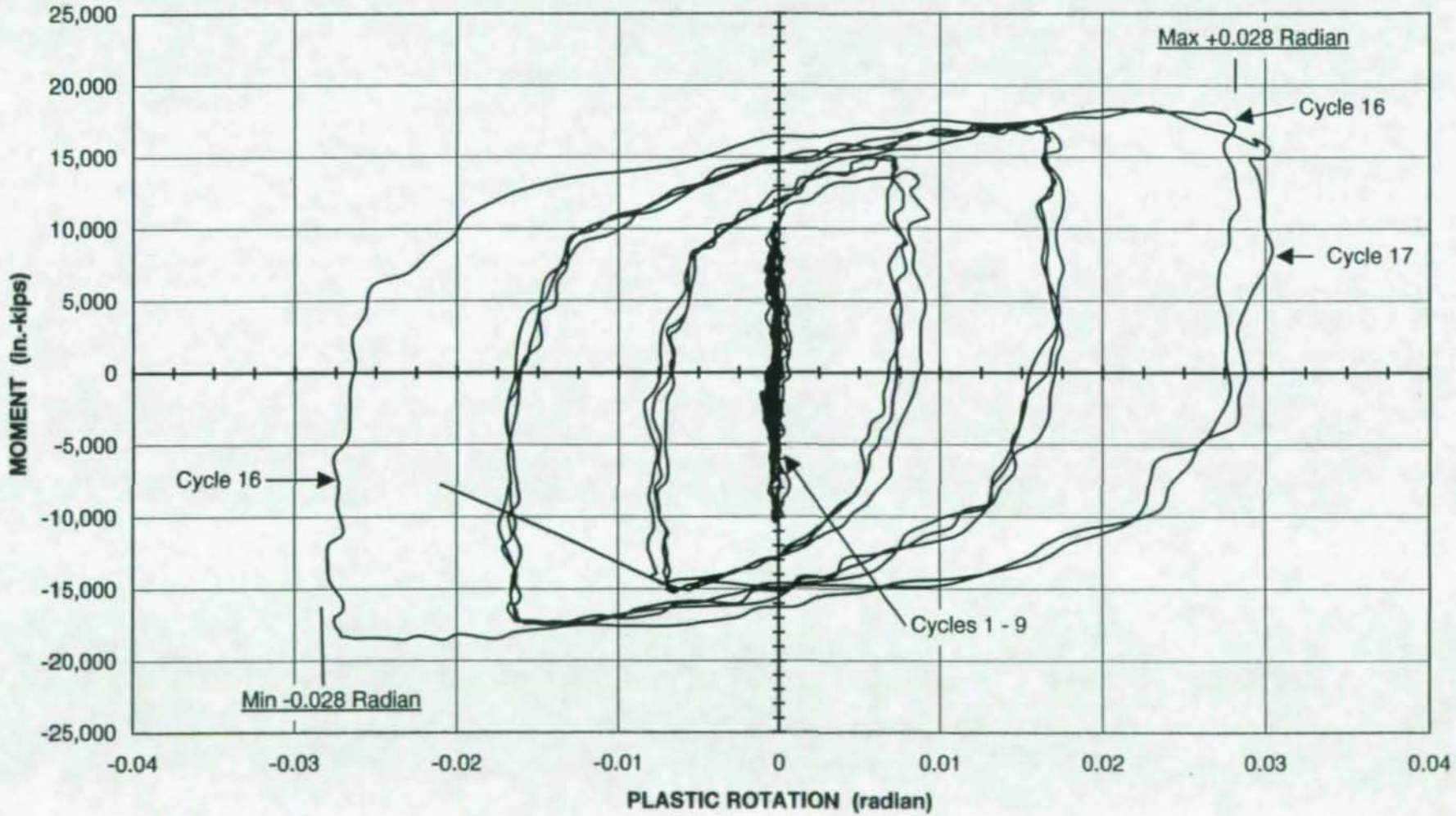


Neg.No.4474-9

b).

Figure 35 Photographs of Bottom Location Fracture at Fusion Line and Ductile Shear Failure of Web of Specimen A4

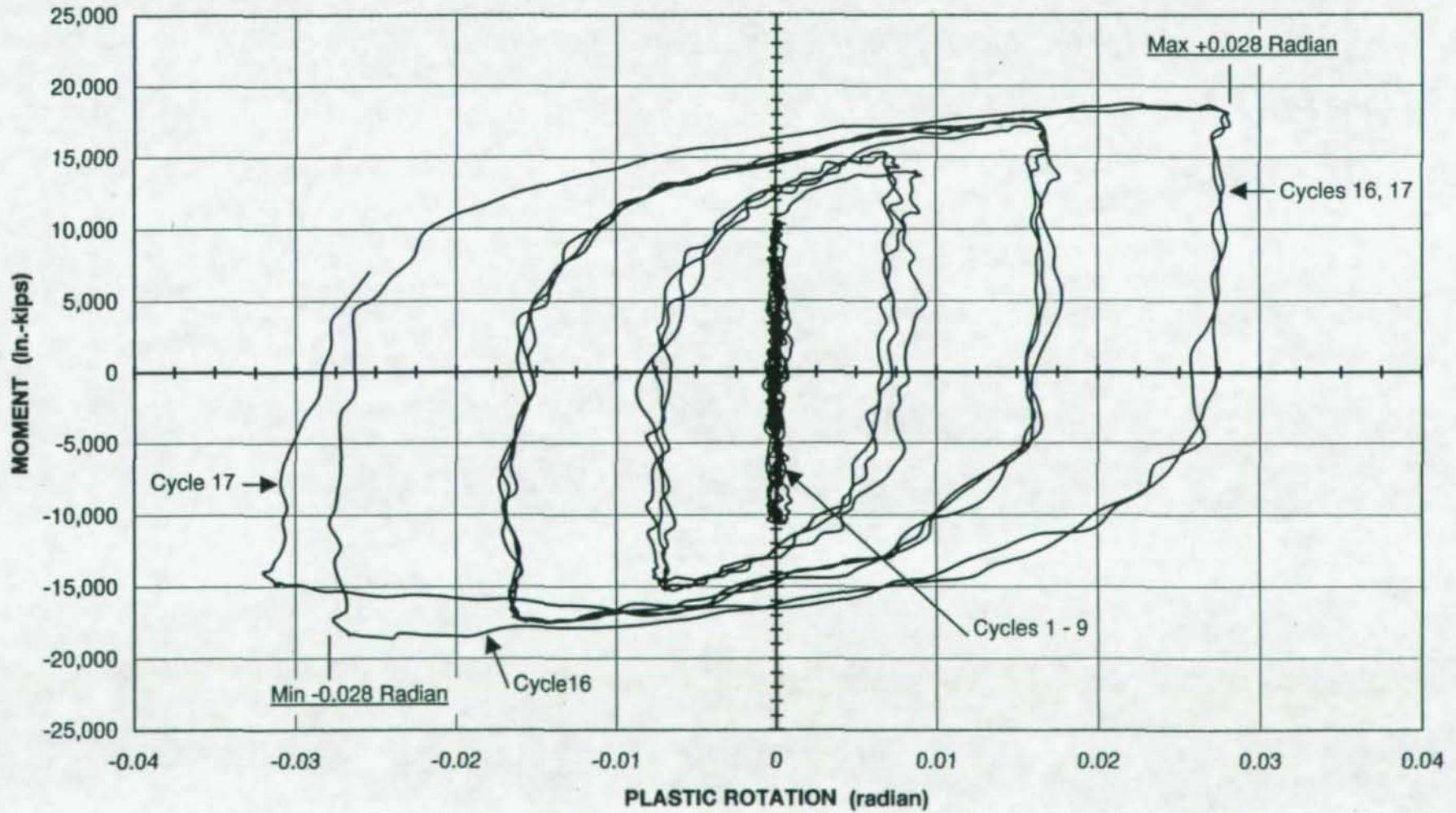
MOMENT vs. PLASTIC ROTATION
SPECIMEN NO. 15
(3-POINT MOVING AVERAGE)



- 114 -

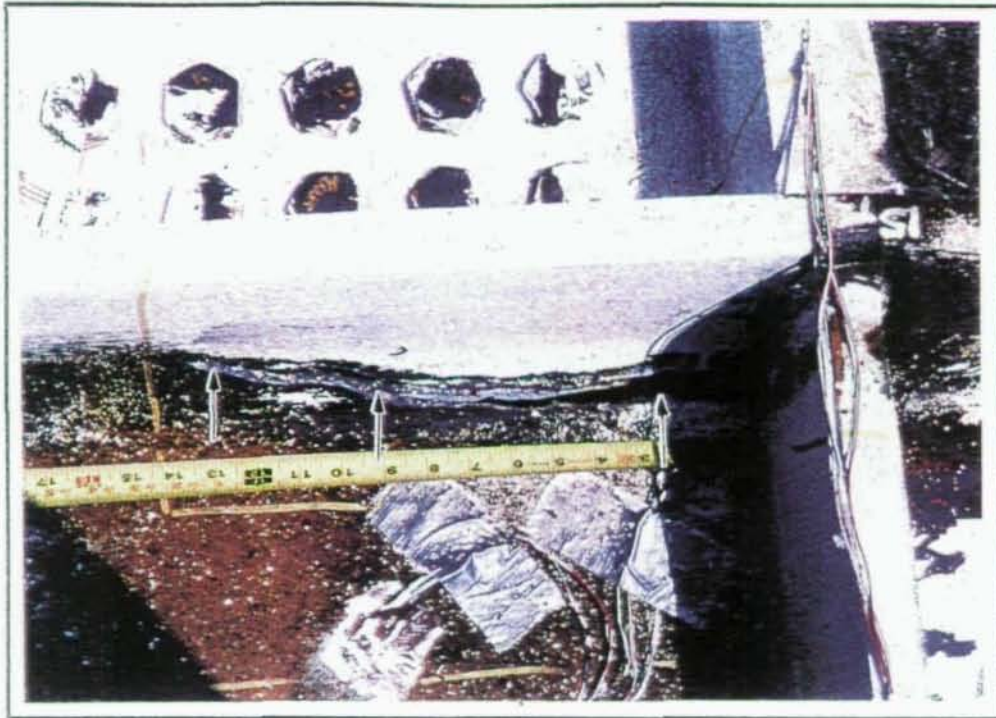
Figure 36 Moment vs. Plastic Rotation Hysteresis Curves for Specimen A6

MOMENT vs. PLASTIC ROTATION
SPECIMEN NO. 16
(3-POINT MOVING AVERAGE)



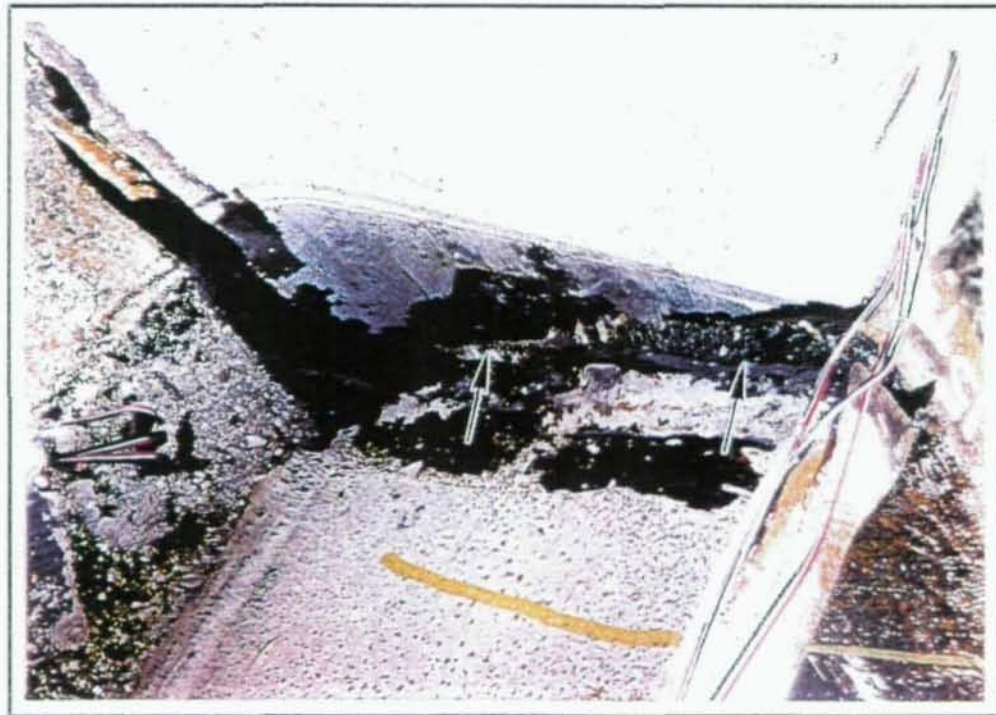
- 115 -

Figure 37 Moment vs. Plastic Rotation Hysteresis Curves for Specimen A7



Neg. No. 8821-23a

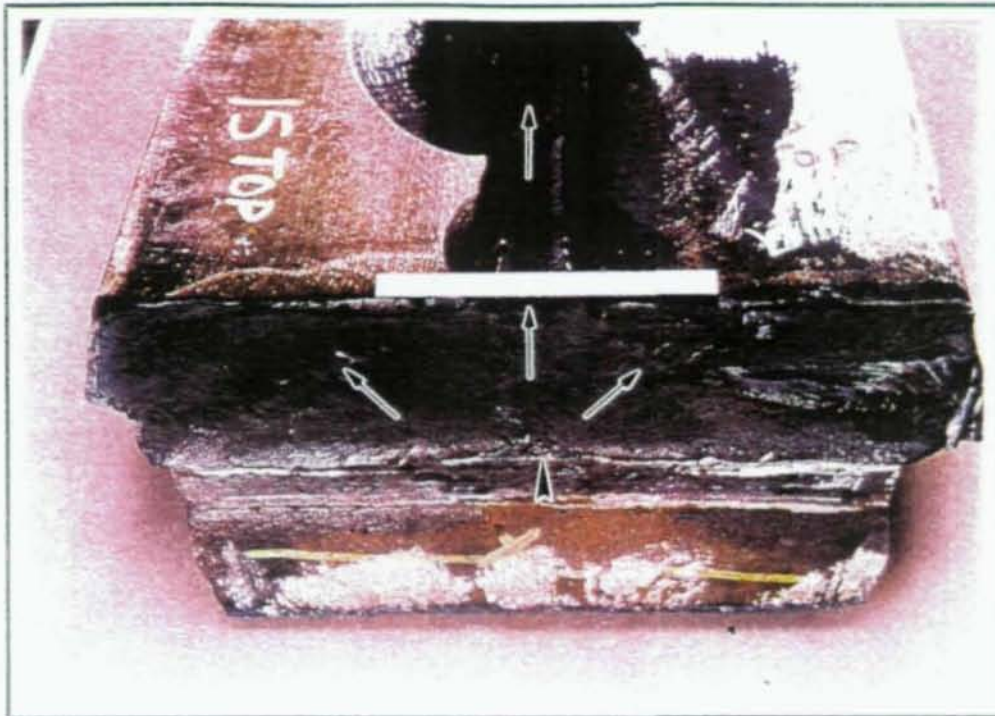
a)



Neg No. 8821-24a

b)

Figure 38 Top Location of Specimen A6, Showing (a) Crack in k-Region and (b) Separation of Continuity Plate from Column Flange



Neg. No. 9615-7a

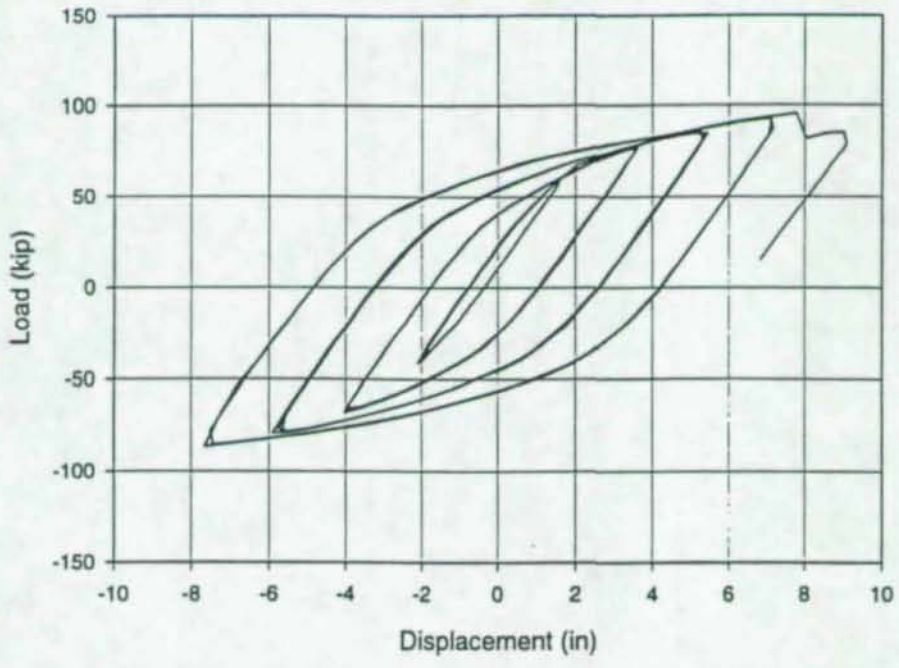
a)



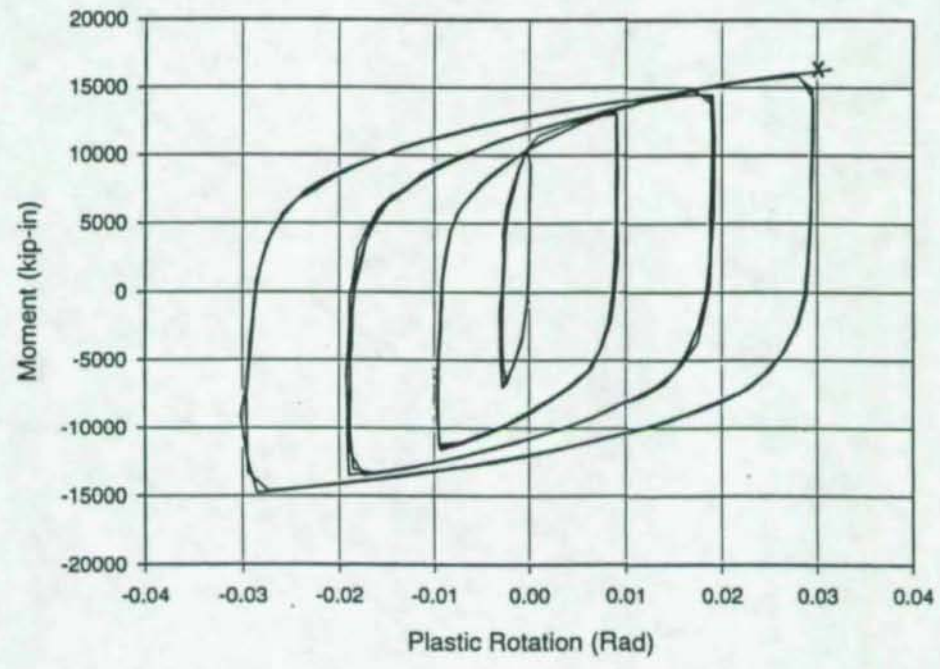
Neg No. 9615-6

b)

Figure 39 Fracture Origin at Top Cover Plate to Column Weld for Specimen A6. Short Arrows Indicate Origin; Long Arrows Show Crack Propagation Direction

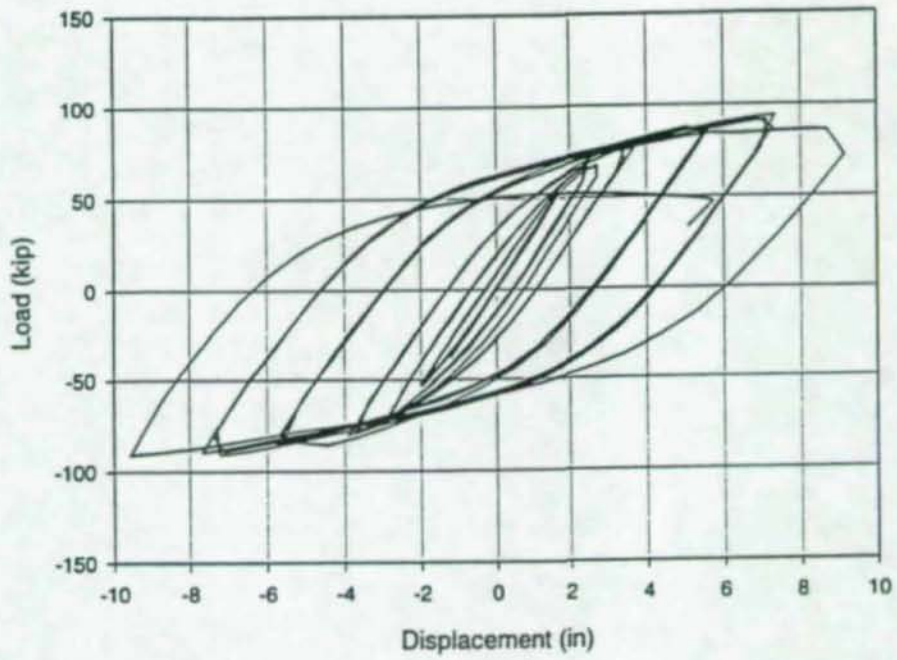


(a)

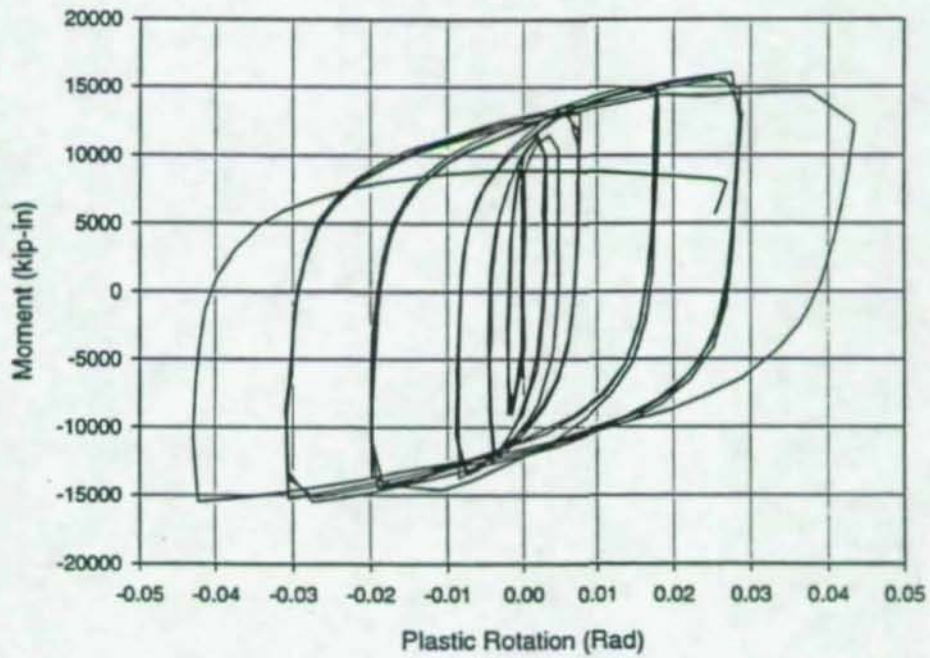


(b)

Figure 40 Load-Displacement and Moment-Plastic Rotation Hysteresis Curves for Specimen A8

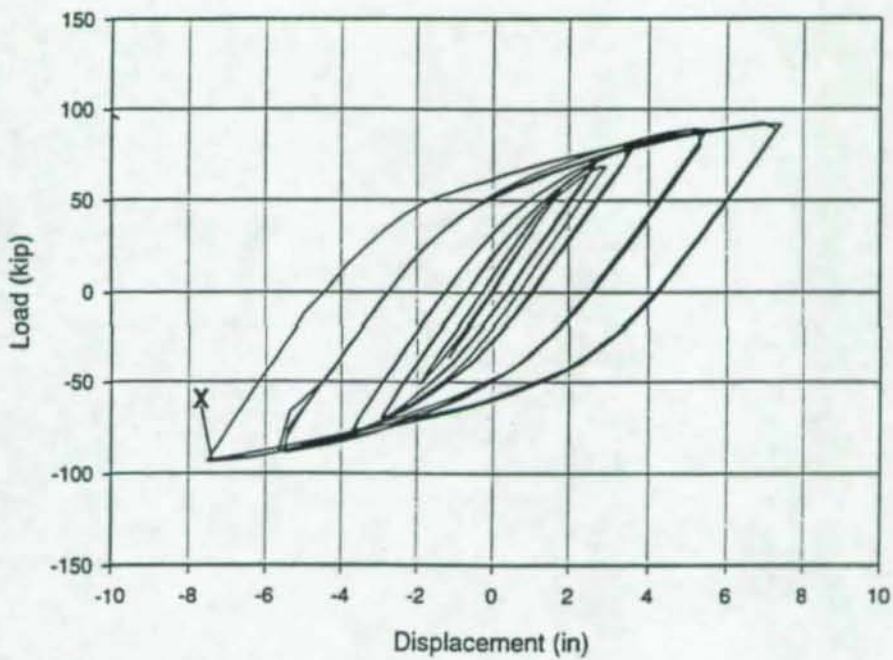


(a)

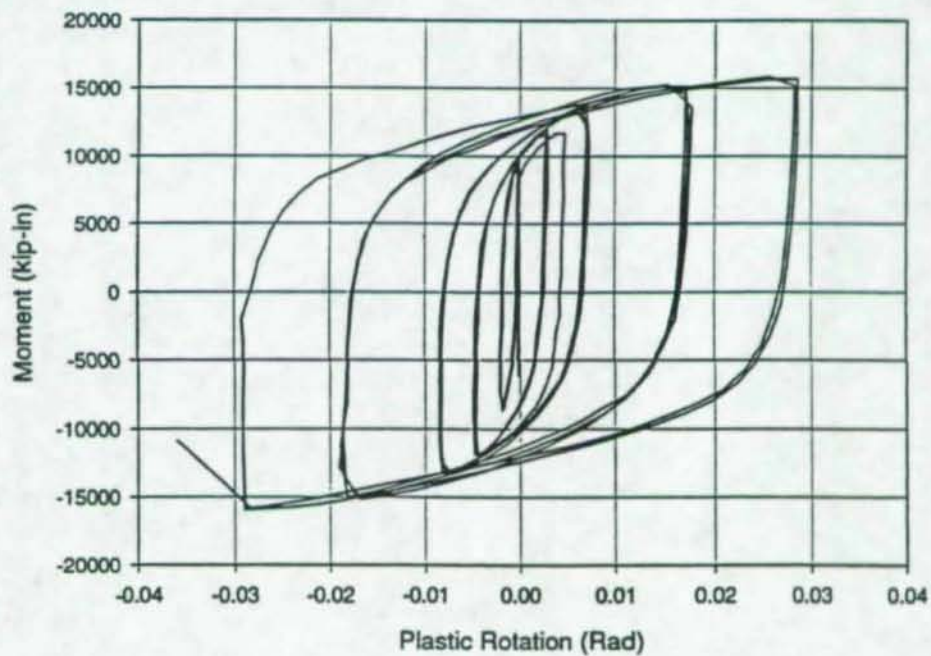


(b)

Figure 41 Load-Displacement and Moment-Plastic Rotation Hysteresis Curves for Specimen R1-1

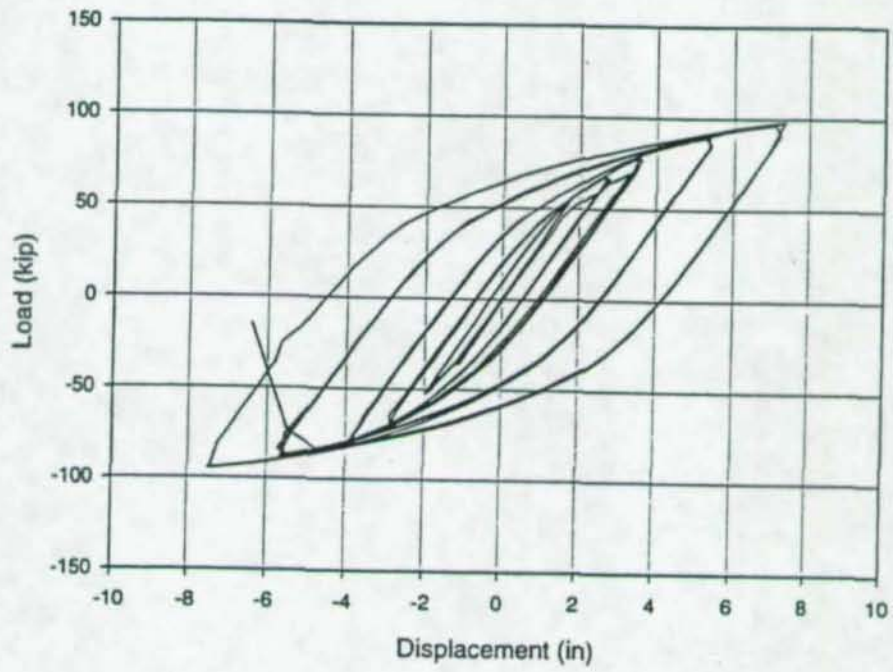


(a)

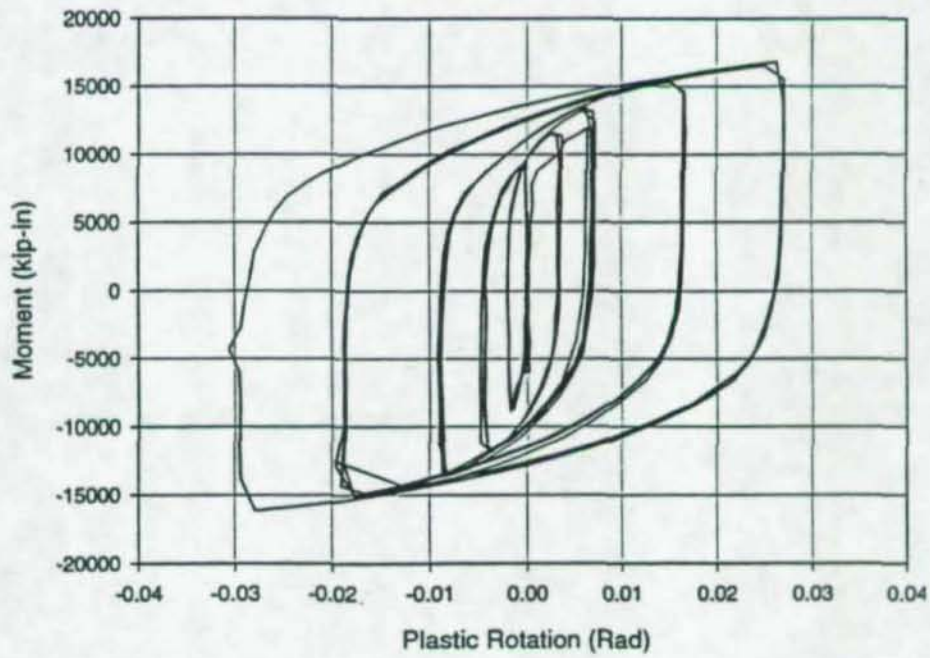


(b)

Figure 42 Load-Displacement and Moment-Plastic Rotation Hysteresis Curves for Specimen R1-2

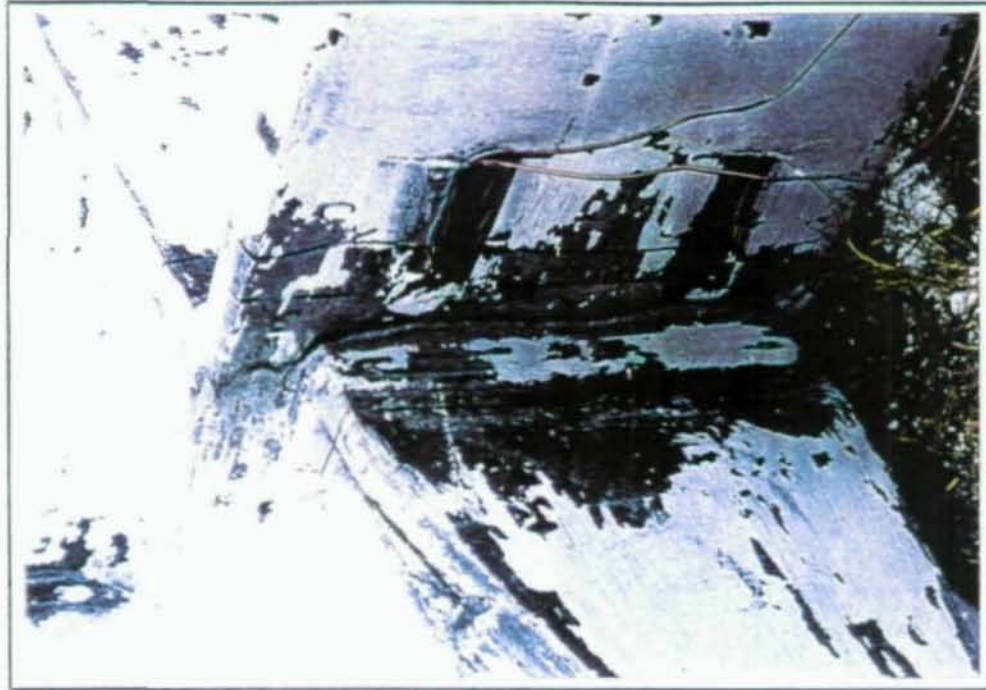


(a)



(b)

Figure 43 Load-Displacement and Moment-Plastic Rotation Hysteresis Curves for Specimen R1-3

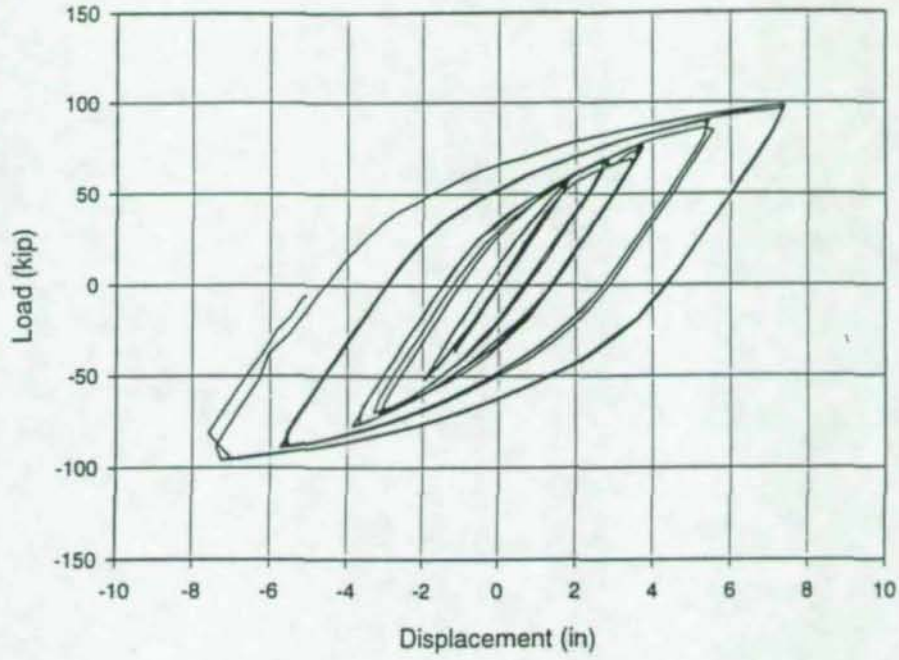


(a)

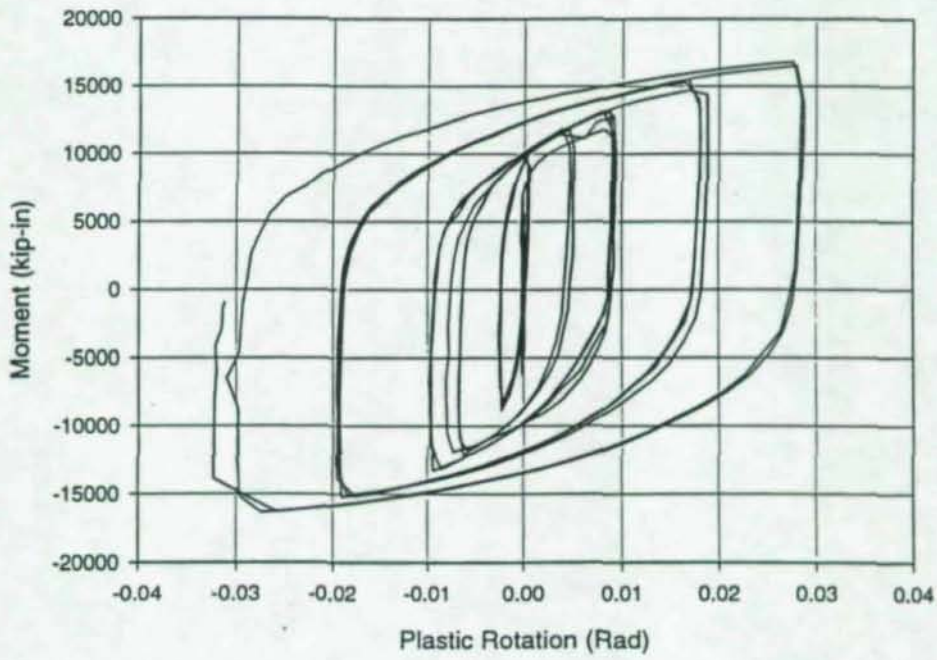


(b)

Figure 44 Photographs of Crack Adjacent to Weld in Specimen R1-3



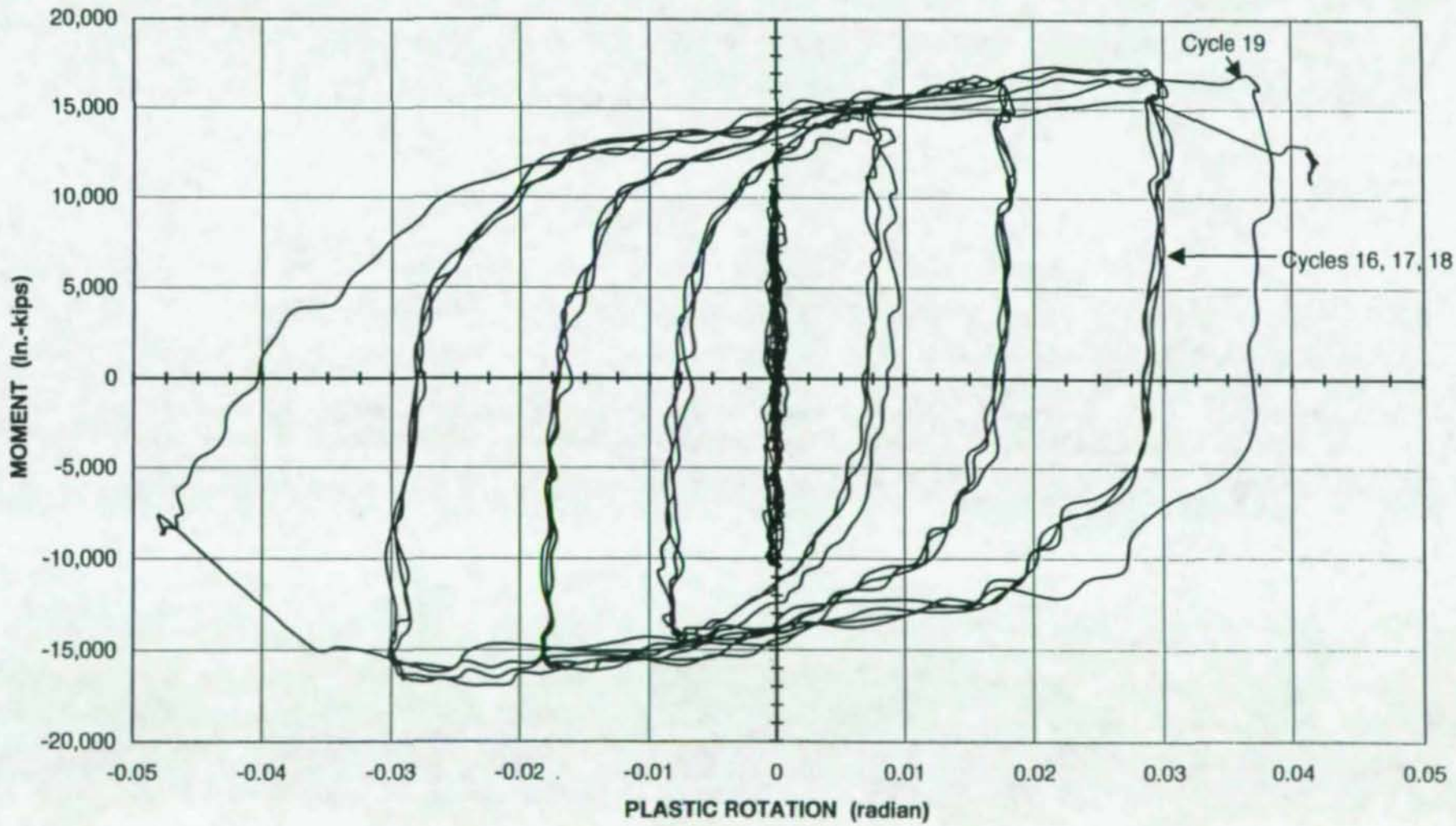
(a)



(b)

Figure 45 Load-Displacement and Moment-Plastic Rotation Hysteresis Curves for Specimen R1-6

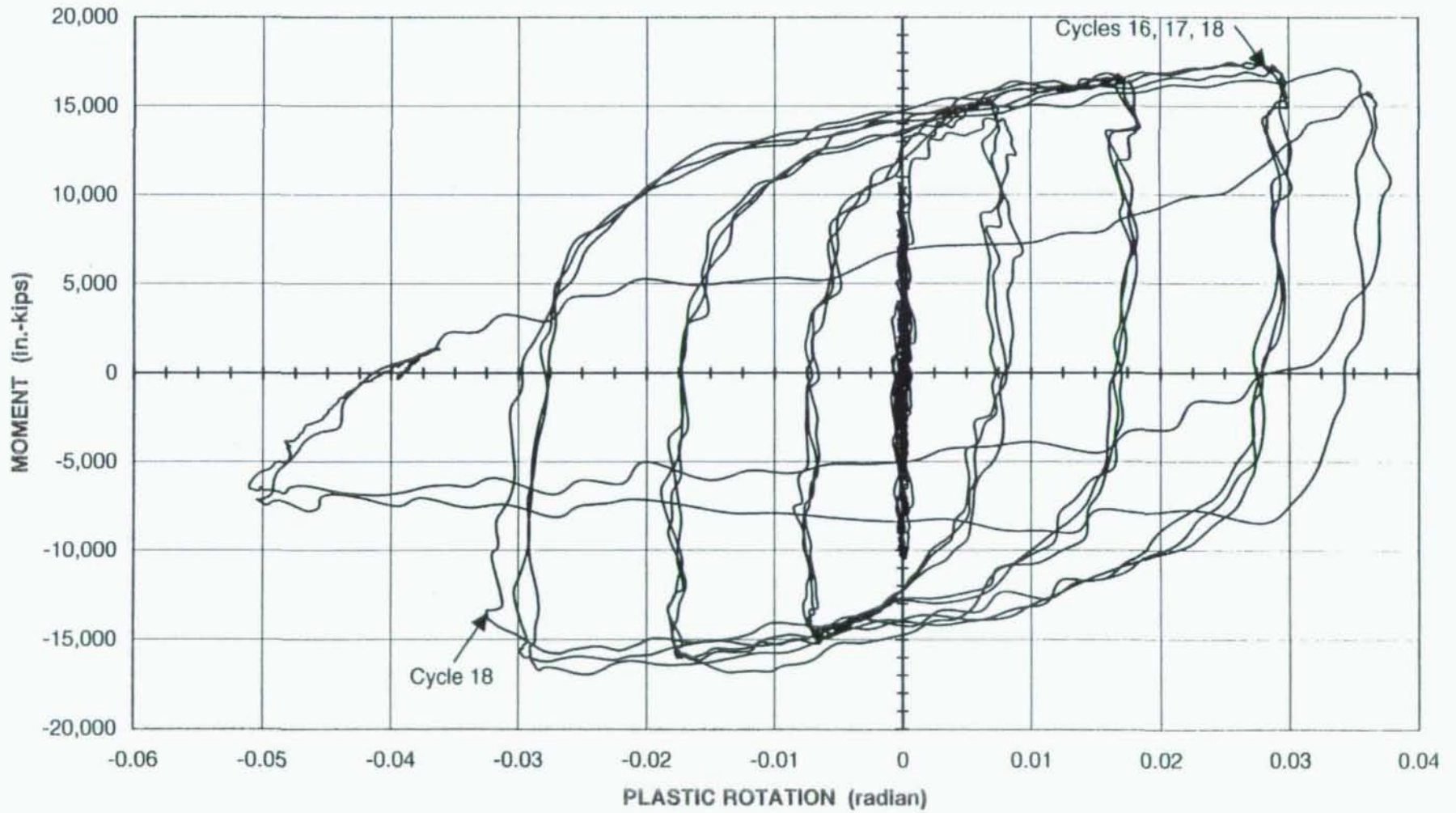
MOMENT vs. PLASTIC ROTATION
SPECIMEN NO. 11
(3-POINT MOVING AVERAGE)



- 124 -

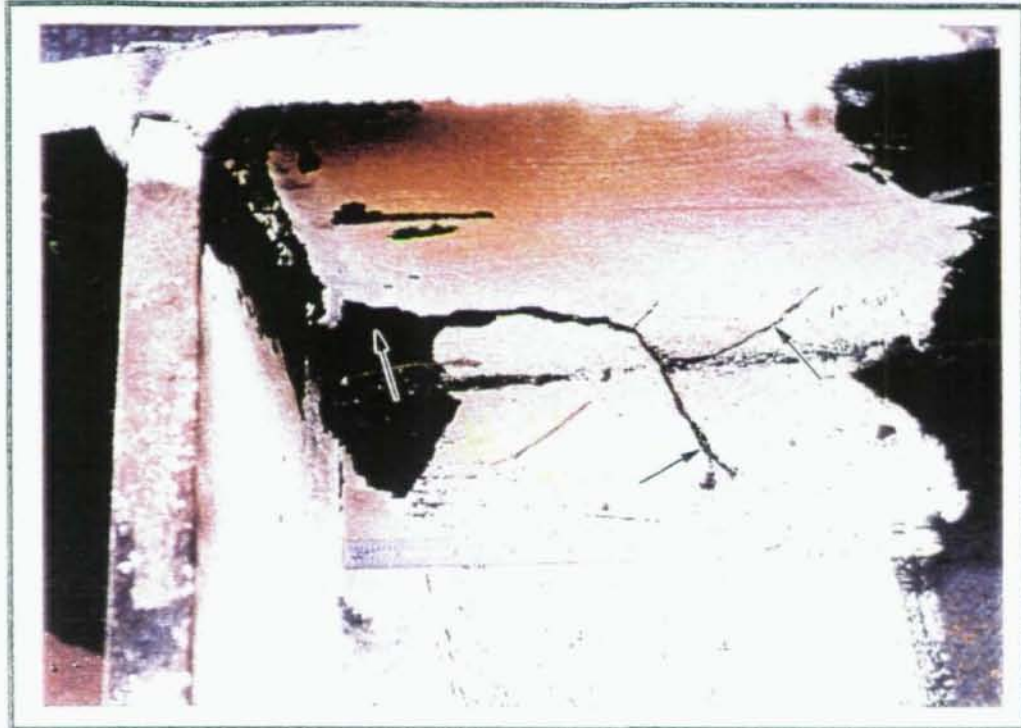
Figure 46 Moment vs. Plastic Rotation Hysteresis Curves for Specimen R1-4

MOMENT vs. PLASTIC ROTATION
SPECIMEN NO. 12
(3-POINT MOVING AVERAGE)



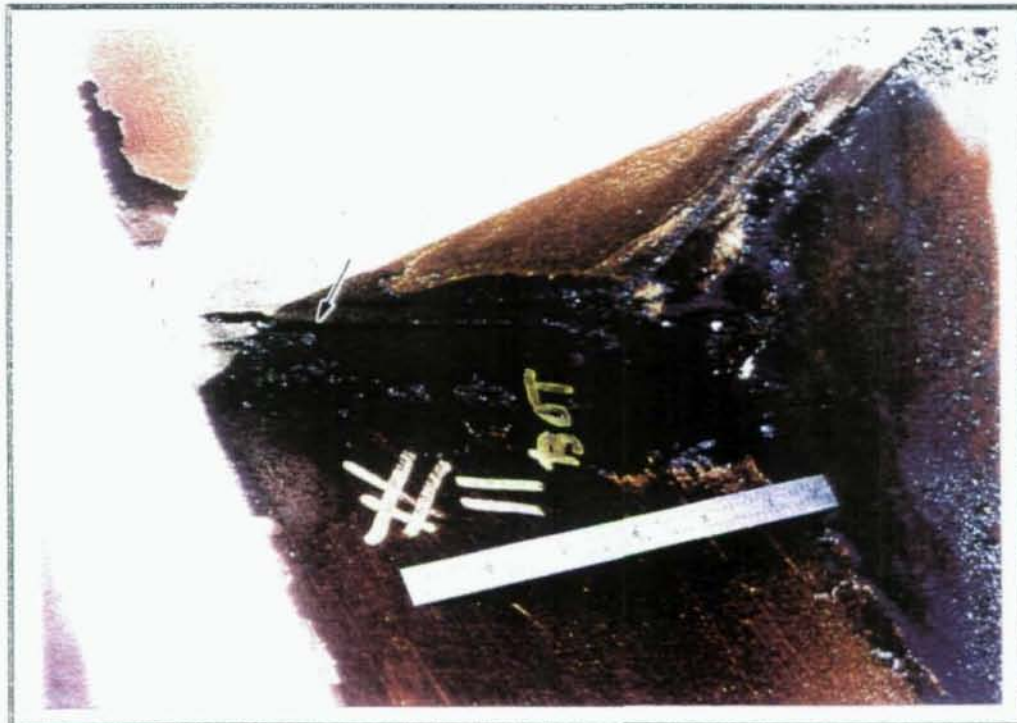
- 125 -

Figure 47 Moment vs. Plastic Rotation Hysteresis Curves for Specimen R1-5



Neg.No.4471-10a

a).



Neg.No.4471-8a

b).

Figure 48 Bottom Location for Specimen R1-4, Showing (a) Crack Extension in k-Region and (b) Failure of Continuity Plate Weld



Neg.No.4596-5a

a).



Neg.No.4596-1ab).

Figure 49 Bottom (a) and Top (b) Locations of Cover Plate to Column Weld for Specimen R1-5. Arrows Indicate Crack between Cover Plate and Flange

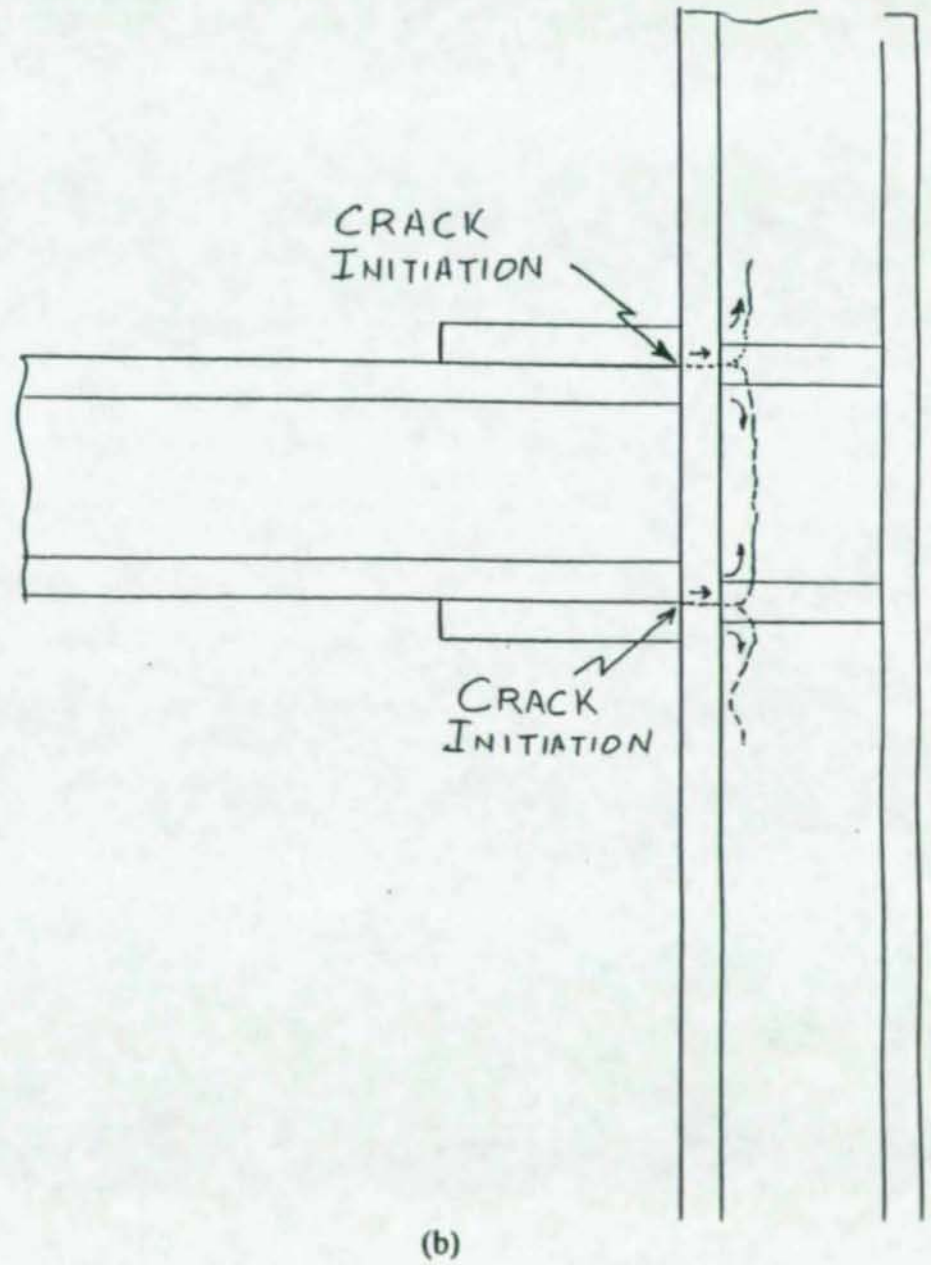
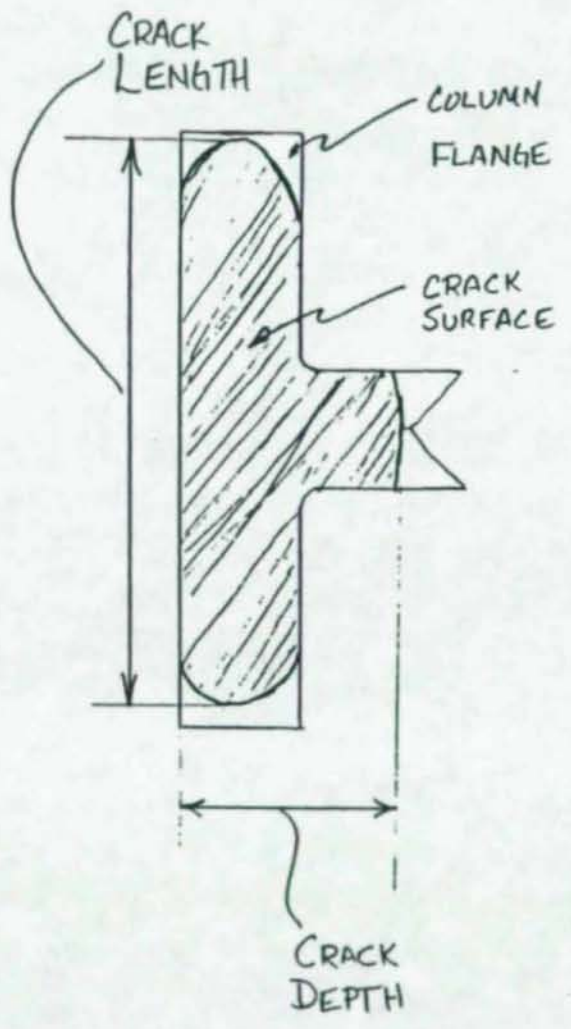


Figure 50 Schematic Illustration of Crack Locations, Depths and Lengths for Specimens R1-4 and R1-5

MOMENT vs. PLASTIC ROTATION
SPECIMEN NO. 13
(3-POINT MOVING AVERAGE)

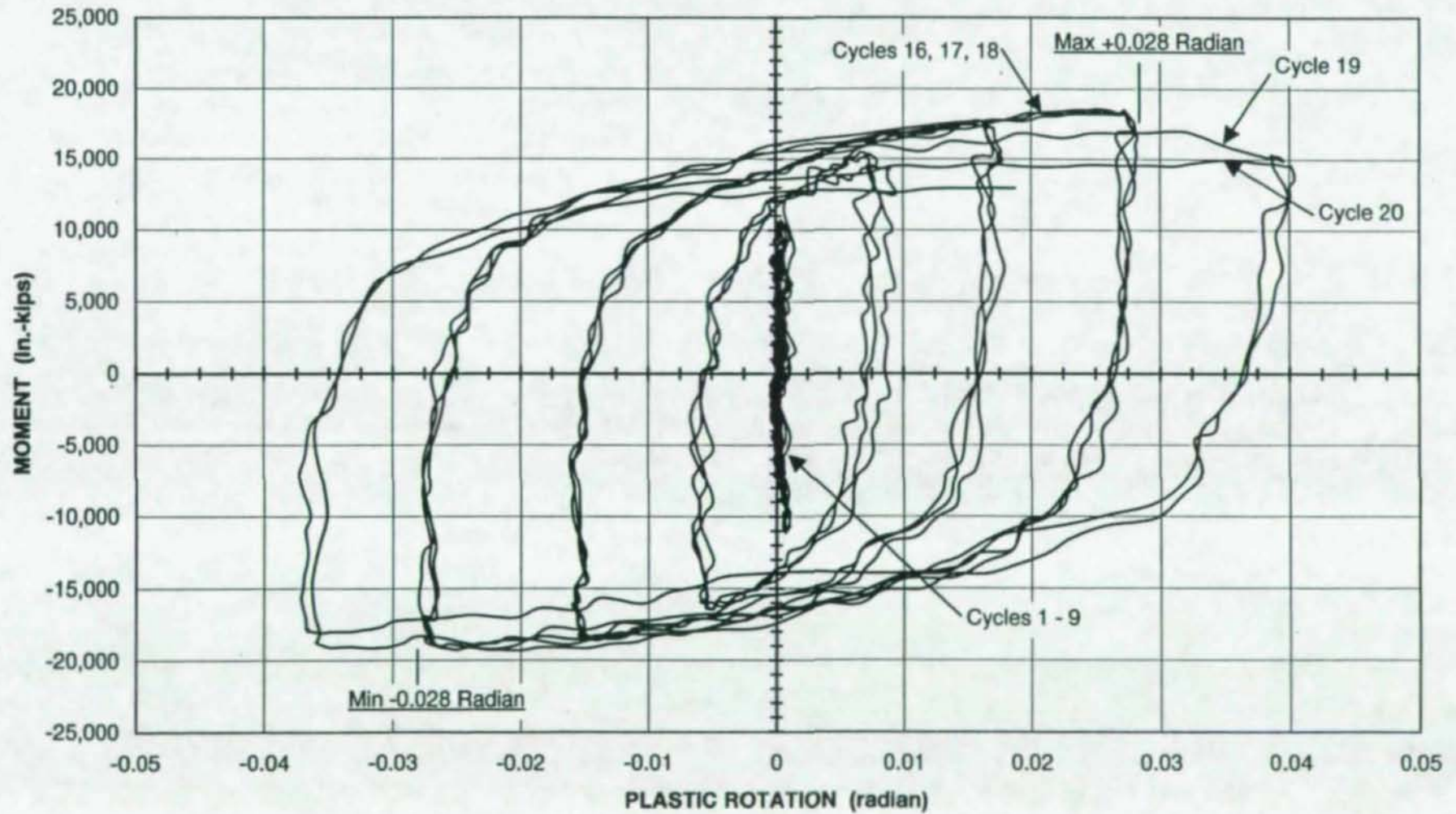


Figure 51 Moment vs. Plastic Rotation Hysteresis Curves for Specimen R2

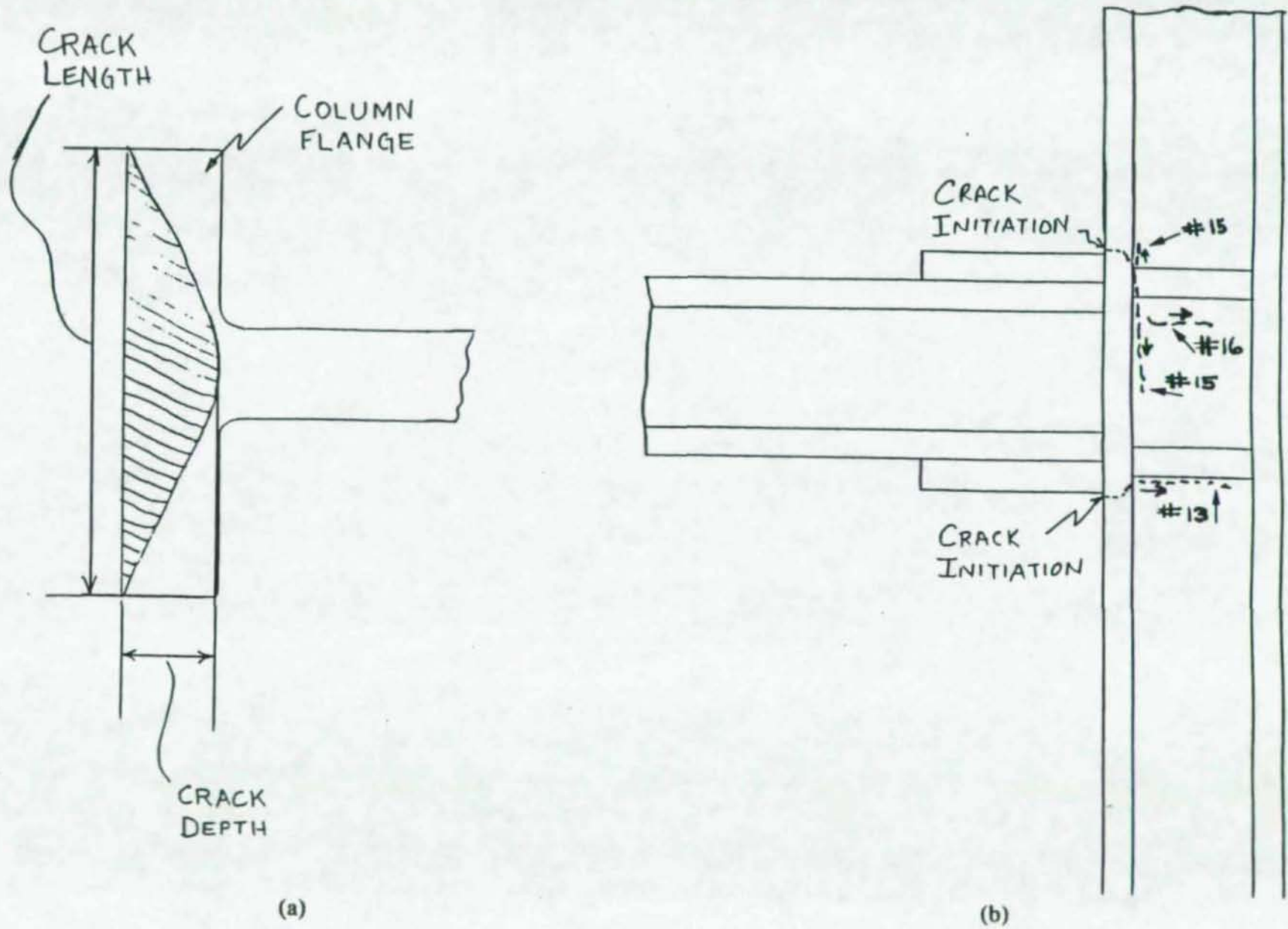
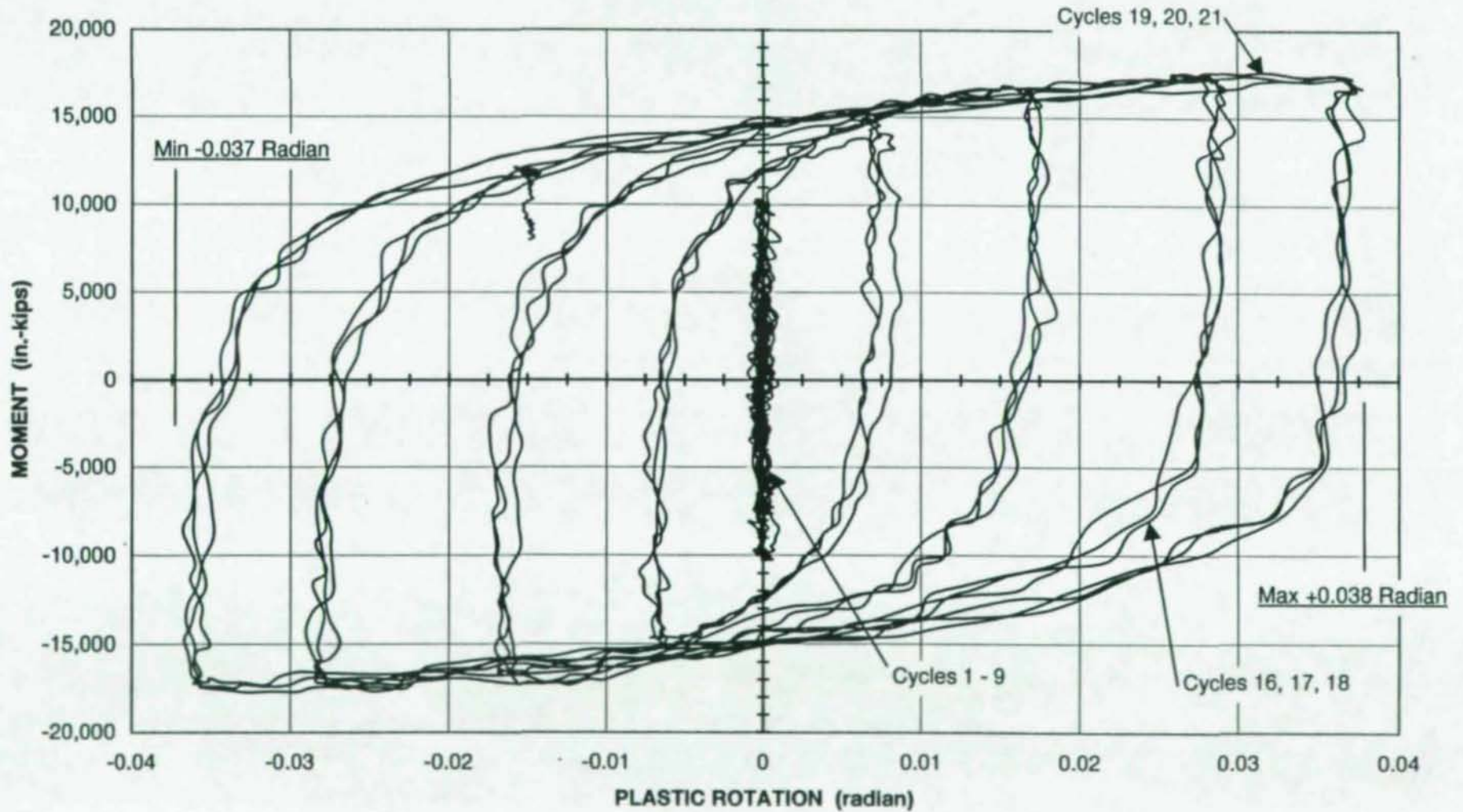


Figure 52 Schematic Illustration of Crack Locations, Depths and Length for Specimens R2, A6 and A7

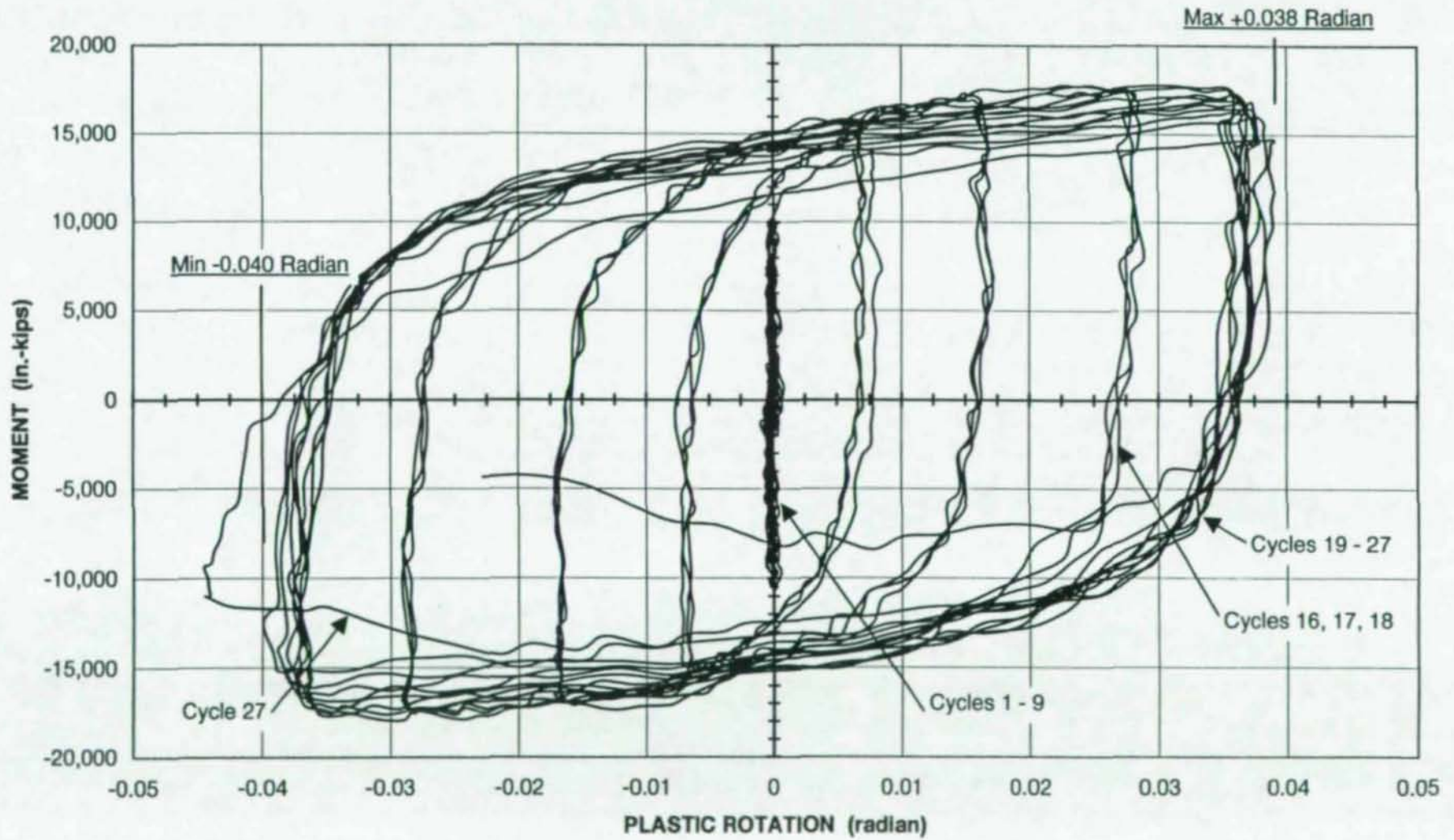
MOMENT vs. PLASTIC ROTATION
SPECIMEN NO. 14
(3-POINT MOVING AVERAGE)



- 131 -

Figure 53 Moment vs. Plastic Rotation Hysteresis Curves for Specimen R3-1

MOMENT vs. PLASTIC ROTATION
SPECIMEN NO. 17
(3-POINT MOVING AVERAGE)



- 132 -

Figure 54 Moment vs. Plastic Rotation Hysteresis Curves for Specimen R3-2



Neg. No. 8585-2a

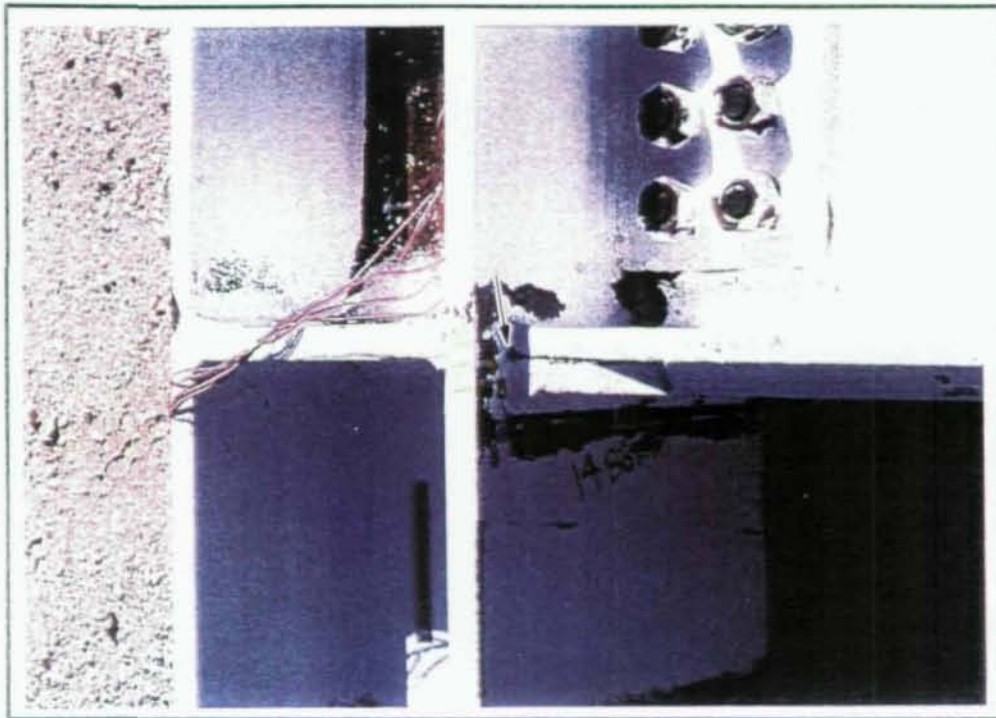
a) Bottom



Neg. No. 8585-7a

b) Top

Figure 55 Photographs of Cover Plate to Column Weld at (a) Bottom and (b) Top for Specimen R3-1, with No Fracture at the Weld Toe



Neg. No. 8585-13a

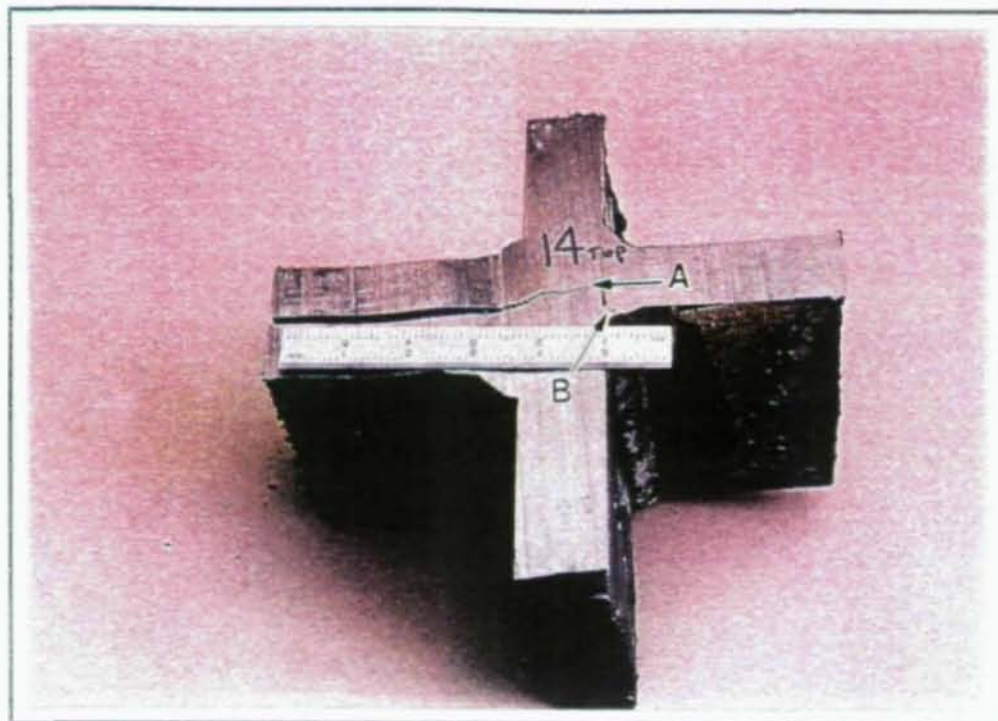
a)



Neg No. 8585-5a

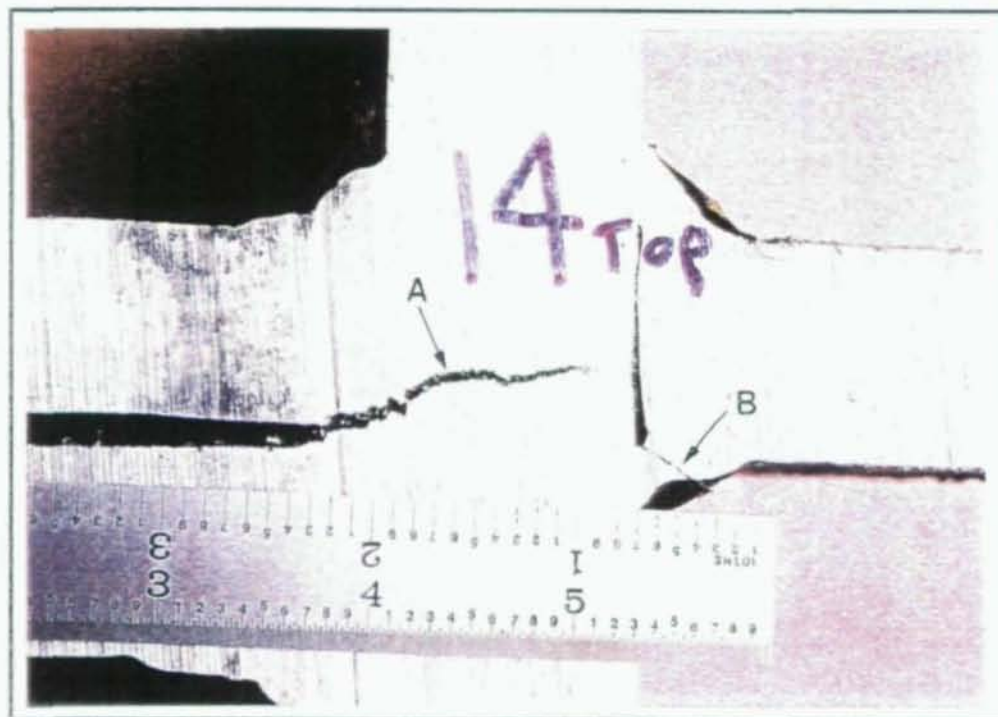
b)

Figure 56 Column Flange near Bottom Cover Plate for Specimen R3-1, with Small Crack Extending into Column



Neg. No. 8821-13a

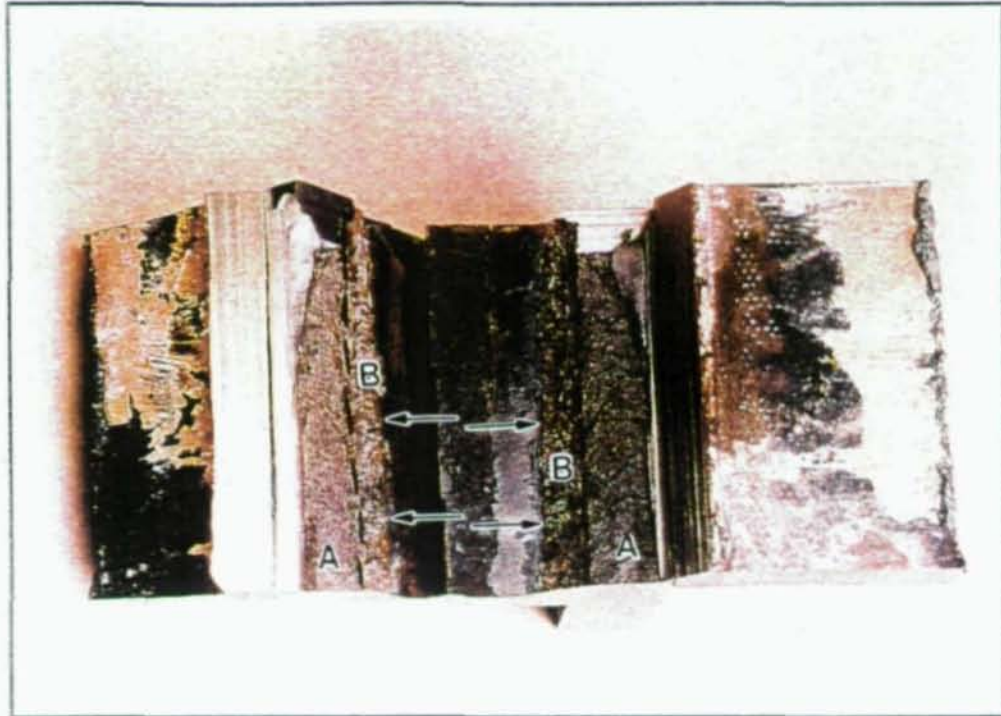
a)



Neg No. 8821-16a

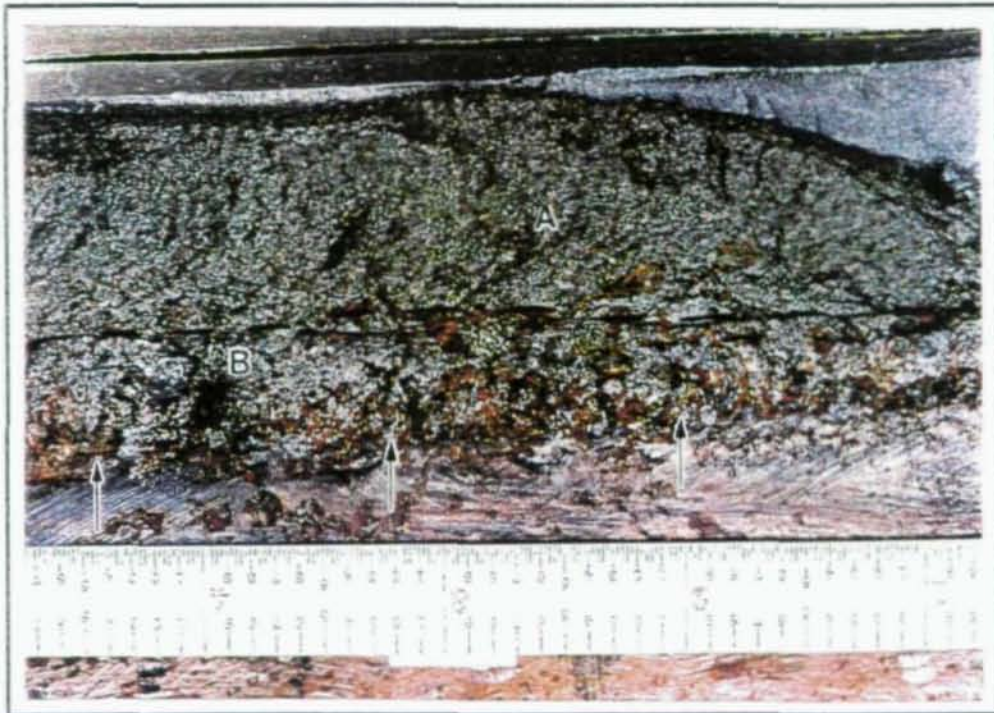
b)

Figure 57 Photographs of Sectioned Top Cover Plate Location for Specimen R3-1, with Arrow A Showing Crack between Cover Plate and Beam Flange, and Arrow B Showing Crack in Continuity Plate Fillet Weld



Neg. No. 8844-11a

a)



Neg No. 8844-24a

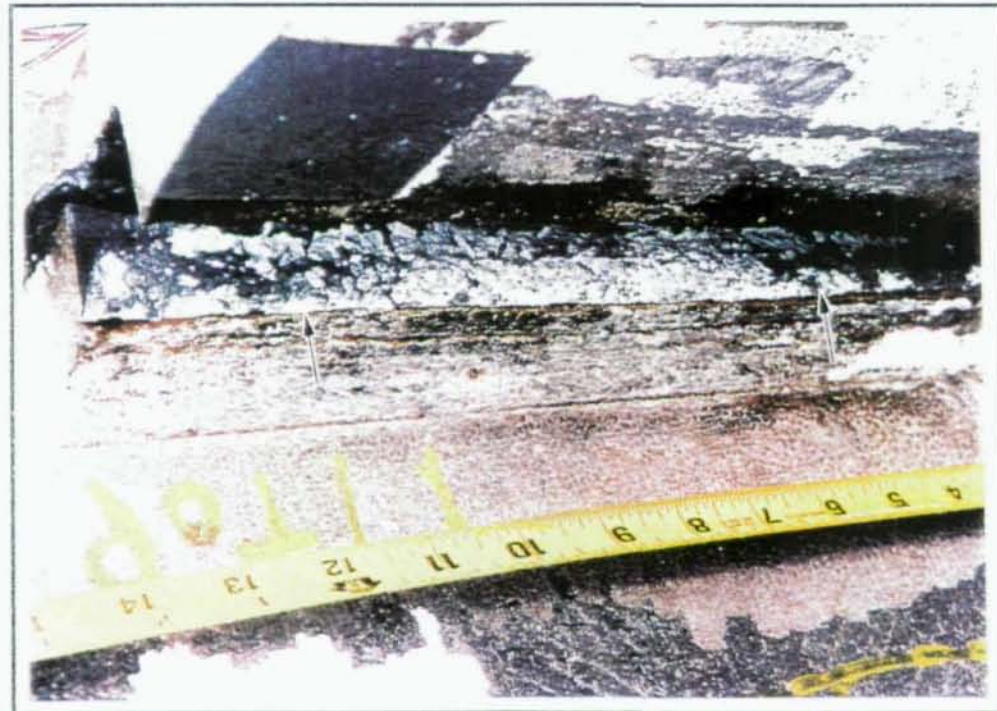
b)

Figure 58 Photographs of Exposed Crack for Specimen R3-1. Arrows show Crack Origin along Weld Root. Dashed Line Separates Flange (A) from Weld (B).



Neg. No. 9532-1

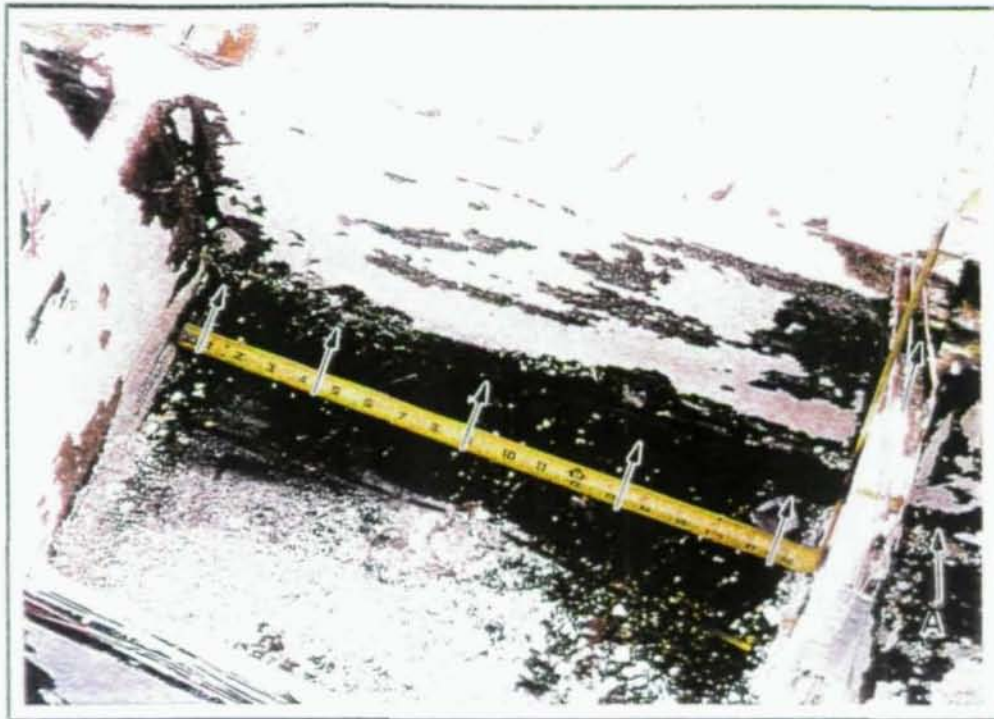
a)



Neg No. 9532-2

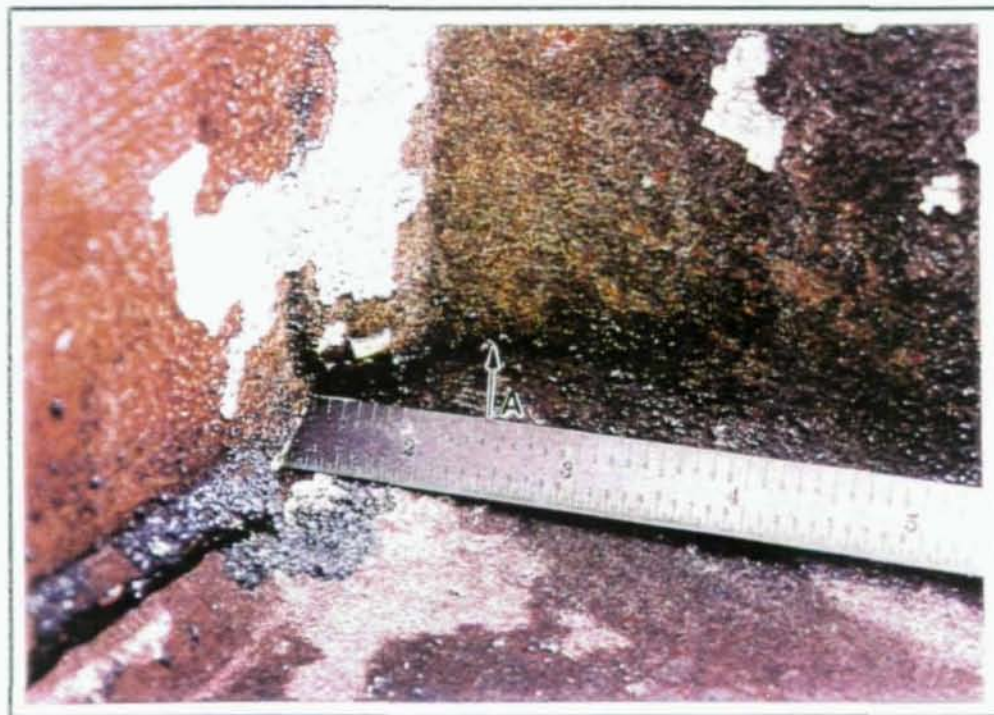
b)

Figure 59 Top Cover Plate to Column Weld for Specimen R3-2.
Arrows Show Fractured Cover Plate and Flange



Neg. No. 9532-11

a)



Neg No. 9616-17

b)

Figure 60 Fracture Path along k-Region for Specimen R3-2.
Arrow A Shows Location of k-Region Crack



Neg. No. 9532-8

a)



Neg No. 9532-14

b)

Figure 61 Photographs of Specimen R3-2, with Arrows Showing Cracks at (a) Column Flange at Bottom Cover Plate and (b) Bottom Continuity Plate



Neg. No. 9616-3a

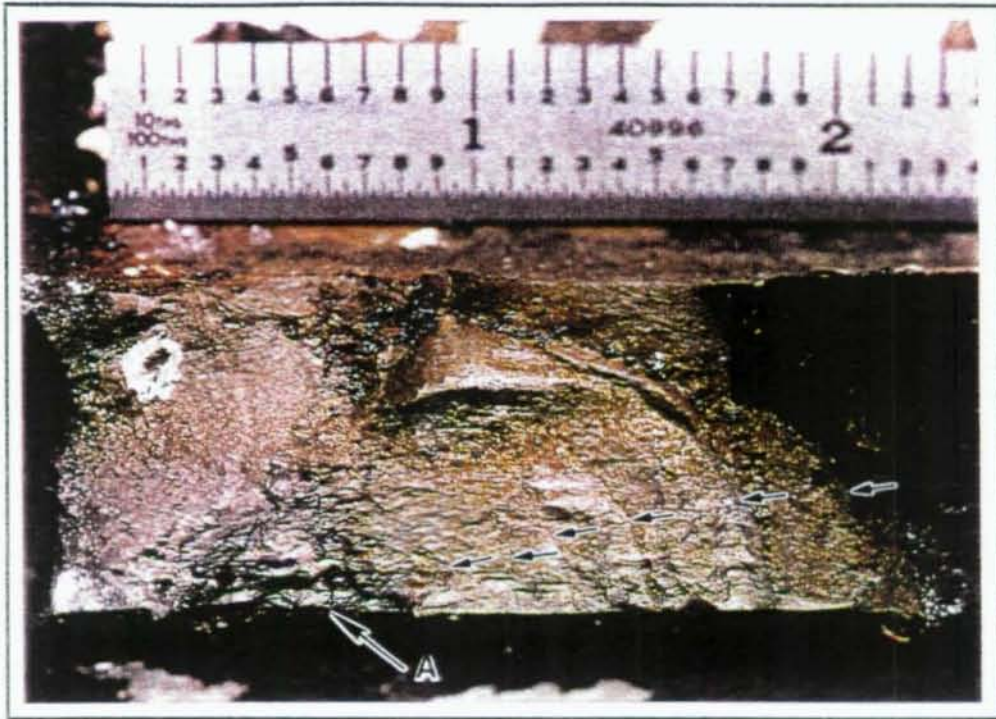
a)



Neg No. 9616-7a

b)

Figure 62 Fractured k-Region for Specimen R3-2. Arrow A Shows Origin at Edge of Continuity Plate Weld. Small Arrows Show Crack Arrest Marks.



Neg. No. 4198-10a

a)



Neg No. 4198-5a

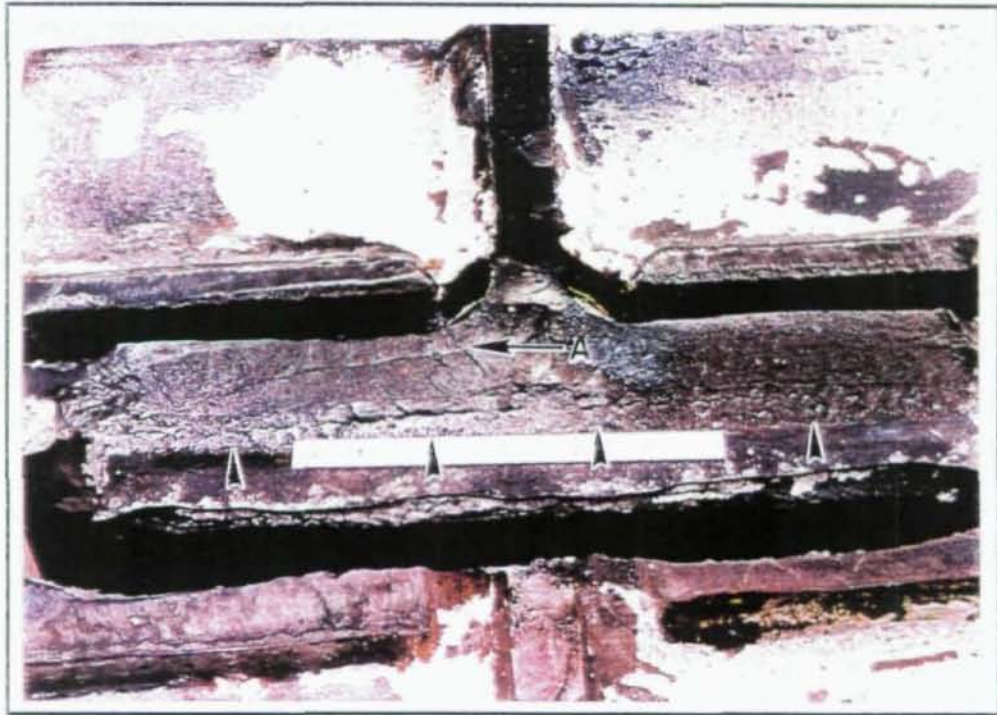
b)

Figure 63 Fractured k-Region for Specimen R3-2. Small Arrows Show Six of the Seven Crack Arrest Marks. Arrow A Shows Continuity Plate Fillet Weld Origin



Neg. No. 9616-1a

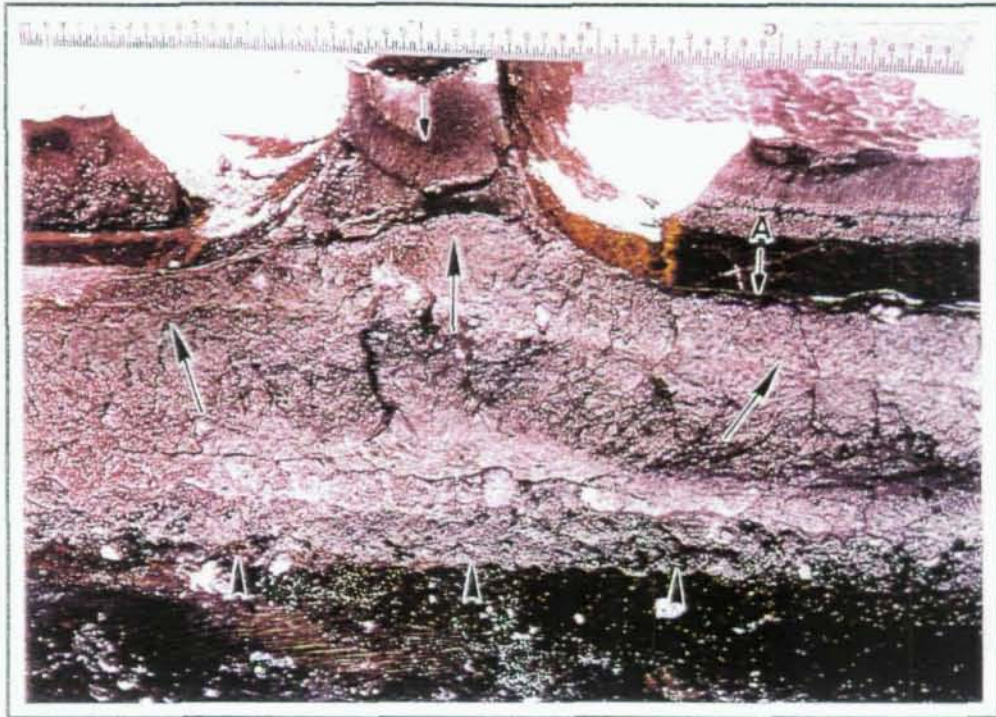
a)



Neg No. 9616-5a

b)

Figure 64 Top Cover Plate Fracture Surfaces for Specimen R3-2. Arrows Indicate Fracture Origin at Weld Root between Cover Plate and Beam Flange. Arrow A Indicates a Crack Arrest Mark in the Flange



Neg. No. 9616-12a

a)



Neg No. 9616-9a

b)

Figure 65 Fractures of Specimen R3-2: (a) Shows Origin at Weld Root between Cover Plate and Flange; (b) Shows Fracture Transition near k-Region. Arrows Show Crack Propagation Direction. Arrow A Indicates Shear Lip on Flange.

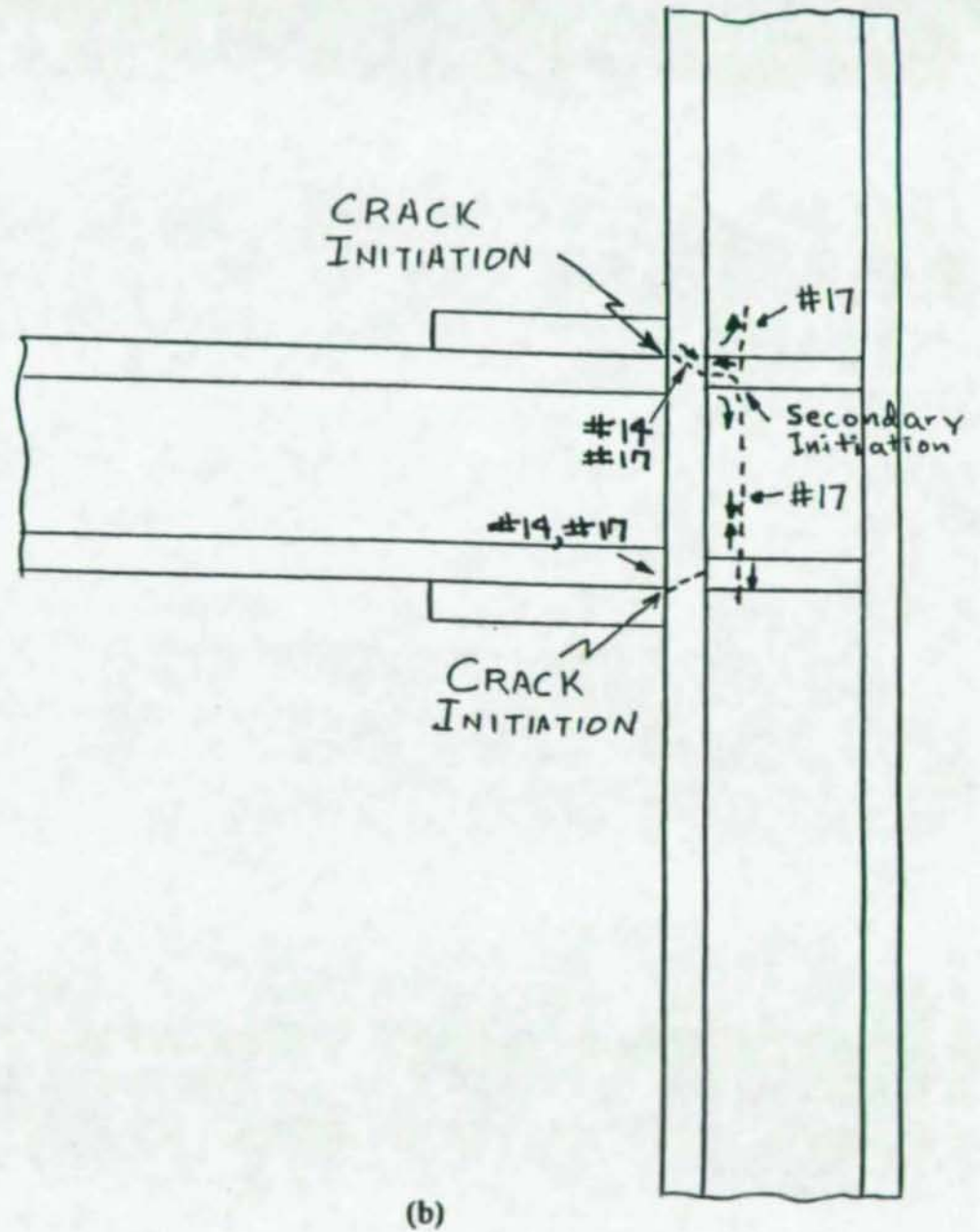
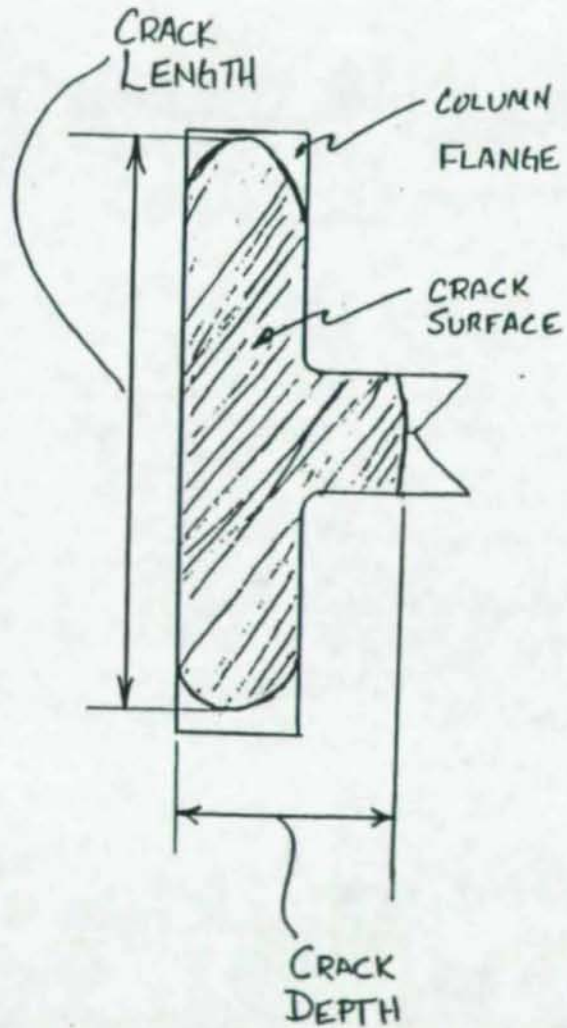


Figure 66 Schematic Illustration of Crack Locations, Depths and Lengths for Specimens R3-1 and R3-2

100-100

